Title
Topological Phase Transitions

Author
Tsui, Lokman

Publication Date
2018

Peer reviewed|Thesis/dissertation

Topological Phase Transitions

by

Lokman Tsui

A dissertation submitted in partial satisfaction of the

requirements for the degree of

Doctor of Philosophy

in

Physics

in the

Graduate Division

of the

University of California, Berkeley

Committee in charge:

Professor Dung-Hai Lee, Chair
Professor Constantin Teleman
Professor Michael Crommie

Spring 2018

Topological Phase Transitions

Abstract

Topological Phase Transitions

by

Lokman Tsui

Doctor of Philosophy in Physics

University of California, Berkeley

Professor Dung-Hai Lee, Chair

The study of continuous phase transitions triggered by spontaneous symmetry breaking has brought revolutionary ideas to physics. Recently, through the discovery of symmetry protected topological phases, it is realized that continuous quantum phase transition can also occur between states with the same symmetry but different topology. The subject of this dissertation is the phase transition between these symmetry protected topological states (SPTs). There are two main parts in this dissertation.

In the first part we consider spatial dimension d and symmetry group G so that the cohomology group, $H^{d+1}(G, U(1))$, contains at least one Z_{2n} or Z factor. We show that the phase transition between the trivial SPT and the root states that generate the Z_{2n} or Z groups can be induced on the boundary of a d+1 dimensional $G \times Z_2^T$-symmetric SPT by a Z_2^T symmetry breaking field. Moreover we show these boundary phase transitions can be "transplanted" to d dimensions and realized in lattice models as a function of a tuning parameter. The price one pays is for the critical value of the tuning parameter there is an extra non-local (duality-like) symmetry. In the case where the phase transition is continuous, our theory predicts the presence of unusual (sometimes fractionalized) excitations corresponding to delocalized boundary excitations of the non-trivial SPT on one side of the transition. This theory also predicts other phase transition scenarios including first order transition and transition via an intermediate symmetry breaking phase.

In the second part, we study the phase transition between bosonic topological phases protected by $Z_n \times Z_n$ in 1+1 dimensions. We find a direct transition occurs when $n = 2, 3, 4$ and in all cases the critical point possesses two gap opening relevant operators: one leads to a Landau-forbidden symmetry breaking phase transition and the other to the topological phase transition. We also obtained a constraint($c \geq 1$) on the central charge for general phase transitions between symmetry protected bosonic topological phases in 1+1D.

To my family

Contents

List of Figures

List of Tables

Acknowledgments

Eight years of PhD has been a long journey. It has been a truely unique life experience. My path crossed with many people, who made this journey fulfilling and meaningful.

First of all, I would like to express my sincere gratitude to my advisor Dr. Dung-Hai Lee for his guidence in my PhD program. Professor Lee is very generous in spending time discussing physics with his students. He often offers words of encouragement while being direct and constructive in his criticisms. He is also very patient in explaining his ideas and takes my ideas seriously. He cares very deeply about my academic and career development. His great passion and dedication to physics and intuitive way of thinking has been very influential to me. I am very lucky to have him as my mentor in the program.

I would also like to thank my collaborators, Yen-Ta Huang, Yuan-Ming Lu and Hong-Chen Jiang. I benefited a lot discussing with Yen-Ta from his meticulous way of thinking and it is great fun to learn physics together. His companionship has been invaluable to me. Dr Lu has been my role model as a hyperactive young researcher. He is energetic, brilliant and always cheerful. I am thankful for Hong-Chen for diligently performing DMRG studies on the models we proposed.

I would like to thank professor Hong Yao and Fa Wang for their discussions and accommodation for me in Tsinghua University and Peking University, where I had a great time discussing physics and meeting with friends including Zi-Xiang Li and Cheung Chan. I am also grateful to have the opportunity to learn physics and mathematics from various people in Berkeley, including John Cardy, Geoffrey Lee, Ryan Thorngren, and Adrian Po.

I would also like to thank the physics department of UC Berkeley and the Lawrance Berkeley National Laboratory for supporting me through my PhD program. I would like to especially thank Anne Takizawa, Donna Sakima and Joelle Miles for clearing my financial and visa problems. I would like to thank Stanford University and the Stanford Research Computing Center for providing computational resources and support that have contributed to these research results. I am also grateful to my qualifying committee and dissertation committee members, professor Michael Crommie, professor Ashvin Vishwanath, and professor Constantin Teleman.

It is also a great honour to be the receipient of the Croucher Fellowship for Postdoctoral Research, which enabled me to pursue a postdoctoral position in MIT in the next two years. I would like to give a special thanks to the Croucher Foundation and its Trustees for the generous award. I must also thanks professor Zheng-Cheng Gu for his strong recommendation and invitations to Hong Kong for workshops in topological phases.

Lastly, I would like to thank my friends and family for their emotional support. I thank my parents and sister for being supportive and loving. I thank Kolen Cheung Ka-Hei, Soarer Siu Ho-Chung and my flatmate Zihao Jing for their friendship. Finally I thank Ms Helena Zeng Hao for being with me, which has made me a much more cheerful person. Our time together taught me how to care for another human being and has greatly enriched the meaningfulness of my life.

Chapter 1

Introduction to Topological Phases

Since the ancient times, humans have been wondering about the phases of matter. It was Laudau[1] who made a breakthrough in the early 20th century. He realized that different phases corresponds to the realization of different symmetries, and in a phase transition, a higher symmetry group is broken into a lower symmetry subgroup. For example, a magnet undergoes a phase transition as temperature is raised past a critical value to go from a ferromagnetic state to a paramagnetic state. The ferromagnetic state has a magnetization which breaks rotation symmetry, which is restored in the paramagnetic state. Another example is the melting of ice. In ice the water molecules are arranged in a periodic crystal which has only a discrete crystalline symmetry, which is a subgroup of the continuous translation and rotation symmetry enjoyed by water molecules in the liquid phase. For some time it appeared convincing that this is the complete story for the classification of phases of matter.

In the last three decades, a strange new class of phases was discovered by humans and is coined the term "topological phases". These phases all enjoy the same symmetry, but one can never continuously deform two distinct phases into one another without closing the energy gap. In other words, a phase transition occurs without any symmetry breaking. An experimental realization of such phases is the celebrated discovery of fractional quantum hall effect(FQHE)[2]. Following the discovery of FQHE, a rapid burst of theoretical and experimental activities uncovered a huge plethora of other topological phases. The word "topology" means the study of properties invariant under continuous deformation. The distinction between topological phases is not in their symmetry, but in their topology. At the current understanding, topological phases are gapped phases of matter and can be divided into two categories. The first category are known as symmetry-protected topological phases(SPT)[3;4;5]. Each of these phases have a unique groundstate with a full energy gap when defined on a closed(i.e., boundary-free) manifold and exhibit the full symmetry of the Hamiltonian. However, these states are grouped into different "topological classes" such that it is not possible to cross from one topological class to another without closing the energy gap while preserving the symmetry. In this class the fundamental degrees of freedom may be fermionic, which includes topological insulators and superconductors, or bosonic, which includes various spin systems. The second category, in contrast, can have degenerate

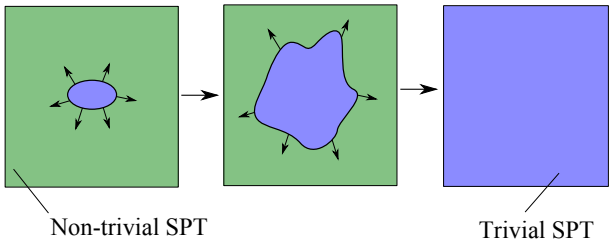

Figure 1.1: (Color online) A caricature showing the necessity of gapless excitations on the boundary of a non-trivial SPT. The blue and green regions represent a trivial and a non-trivial SPT respectively. If the interface between a trivial and non-trivial SPT were gapped, then a small island of trivial SPT may be grown inside a non-trivial SPT, and gradually expand to occupy the entire system without closing the energy gap hence adiabatically connecting a trivial and non-trivial SPT.

groundstates when defined on a topologically non-trivial closed manifold. They are called "topologically ordered" states. In this dissertation we will focus on the bosonic SPTs which belong to the first category.

1.1 Symmetry-Protected Topological Phases

Symmetry protected topological(SPT) phases are the non-degenerate ground states of local lattice Hamiltonians each respecting the same global symmetry group G. These ground states remain invariant under G and are separated from their respective excited states by an energy gap. If two Hamiltonians can be made equal by adding or removing symmetry preserving local terms while preserving the excitation gap, they are viewed as equivalent. Correspondingly ground states of equivalent Hamiltonians are viewed as the same phase.

Given two SPTs in the same dimension, we may try to stack them on top of each other. This stacking operation provides an abelian group structure to the SPTs. The trivial group element is the direct product state. All the other states which cannot be smoothly deformed to the trivial state are non-trivial SPTs.

The hallmark of non-trivial SPTs is the presence of gapless boundary excitations. The fact that a non-trivial SPT must have a gapless boundary can be understood as follows. A SPT with boundary can be alternatively viewed as the same SPT interfaces with vacuum, i.e., a trivial SPT. If there were no gapless excitations at the interface we can gradually expand an island of trivial SPT embedded in the non-trivial one until it occupies the entire system without closing the energy gap (See Fig. 1.1). Since such expansion, or more precisely the local modification of the Hamiltonian which causes such expansion, does not have to break the symmetry, this contradicts the notion of trivial and non-trivial SPT being in two inequivalent classes. Hence a non-trivial SPT must have gapless boundary excitations which cannot be gapped out if the protection symmetry is not broken.

Example of fermionic SPT: Chern Insulator

To be concrete, lets consider an example of fermionic SPT, a Chern insulator. Consider a 2-by-2 single particle Bloch Hamiltonian in two spatial dimensions. Such a hamiltonian has the general form

$$h(\vec{k}) = a_0(\vec{k})\sigma_0 + a_x(\vec{k})\sigma_x + a_y(\vec{k})\sigma_y + a_z(\vec{k})\sigma_z$$

And the single-particle energy eigenvalues are $E(\vec{k}) = \sigma_0 \pm \sqrt{a_x^2 + a_y^2 + a_z^2}$. Focusing on gapped phases, and deforming the energy gap to a constant, we may assume $\sigma_0 = 0$ and $a_x^2 + a_y^2 + a_z^2 = const.$ Thus the space of gapped 2-by-2 Bloch hamiltonians with constant energy gap forms a 2-sphere parametrized by (a_x, a_y, a_z). As a function of $\vec{k}$ belonging to the Brillouin zone, the hamiltonian $h(\vec{k})$ is a map from the torus T^2 to the sphere S^2. Such maps form distinct equivalent classes under continuous deformation. They can be distinguished by computing a topological invariant known as the Chern number, which is the integral of the Berry phase curvature over the Brillouin zone. If the function $h(\vec{k})$ can be deformed to a constant map, it is considered as a "trivial" insulator. Otherwise it is a non-trivial topological insulator. It turns out that when the corresponding lattice hamiltonian is defined on a manifold with open boundary, the "trivial" insulator will still be gapped while the "non-trivial" topological insulator will have gapless excitations (a chiral complex fermionic mode) on the boundary. The direction of the chiral mode (left or right moving) depends on the sign of the Chern number. Under stacking, these Chern insulators form the group of integers Z. Physically the inequivalent phases are labelled by the difference between the number of right moving chiral modes and left chiral modes $n_R - n_L$.

In the above example, since the gapless mode is chiral, no symmetry is needed to protect it from being gapped out. In other words, the protection symmetry is actually just the trivial group with only the identity element. We may use the Chern insulator to engineer another SPT with a non-trivial protection group as follows. If we combine a Chern insulator for spin up electrons with one right-moving chiral edge modes and a Chern insulator for spin down electrions with one left-moving chiral edge modes, the result is another fermionic SPT. Without any symmetry, we may gap out the boundary edge modes (labelled by $\psi_{R\uparrow}, \psi_{L\downarrow}$) via the mass coupling $\psi_{R\uparrow}^\dagger \psi_{L\downarrow} + h.c.$. However if we impose the time reversal symmetry $\hat{T}$ which transforms $\psi_{R\uparrow} \to \psi_{L\downarrow}$ and $\psi_{L\downarrow} \to -\psi_{R\uparrow}$ so that $\hat{T}^2 = (-1)^{n_F}$ is the fermion parity, then the mass term $\psi_{R\uparrow}^\dagger \psi_{L\downarrow} + h.c.$ is forbidden. Hence in this case the fermionic SPT is protected by the time-reversal symmetry. This is known as the spin hall insulator and has a Z_2 classification.

Example of bosonic SPT: Haldane Chain

Another example of SPT is the Haldane chain. In this case the degree of freedoms are bosonic integer-spin variables, arranged in a one spatial dimensional chain geometry. Each unit cell consists of two spin-1/2 variables, hence forming an integer (spin-0 or spin-1) variable in each

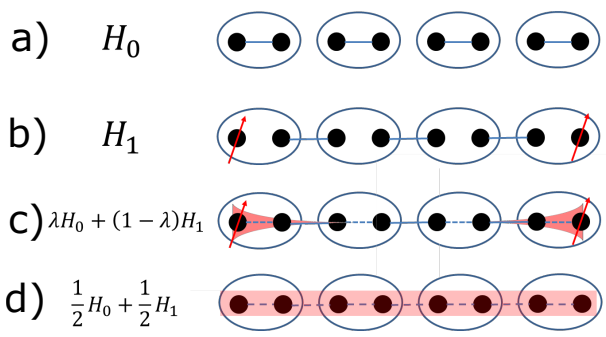

Figure 1.2: (Color online) (a) The Hamiltonian and groundstate wavefunction for a trivial bosonic SPT. The oval is a unit cell consisting of two spin-1/2 denoted as a black dot. The Hamiltonian is $H_0 = \sum_{<i,j>} \vec{s_i} \cdot \vec{s_j}$ where $< i, j >$ are summed over the blue bonds. In the groundstate, spin-1/2's form spin singlets within each unit cell resulting in a direct product state. (b) The groundstate wavefunction of the non-trivial SPT(Haldane chain). The hamiltonian consists of singlet coupling for spin-1/2s across different unit cells. A dangling spin-1/2 remains on each edge when defined on an open chain. (c) Tuning a parameter λ to interpolate between the trivial and non-trivial SPTs. As λ approaches the critical value $\lambda_c = 1/2$, the dangling spin-1/2 becomes more and more delocalized from the edge. (d) The critical state at $\lambda = \lambda_c$. The dangling spin-1/2 from the edge becomes completely delocalized and freely propagate in the gapless bulk. As a result the bulk has fractionalized (spin-1/2) excitations (spinons) despite each unit cell having integer spin.

cell. Suppose each unit cell enjoys the $SO(3)$ spin rotation symmetry for integer spins. In the trivial SPT state, the spin-1/2's within each unit cell forms a singlet. The groundstate is hence a direct product state of spin singlets over all cells. In the non-trivial SPT state, the spin-1/2's form singlet with a neighbour spin-1/2 in an adjacent cell (see Figure 1.2(a,b)). It is observed that a dangling spin-1/2 resides on the edge of the non-trivial SPT state when defined on an open chain. The dangling spin-1/2 cannot be gapped out while preserving the $SO(3)$ symmetry on each unit cell. This leads to a four-fold groundstate degeneracy on an open chain since on each edge there is a two-fold degeneracy assocated with the spin-1/2. Such edge degeneracy is the manifestation of "gapless" boundary states in the case of a 0-d boundary.

If two non-trivial spin chains are stacked together, then on each edge there will be two dangling spin-1/2's. It will be possible to couple the two spin-1/2's on each edge to gap out the boundary, resulting in a trivial SPT state. Hence the bosonic SPT protected by $SO(3)$ in 1d have a Z_2 classification.

Classification of bosonic SPT via group cohomology

The Z_2 classification for the Haldane chain example is a special case of a general classification result. For fixed spatial dimension d and symmetry group G, it is proposed[5] that the SPT phases form an 1-1 correspondence with the cohomology group $H^{d+1}(G, U(1))$. For example, $H^2(SO(3), U(1)) = Z_2$. Its definition is presented in Appendix A.1. In the 1-d case, $H^2(G, U(1))$ corresponds to the projective representations of group G. We remark that this proposal does not provide a complete classification result. In fact, some exceptional phases are discovered outside the cohomology classification[7]. In the dissertation we simply focus on the phases transition between the SPTs classified by the cohomology group[8;9].

1.2 Quantum Phase transitions between topological phases

Having familiarized ourselves with topological phases, we will now turn to the focus of this dissertation: the study of phase transitions between topological phases. In particular we focus on the quantum(*i.e.* zero temperature) phase transitions. Before we begin, we should explain our motivations: why study phase transitions?

The study of phase transitions brought tremendous impact on theoretical physics, stimulating the development of very deep understanding of nature including the concept of universality class, renormalization group flow, and conformal field theory. As explained before, Landau's theory of symmetry breaking phase transitions is a very successful theory. A generic phases transition involves the breaking of a higher symmetry group into a lower symmetry group. This can be quantified through the measurement of an order parameter. In the state of higher symmetry, the order parameter remains zero while it gains a non-zero value in the lower symmetry phase. In the example of ferromagnetic to paramagnetic phase transition, the magnetization is the order parameter. When people measure how this order parameter vanishes as one approaches the critical point, they noticed something immensely preculiar. As some control parameter t is tuned towards the critical value t_c at which the phase transition occurs, the order parameter m vanishes. In general m vanishes as some power law: $m \propto |t - t_c|^\beta$, where β is a dimensionless number known as a critical exponent. We can study how various other quantities(e.g. heat capacity, susceptibility, correlation length) behave near the critical point and define a variety of other critical exponents. Amazingly, across a variety of seemingly different experiments with different materials, the measured sets of critical exponents are identical as long as they have the same spatial dimensions and the same symmetry breaking pattern. This allows physicists to neatly group many different phase transitions into a single "universality class".

The root of this phenomenon is the emergence of conformal symmetry, or scale invariance, at the critical point. This is best understood in 1+1 spacetime dimensions. As the control parameter approaches its critical value, the energy gap closes and the correlation length diverges. The system becomes self-similar upon rescaling and acquires a very large emergent

symmetry group of conformal transformations. In 1+1 spacetime dimension, the conformal symmetry turned out to be so large that they impose severe constraints on the possible representations of the symmetry (with some assumptions). Thus the critical points which fall into different representations of the conformal symmetry also becomes highly constrained. This lead to the distinct universality classes which are observed.

Thus the study of phase transitions have far reaching consequences and is highly interesting. After the discovery of topological phases, it is a natural question to ask what is so special about the quantum phase transitions between topological phases. This dissertation is born out of an attempt to answer this question.

1.3 Outline

The following two chapters summerize our study on topological phase transitions. In Chapter 2 we develop a holographic theory of phase transitions between a class of bosonic SPTs. We find that a critical point between topological phases protected by group G can be interpreted as the boundary state of another SPT in one higher dimension protected by $G \times Z_2^T$. The higher dimensional SPT can be interpreted as having Z_2^T domain walls decorated by the lower dimensional SPT. The extra Z_2^T symmetry acts as a duality transformation between the two distinct lower dimensional SPTs living on the boundary. It also elucidates a physical picture that the critical point is the proliferation of gapless boundary states of the non-trivial SPT.

In Chapter 3 we study the critical point between 1-d SPTs protected by $Z_n \times Z_n$. We found that a direct transition occurs for $n \leq 4$ and obtained an exactly solvable analytical model which is verified by DMRG simulations. We observe that the central charge is always greater than or equal to 1, which can be generalized to 1D phase transition between topological phases protected by any discrete unitary symmetries. We also found the critical point is a multicritical point, in the sense that it has two relevant symmetric operators. One drives the SPT transition and the other drives the transition between two spontaneous symmetry breaking phases whose symmetries do not have subgroup relations, *i.e.* a Laudau forbidden transition.

Chapter 2

A Holographic Theory of Phase Transitions Between Symmetry Protected Topological States

2.1 Introduction

Suppose we have a bulk Hamiltonian describing a bosonic SPT. This hamiltonian has a tuning parameter λ, and by changing λ the ground state of $H(\lambda)$ goes from one SPT to another inequivalent SPT. Our purpose is to study the possible phase transition(s) occurring for intermediate values of λ. We propose the following conjecture: in a direct transition, the critical state is a proliferation of the gapless boundary states that lives on the boundary between the two SPTs. (Recall that from section 1.1, the boundary of a non-trivial SPT carries gapless boundary states which cannot be gapped out while preserving the protection symmetry G.)

The motivation of the conjecture is as follows. Take the Haldane chain (Figure 1.2) as an example. Suppose the Hamiltonian is now a linear interpolation between the trivial (H_0) and non-trivial (H_1) chains parametrized by λ. As we tune λ so that the system approaches the critical point $\lambda_c = 1/2$, the energy gap closes and the spin-1/2's on the edge becomes more and more delocalized (with localization length inversely proportional to the energy gap)(Figure 1.2(c)). At the critical point λ_c, the gap completely closes and the localization length becomes infinity. Thus the edge modes becomes free to propagate throughout the bulk at the critical point.

Put it another way, we can imagine a spatially dependent parameter $\lambda(\vec{x})$ such that on one side of the system ($x > 0$), it is in one SPT ($\lambda(\vec{x}) > \lambda_c$) while on the other side ($x > 0$), the system belongs to the other SPT ($\lambda(\vec{x}) < \lambda_c$). Near $x = 0$, the value of $\lambda \sim \lambda_c$. Thus we can view the gapless boundary state that lives near $x = 0$ as a spatially confined bulk critical state. In other words the gap closure at the boundary between two inequivalent SPTs can be viewed as a spatial coordinate tuned phase transition between the two SPTs[6].

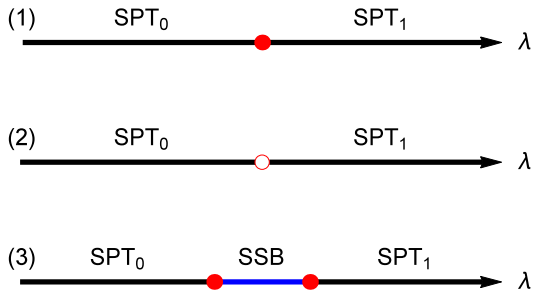

Figure 2.1: (Color online) Three possible scenarios for the phase transition between two different SPTs. Red dots represent continuous quantum critical points, red circle represents first order phase transition, and "SSB" stands for spontaneous symmetry breaking.

To elucidate the above physical picture, we arrived at the following theorem, which is the main result of this chapter:

Theorem The three scenarios of phase transition (see Fig. 2.1) between a trivial d-dimensional G-symmetric SPT and a non-trivial SPT satisfying a special condition can be realized at the boundary a d+1 dimensional $G \times Z_2^T$ symmetric SPT under the influence of a *boundary* Z_2^T symmetry breaking field. The condition the non-trivial G-symmetric SPT must satisfy is that it is not equivalent to the stacking of any two other identical G-symmetric SPTs. This condition will be referred to as the "non double stacking condition" (NDSC) in the rest of the chapter. Any G whose $H^{d+1}(G, U(1))$ contains a Z_{2n} or Z factor will have SPTs, e.g., that corresponds to the generator of Z_{2n} or Z, satisfy this condition.

Here the Z_2^T transformation inverts the sign of a local Ising variable and performs a complex conjugation on the wavefunction. Because the Ising variable in question is not necessarily time reversal odd, this Z_2^T is not the usual time reversal symmetry. This theorem allows us to construct explicit lattice models to describe the SPT phase transition. In particular these lattice models possess a non-local transformation (a "duality transformation") relating the trivial and non-trivial SPTs on the opposite sides of the transition. In the case of continuous phase transition, the critical theory exhibits an emergent (non-local) symmetry. The excitations at such critical point, sometimes fractionalized, correspond to "dynamically percolated" boundary excitations of the non-trivial SPT on one side of the transition.(The last statement was conjectured in Ref.[6].)

Most of the remaining of the main text, namely, section 2.2 – section 2.4 presents a sketch of the proof for the theorem. In these discussions we shall focus on physical arguments while keeping mathematics to a minimum level. The formal proofs are left in the appendices. The mathematical tool we use in this chapter is the standard group cohomology cocycle manip-

ulation. In the following we give the outline for the main text and appendices separately.

The outline of the main text

In section 2.2 we discuss the special $G \times Z_2^T$ SPT whose boundary, in the presence of Z_2^T symmetry breaking field, exhibits the phase transition between a trivial and non-trivial G-symmetric SPTs *in one space dimension lower*. In section 2.3 we discuss the NDSC condition imposed on the non-trivial G-symmetric SPTs on one side of the transition. In section 2.4 we discuss the three possible scenarios (Fig. 2.1) of the SPT transition and relate them to the boundary physics of the $G \times Z_2^T$ SPT. In section 2.5 we present simple examples of lattice models in one and two dimensions. These models are constructed under the framework enabled by the theorem. We shall discuss the phase transitions they exhibit. Finally in section 2.6 we conclude and discuss directions for future studies.

The outline of the appendices

In Appendix A.1 we show how to construct the (fixed point) ground state wavefunction and their associated exactly solvable hamiltonian for $\mathcal{G}$-symmetric SPTs in general dimensions. Here $\mathcal{G}$ can contain both unitary and anti-unitary elements. In Appendix A.2 we construct the basis states spanning the low energy Hilbert space for the boundary of a $\mathcal{G}$-symmetric SPT, and derive how do they transform under the action of $\mathcal{G}$. In Appendix A.3 we focus on $\mathcal{G} = G \times Z_2^T$ and dimension=d+1. In (A.3) we focus on a particular subset of the cocycles of $H^{d+2}(G \times Z_2^T, U(1))$. In (A.3) we determine the condition for the non-trivialness of the chosen cocycles. In (A.3) we show that the SPTs constructed from these cocycles correspond to decorating the proliferated Z_2^T domain walls with G-symmetric SPTs. In Appendix A.4 we show that the boundary Hilbert space of the $G \times Z_2^T$ SPT contains an invariant subspace which is spanned by a basis isomorphic to the usual basis for studying G-symmetric SPTs in d dimension. In part (A.4) we show how to utilize this basis to write down a family of d-dimensional lattice models exhibiting phase transition(s) between two inequivalent G-symmetric SPTs. For these models we show that the extra Z_2^T symmetry acts non-locally. In Appendix A.5 we show how the extra Z_2^T symmetry implies there is no local $G \times Z_2^T$ symmetric hamiltonian that can gap out the d-dimensional system without spontaneous symmetry breaking. In Appendix A.6 and A.8 we show how the framework developed in the chapter can be applied to obtain simple lattice hamiltonians in one and two space dimensions.

2.2 The $G \times Z_2^T$ symmetric SPT in $d+1$ dimensions from proliferating decorated Z_2^T domain walls

Generalizing the work of Ref. [10], we consider a *subset* of $d+1$ dimensional $G \times Z_2^T$ symmetric SPTs constructed by proliferating Z_2^T domain walls each "decorated" with a non-trivial d-dimensional G-symmetric SPT (satisfying the NDSC). The basis states spanning the Hilbert space for this problem is $\prod_i |\rho_i, g_i\rangle$ where i labels the lattice sites and $\rho_i = \pm 1 \in Z_2^T, g_i \in G$. Hence each site has an Ising-like variable. This variable reverses sign under the action of Z_2^T. A state with non-zero expectation value of such Ising variable breaks the Z_2^T symmetry. From such a symmetry breaking state we can construct a Z_2^T-symmetric state by "proliferating" the domain walls separating regions with opposite value of the Ising variable . (This means the ground state is a superposition of all possible Ising configurations.) Such domain walls are orientable d-dimensional manifolds and we choose the orientation consistently. To construct the $d+1$ dimensional SPT, these domain walls are decorated with the G-symmetric SPT_1 or $\overline{SPT_1}$ (the inverse of SPT_1) according to the following rule. If the orientation of a domain wall points from the $+1$ domain to the -1 domain it is decorated with SPT_1. If the reverse is true it is decorated with $\overline{SPT_1}$. Because the Z_2^T operation reverses the sign of the Ising variable, it must transforms SPT_1 into $\overline{SPT_1}$. A domain wall decorated with $\overline{SPT_1}$ is said to be conjugate to the one decorated with SPT_1 because when they are stacked together their respective SPTs combine to become trivial.

If we construct the wavefunctions for SPT_1 and $\overline{SPT_1}$ according to Appendix A.1, the wavefunction associated with $\overline{SPT_1}$ is the complex conjugate of that of SPT_1. Hence *the non-trivial element of Z_2^T has two effects – it inverts the sign of the Ising variable as well as performing the complex conjugation on the wavefunction.* Because the Ising variable in question does not have to be time-reversal odd, the Z_2^T discussed here can be different from the usual time reversal symmetry.

If the $d+1$ dimensional system has boundary, and which respects the Z_2^T symmetry, the proliferated fluctuating bulk domain walls can intersect it. The intersection is $d-1$-dimensional (see Fig. 2.2) and is itself the boundary of the domain wall. Thus they harbor gapless boundary excitations of the SPT on the domain wall. However when two "conjugate" intersections come close the gapless excitations on them can quantum tunnel. (A pair of conjugate intersections are the respective intersections of a pair of conjugate domain walls with the boundary.) When such quantum tunneling is strong a gap can open and effectively the two conjugate intersections annihilate each other.

2.3 The NDSC and the non-trivialness of the $G \times Z_2^T$-symmetric SPT

In Appendix (A.3) we prove mathematically that the state arises from proliferating the decorated Z_2^T domain walls is non-trivial only if the SPT on the wall satisfies the NDSC.

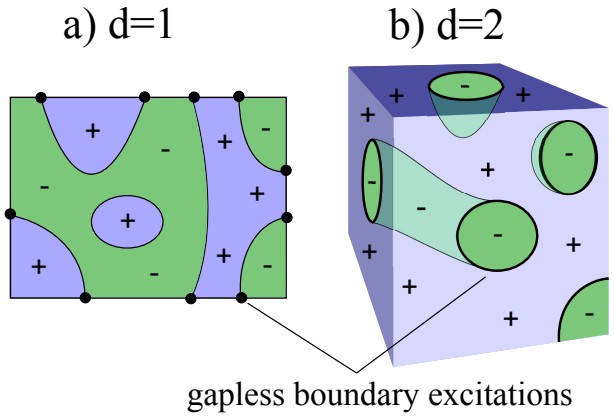

Figure 2.2: (Color online) Intersection of domain walls with the boundary of a $d+1$ dimensional system, for (a) $d = 1$ and (b) $d = 2$. The value of the Z_2^T Ising variable for regions colored blue and green are +1 and -1 respectively. The domain walls are decorated with a d-dimensional SPT. Their intersections with the boundary are $d-1$-dimensional, denoted by black dots in (a) and solid lines in (b) respectively. These intersections host gapless boundary excitations of the SPT living on the domain walls.

Now we explain why this condition is necessary. Let's suppose SPT_1, the SPT that the domain walls are decorated with, violates the NDSC and $SPT_1 = (SPT_{1/2})^2$ for certain G-symmetric $SPT_{1/2}$. In the following we show it is possible to perturb the boundary with a local $G \times Z_2^T$ symmetric hamiltonian ΔH and gap out the gapless excitations.

Let ΔH coats the boundary with an additional layer of a $\overline{SPT_{1/2}}$ or $SPT_{1/2}$ depending on whether the Z_2^T variable on the boundary is $+1$ or -1. Since $SPT_{1/2}$ is G-symmetric, ΔH respects the G-symmetry. Moreover because the coating switches from $SPT_{1/2}$ to $\overline{SPT_{1/2}}$ when the Z_2^T variable is flipped, ΔH also respects the Z_2^T symmetry. The fact ΔH is local is because the coating only depends on the value of the Z_2^T variable locally.

Without loss of generality let's suppose the orientation of the domain wall points from the $+1$ domain to the -1 domain. This will induce an orientation on the intersection of the domain wall and the boundary. In Fig. 2.2 this means the blue region is "inside" and the green is "outside". Also let us choose the orientation of the coated film so that the orientation of the boundary between $SPT_{1/2}$ and $\overline{SPT_{1/2}}$ agrees with that of the domain wall intersection. Without the coating the domain intersection carries the boundary gapless excitations of SPT_1. After the coating the interface between $SPT_{1/2}$ and $\overline{SPT_{1/2}}$ will be stacked on top of the original intersection. In the coated film of Fig. 2.3, when viewed from the $\overline{SPT_{1/2}}$ domain, the interface should host the boundary modes of $\overline{SPT_{1/2}}$. On the other hand when viewed from the $SPT_{1/2}$ domain the interface has the opposite orientation, thus it should host the conjugate of the $SPT_{1/2}$, i.e., the $\overline{SPT_{1/2}}$ boundary modes. As a result the stacked intersection/interface hosts the stacked boundary modes of SPT_1 and $\overline{SPT_{1/2}}^2 = \overline{SPT_1}$. Therefore they cancel and the gapless excitation on the domain wall/boundary intersection

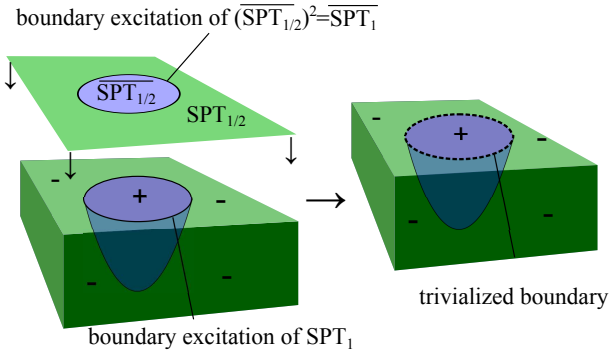

Figure 2.3: (Color online) Getting rid of the gapless boundary excitations if the SPT (SPT_1) used to decorate domain walls can be written as the square of another SPT ($SPT_{1/2}$). This is achieved by coating the surface with a layer of ($SPT_{1/2}$) on -1 domains and $\overline{SPT_{1/2}}$ on +1 domains (left panel). The combined boundary excitations on the intersection is gapped as denoted by the dashed line in the right panel.

are gapped out. This means the $G\times Z_2^T$-symmetric SPT must be trivial because it is possible to add totally symmetric boundary perturbation to remove the gapless excitations. Hence in order for the SPT derived from proliferating the decorated Z_2^T domain wall to be non-trivial the NDSC must be satisfied.

2.4 The Z_2^T symmetry breaking field and the three possible phase transition scenarios

Now let's assume the proliferated domain walls are decorated with the SPT satisfying the NDSC. In Appendix A.4 we show that the boundary of such $G\times Z_2^T$ SPT has an invariant subspace "transplantable" to one dimension lower[11]. This invariant subspace can be made into the lowest-energy subspace by turning on *fully* $G\times Z_2^T$ symmetric *boundary* perturbation. The basis set of such subspace is $\prod_\mu |g_\mu\rangle_B$, $g_\mu\in G$ where μ labels the boundary sites. They transform under G and the non-trivial element of Z_2^T according to

$$S_g\prod_\mu |g_\mu\rangle_B=\prod_\mu |gg_\mu\rangle_B,\quad g\in G \tag{2.1}$$

$$S_{-1}\prod_\mu |g_\mu\rangle_B=\phi(\{g_\mu\})K\prod_\mu |g_\mu\rangle_B,\quad -1\in Z_2^T \tag{2.2}$$

where the pure phase

$$\phi(\{g_\mu\})=\prod_\Delta[\nu_{d+1}(e,\{g_\mu\}_\Delta)]^{\sigma(\Delta)} \tag{2.3}$$

is the ground state wavefunction of the G-symmetric SPT used to decorate the domain wall, and K stands for complex conjugation. Here ν_{d+1} is a $U(1)$ phase factor whose arguments are $d+2$ elements in G. It is a representative in the group cohomology class of G that corresponds to the G-symmetric SPT, so it is fully determined by the group structure and the choice of a particular G-symmetric SPT (See Appendix A.1 for a review of group cohomology). The product is carried over the d-dimensional simplices Δ which triangulate the d-dimensional boundary. $\sigma(\Delta) = \pm 1$ is the orientation of each simplex and $\{g_\mu\}_\Delta$ is a shorthand for the $d+1$ group elements assigned to the vertices of Δ.

In Appendix (A.4) we show how to construct a family of d-dimensional lattice models using the above basis set. These models depend on a parameter $\lambda \in [0,1]$,

$$H(\lambda) = (1-\lambda)H_0 + \lambda H_1, \tag{2.4}$$

where

$$H_0 = -J \sum_\mu \sum_{g_\mu, g'_\mu} |\{g'_\mu\}\rangle_B \ {}_B\langle\{g_\mu\}|, \tag{2.5}$$

and

$$H_1 = -J \sum_\mu \sum_{g_\mu, g'_\mu} \frac{\phi(\{g'_\mu\})}{\phi(\{g_\mu\})} \overline{|\{g'_\mu\}\rangle_B} \ \overline{{}_B\langle\{g_\mu\}|}. \tag{2.6}$$

In the above equations $J > 0$ (and can be taken to very large value) and $\overline{|\{g'_\mu\}\rangle_B}$ stands for the complex conjugation of $|\{g'_\mu\}\rangle_B$. It is shown in Appendix A.3 that both H_0 and H_1 are invariant under the action of G, and that the ground state of H_0 is the trivial G-symmetric SPT while the ground state of H_1 is the non-trivial G-symmetric SPT described by the wavefunction in Equation (2.3). Upon the action of the non-trivial element of Z_2^T transforms H_0 and H_1 according to

$$S_{-1} H_0 S_{-1}^{-1} = H_1 \quad \text{and} \quad S_{-1} H_1 S_{-1}^{-1} = H_0. \tag{2.7}$$

Consequently $H(\lambda = 1/2)$ has an extra Z_2^T symmetry (Equation (2.2)). For other values of λ there is only the G symmetry (Equation (2.1)). (Therefore we can view $\lambda - 1/2$ as a Z_2^T symmetry breaking field.)

In Appendix A.5 we prove that due to the non-local action of S_{-1}, $H(\lambda = 1/2)$ is either gapless or the $G \times Z_2^T$ symmetry is spontaneously broken. This implies at $\lambda = 1/2$ the d-dimensional system can be in one of the three following phases. (1) Gapless and $G \times Z_2^T$ symmetric. (2) Gapped but spontaneously breaks the Z_2^T symmetry. (3) Gapped and spontaneously breaks the G (or both the G and Z_2^T) symmetry. Because at $\lambda = 1/2$ the system must be in one of the three phases discussed above, there are three possible routes for the phase transition from the trivial to non-trivial G-symmetry SPTs (Fig. 2.1). We discuss these three scenarios in the following. We shall do so from the view point of the d-dimensional system or that of the boundary of the d+1 dimensional system interchangeably.

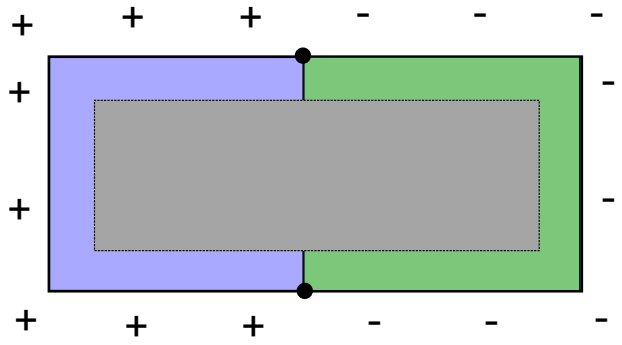

Figure 2.4: (Color online) The two inequivalent G-symmetric SPTs induced by opposite values of the boundary Z_2^T symmetry breaking field. Here blue and green denote the trivial and non-trivial SPT, respectively. The interface between these two SPT's are also an Z_2^T domain walls whose intersections with the boundary (the black dots) host the gapless boundary excitations of the SPT used to decorate the domain wall. The grey region in the center denotes the $G \times Z_2^T$ SPT with unbroken Z_2^T symmetry.

Continuous phase transition

This scenario corresponds to the boundary of the $G \times Z_2^T$ SPT being gapless. Under such condition the gapless excitations on the intersections of the fluctuating bulk domain walls and the boundary gives rise to a gapless boundary. These gapless-modes-infested domain wall intersections quantum fluctuate and delocalize throughout the boundary of the $d+1$ dimensional system. This is the "dynamic percolation" picture conjectured in Ref. [6].

Now let's imagine introducing the Z_2^T symmetry breaking field on the boundary (and only on the boundary). Now the Z_2^T domain wall can no longer intersect the boundary at sufficiently low energies. As a result the boundary is gapped. The two possible directions of the Z_2^T symmetry breaking field leads to two G-symmetric SPTs corresponding to the Z_2^T variable having opposite expectation values. In the following we show that these two SPTs are topologically inequivalent.

To do that we just need to demonstrate the interface between the two SPTs is necessarily gapless. This can be achieved by breaking the Z_2^T symmetry so that half of the boundary has positive and the other half has negative Z_2^T symmetry breaking field. The interface between these two halves are Z_2^T domain walls and they have to connect to the fluctuating domain wall in the bulk (See Fig. 2.4). Hence they host gapless excitations. This implies the two G-symmetric SPTs on the boundary induced by opposite Z_2^T-breaking field are indeed inequivalent.

First order phase transition

Here we consider the case when the state at $\lambda = 1/2$ spontaneously breaks the Z_2^T symmetry. In this case there will be degenerate ground states corresponding to the Z_2^T variable having opposite expectation values. An infinitesimal Z_2^T symmetry breaking field will lift the degeneracy and result in uniquely gapped G-symmetric phases on either side of $\lambda = 1/2$. From the boundary point of view because the Z_2^T symmetry is spontaneously broken the fluctuating domain walls no longer intersect the boundary at low energies. This removes the gapless excitations associated with the interaction. The same argument associated with Fig. 2.4 implies the two gapped G symmetric phases induced by opposite value of the symmetry breaking field are topologically inequivalent. Thus we have two distinct G-symmetric SPTs whose energy crosses at the transition point – i.e. a first order phase transition has occured. This is depicted as the second scenario in Fig. 2.1.

An intermediate symmetry breaking phase

In the third scenario the boundary of the $G \times Z_2^T$ symmetric SPT spontaneously breaks the G (or both the G and Z_2^T) symmetry. Because of the G symmetry breaking the gapless excitations at the domain wall intersections are gapped out. From the point of view of the d-dimensional system the Z_2^T symmetry breaking field, i.e., the perturbation induced by λ deviating from 1/2, is G-symmetric. Because of the existence of energy gap, infinitesimal symmetry breaking field can only act within the degenerate ground state manifold (i.e. the subspace spanned by the degenerate ground states) . Because the G symmetry is spontaneously broken such ground state manifold must carry a multi-dimensional irreducible representation of G. Since the Z_2^T symmetry breaking field is G symmetric, it should be proportional to the identity operator within the ground state manifold. Consequently for values of λ in the immediate neighborhood of 1/2 the ground states remain degenerate and the G symmetry remains spontaneously broken. When λ deviates sufficiently from 1/2 the G-symmetry has to be restored at some point because the limiting states at $\lambda = 0$ and $\lambda = 1$ are G-symmetric. Thus two Landau-like G symmetry restoring critical points must intervene at intermediate λ. This gives rise to the possibility depicted as scenario (3) in Fig. 2.1.

In section 2.5 we construct a simple solvable models for which scenario (1) and (3) are realized. Scenario (2) is suggested to occur in a numerical study on 2D Z_2 SPT phase transition[12]. We have not encountered an example where topological ordered[13] state appears on the boundary as discussed in Ref.[14;15;16;17;18;19;20;21], though it would be interesting for future studies.

2.5 Example: phase transition between $Z_2 \times Z_2$-symmetric SPTs in $d = 1$

A solvable case in one dimension

In one dimension there are two inequivalent $Z_2 \times Z_2$-symmetric SPTs ($H^2(Z_2 \times Z_2, U(1)) = Z_2$). We follow the recipe in Appendix A.3 to construct the solvable Hamiltonians for the trivial and non-trivial $Z_2 \times Z_2$-symmetric SPTs and a family of interpolating hamiltonians which realize scenario (1) of Fig. 2.1. Consider two spin-1/2 variables σ_{2i-1} and σ_{2i} in each unit cell i. The $Z_2 \times Z_2$ group acts as global π rotations along x and z directions on all spins. As detailed in Appendix A.6 the trivial/non-trivial Hamiltonians and the non-trivial element of Z_2^T transformation are given by

$$H_0 = \sum_i (\sigma^x_{2i-1}\sigma^x_{2i} + \sigma^z_{2i-1}\sigma^z_{2i}) \tag{2.8}$$

$$H_1 = \sum_i (\sigma^x_{2i-2}\sigma^x_{2i-1} + \sigma^z_{2i}\sigma^z_{2i+1}) \tag{2.9}$$

$$H(\lambda) = (1-\lambda)H_0 + \lambda H_1 \tag{2.10}$$

$$S_{-1} = \prod_i (\frac{1+\sigma^z_{2i-1}\sigma^z_{2i+1}}{2} + \frac{1-\sigma^z_{2i-1}\sigma^z_{2i+1}}{2}\sigma^x_{2i})K \tag{2.11}$$

Here K stands for complex conjugation. It is straightforward to show that the trivial/non-trivial Hamiltonians transform into each other under S_{-1}. Equation (2.8) and Equation (2.9) and any linear combination of them are exactly solvable by going to the Majorana fermion representation (see Fig. A.4). In such representation H_0 contains intra-unit-cell (the rectangle boxes) coupling and H_1 contains inter-unit-cell coupling. The critical Hamiltonian $(H_0 + H_1)/2$ consists of two decoupled critical Majorana chains. As a result it exhibits central charge $c = 1$. In the spin 1/2 representation $(H_0 + H_1)/2$ is the XX model which possesses gapless spin-1/2 excitations. Since H_1, the dimerized XX model, has spin-1/2 edge states, this gives an explicit example where the gapless excitations of the critical state are delocalized, or dynamically percolated, edge excitations.

Although the hamiltonians in Equation (2.10) is exactly solvable it has one undesirable feature, namely, it actually has higher symmetry ($U(1)$) than $Z_2 \times Z_2$ ($U(1) \times Z_2^T$ rather than $Z_2 \times Z_2 \times Z_2^T$ in the case of $\lambda = 1/2$). In the following we add perturbations to Equation (2.10) to break the extra symmetry while maintain the solvability. Consider the following hamiltonian

$$\begin{aligned} H(\lambda, \alpha) = &\sum_i (1-\lambda)\left[\alpha\sigma^x_{2i-1}\sigma^x_{2i} + (1-\alpha)\sigma^z_{2i-1}\sigma^z_{2i}\right] \\ &+ \lambda\left[\alpha\sigma^x_{2i-2}\sigma^x_{2i-1} + (1-\alpha)\sigma^z_{2i}\sigma^z_{2i+1}\right], \end{aligned} \tag{2.12}$$

where $\alpha, \lambda \in [0, 1]$. For $\alpha \neq 1/2$ the symmetry of the model is reduced to $Z_2 \times Z_2$. Like Equation (2.10) this model is exactly solvable after going to the Majorana basis. The phase

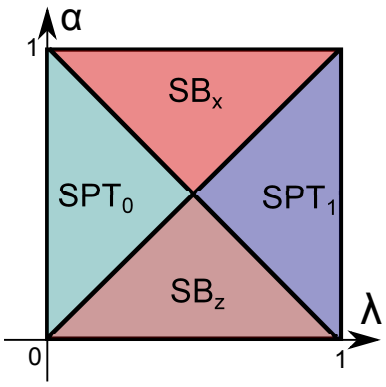

Figure 2.5: (Color online) The phase diagram of Equation (2.12). The regions SPT_0, SPT_1 correspond to trivial and non-trivial SPTs, respectively. SB_x, SB_z correspond to spontaneous symmetry-breaking with $\langle\sigma_x\rangle$ and $\langle\sigma_x\rangle$ non-zero, respectively. The solid black lines mark continuous phase transitions. Along the $\lambda = 1/2$ line there is either spontaneous symmetry breaking or gapless excitation.

diagram is shown in Fig. 2.5. Under S_{-1}, λ transforms into $1-\lambda$ while α remains fixed. Along the line $(\lambda, \alpha) = (1/2, \alpha)$ the Z_2^T symmetry is respected. Under that condition the system is either gapless or exhibits spontaneous symmetry breaking as predicted by the theorem in Appendix A.5. Interestingly the critical point between SPT_0 and SPT_1 at $(\lambda, \alpha) = (1/2, 1/2)$ is also the transition point between two symmetry breaking phases. Moreover because the residual symmetry groups respected by the two symmetry breaking phases do not have subgroup relationship, the transition is an example of Landau forbidden transitions. Hence in this example the critical point between two SPTs is simultaneously the critical point of a Landau forbidden transition. Along the line (λ, α_0) where $\alpha_0 \neq 1/2$, the two SPT phases are intervened by a spontaneous symmetry breaking phase hence realizing the third scenario discussed in section 2.4.

Continuous phase transition in models with only $Z_2 \times Z_2^T$ symmetry (except at the critical point)

In the last subsection after the removal of the extra $U(1)$ symmetry the transition between the SPTs is no longer direct. As a result one might wonder whether the continuous critical point is realizable without enlarging the symmetry group.

This motivates us to look for models with *only* $Z_2 \times Z_2$ symmetry (except at the critical point) while exhibiting a continuous direct transition between two inequivalent SPTs. The more general model is still exactly solvable at two limits, namely $\lambda = 0$ and 1 where it gives two inequivalent SPTs. However unlike the simple example the model is not solvable for intermediate values of λ. In the following we perform density matrix renormalization group

(DMRG)[22] calculation to study the intermediate λ including the critical point.

The Hamiltonian we consider is given by (as shown in Fig.2.6(a))

$$\begin{aligned} H &= \sum_{i=1}^{N/6} [\lambda(S^x_{6i-5}S^x_{6i-4} + bS^y_{6i-5}S^y_{6i-4}) \\ &\quad +(1-\lambda)(S^y_{6i-4}S^y_{6i-3} + bS^z_{6i-4}S^z_{6i-3})] \\ &\quad +\lambda(S^z_{6i-3}S^z_{6i-2} + bS^x_{6i-3}S^x_{6i-2}) \\ &\quad +(1-\lambda)(S^x_{6i-2}S^x_{6i-1} + bS^y_{6i-2}S^y_{6i-1}) \\ &\quad +\lambda(S^y_{6i-1}S^y_{6i} + bS^z_{6i-1}S^z_{6i}) \\ &\quad +(1-\lambda)(S^z_{6i}S^z_{6i+1} + bS^x_{6i}S^x_{6i+1})], \end{aligned} \tag{2.13}$$

where S^x, S^y and S^z are spin 1/2 operators, λ and b are coupling parameters. The unit cell of Equation (2.13) contain 6 sites each possessing a spin 1/2. These six spin 1/2s in each unit cell add to form integer total spins. The $Z_2 \times Z_2$ group is generated by π rotation around any two, e.g., x, y, spin axes for all spins.

When $b = 1$, the Z_2^T transformation S_{-1} flips $\lambda \leftrightarrow 1-\lambda$, is defined by $S_{-1} = U_1U_2K$, where

$$\begin{aligned} U_1 &= \prod_{i=1}^{N/3} U_{XY,3i-2}U_{YZ,3i-1}U_{ZX,3i} \\ U_{AB,j} &= \left(\frac{1+\sigma^A_j}{2} + \frac{1-\sigma^A_j}{2}\sigma^B_{j+1}\right)\left(\frac{1+i\sigma^B_{j+1}}{\sqrt{2}}\right) \\ U_2 &= \prod_{i=1}^{N/3} \sigma^y_{3i-2}\sigma^z_{3i-1}\sigma^x_{3i} \end{aligned}$$

It may be checked that $S^2_{-1} = 1$ and it commutes with global $Z_2 \times Z_2$ rotations generated by $\prod_i \sigma^x_i$ and $\prod_i \sigma^z_i$.

In the limits $\lambda = 0$ and $\lambda = 1$ the system consists of decoupled dimers. It is simple to check that for $b > 0$ the ground state of each dimer is a spin singlet, and the bulk energy spectrum is gapped under periodic boundary condition. Under the open boundary condition there are gapless edge modes for $\lambda = 0$, while there is no edge state for $\lambda = 1$. So, these two limits are topologically distinct and we expect a phase transition between them for some intermediate value of λ.

The phase diagram of Equation (2.13) is illustrated by Fig.2.6(b). We find that for $\lambda < 0.5$ the system is in a non-trivial SPT phase. This is manifested by the fact that under periodic boundary condition (PBC) there is an energy gap while in open boundary condition (OBC) it is gapless (see Fig. 2.7). In contrast for $\lambda > 0.5$ the system is in a trivial SPT phase. This is manifested by the existence of an energy gap in both periodic and

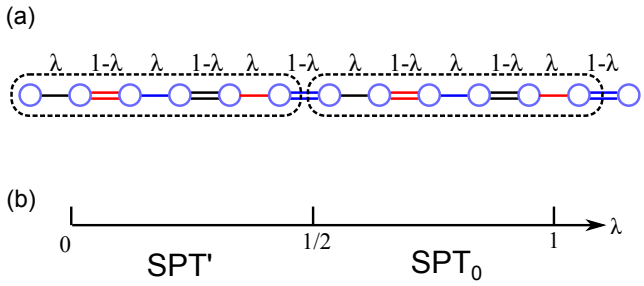

Figure 2.6: (Color online) (a) Sketch of the interactions in the model Hamiltonian of Equation (2.13). Three different types of the interaction are represented by three different colored bonds. For example, black bonds denote $(S_i^x S_{i+1}^x + bS_i^y S_{i+1}^y)$, red bonds denote $(S_i^y S_{i+1}^y + bS_i^z S_{i+1}^z)$, and blue bonds denote $(S_i^z S_{i+1}^z + bS_i^x S_{i+1}^x)$. λ and $(1-\lambda)$ are the strength of the interactions. It is represented by single bonds and double bonds respectively. A dashed box denotes one unit cell. (b) Phase diagram for Equation (2.13). The $\lambda < 1/2$ region is occupied by a non-trivial SPT, while the $\lambda > 1/2$ region is occupied by trivial SPT.

open boundary conditions (Fig. 2.7(a,b)). Interestingly, there is indeed a continuous phase transition between the two SPT phases occurring at $\lambda = 1/2$ for all $b > 0$ we have studied. Numerics indicate the central charge of this critical point is $c = 1$ (see Fig. 2.8)), the same as that of the solvable case. Since $c = 1$ allows continuous varying critical exponents, we go on to extract the energy gap exponent α,

$$\Delta \sim |\lambda - 1/2|^{\alpha}, \tag{2.14}$$

for different values of b. The results are shown in Fig. 2.9. For more details of the DMRG calculation see Appendix B.7.

The above example proves that scenario (1) in Fig. 2.1 is indeed attainable for phase transition between SPTs protected by *only* $Z_2 \times Z_2$.

Phase transition between Z_2 symmetric SPTs in 2D

In this subsection we follow the framework set in previous sections to construct a lattice model describing phase transition between by 2D Z_2-symmetric SPTs. (According to the cohomology group classfication there are two inequivalent Z_2-symmetric SPTs in 2D).

Consider a triangular lattice. For each site i there is an Ising variable $\sigma_i := \sigma_i^z = \pm 1$. The trivial SPT hamiltonian is

$$H_0 = -\sum_i \sigma_i^x. \tag{2.15}$$

After some math the non-trivial SPT Hamiltonian can be reduced to

$$H_1 = \sum_i \left[\Pi_{\langle j,k\rangle} i^{\left(\frac{1-\sigma_j\sigma_k}{2}\right)}\right] \left[i^{(\sum_{j=1}^6 \sigma_j)}\right] \sigma_i^x. \tag{2.16}$$

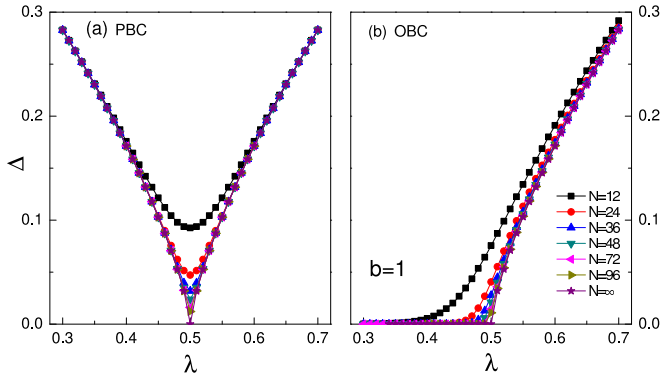

Figure 2.7: (Color online) Excitation gap Δ as a function of λ at $b = 1$ (Equation (2.13)). (a) For periodic boundary condition, Δ is finite except the critical point ($\lambda = 1/2$). (b) For open boundary condition, $\Delta = 0$ for $\lambda < 1/2$ due to the presence of gapless edge modes in the non-trivial SPT phase. For $\lambda > 1/2$ the SPT is trivial hence $\Delta > 0$.

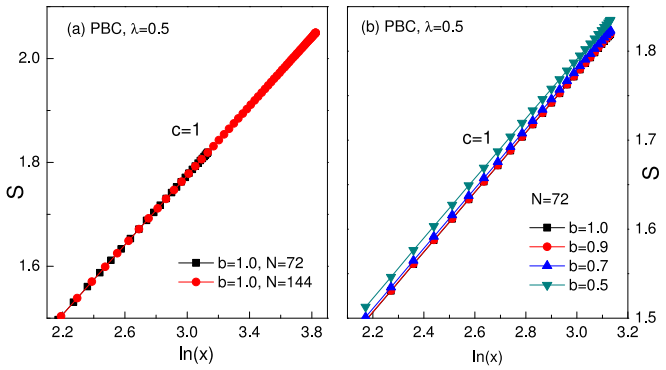

Figure 2.8: (Color online) Entanglement entropy scaling for Equation (2.13) at $\lambda = 1/2$ and various values of b. Panel (a) shows the result for periodic $N = 72$ and 144 site chains for $b = 1$. Panel (b) shows the result for a periodic $N = 72$ site chain for various b values. The fit to $S(x) = \frac{c}{3}\ln(x) + const$ extrapolates to a central charge $c = 1$. Here $x = \frac{N}{\pi}\sin(\frac{\pi l}{N})$, and l is the subsystem length.

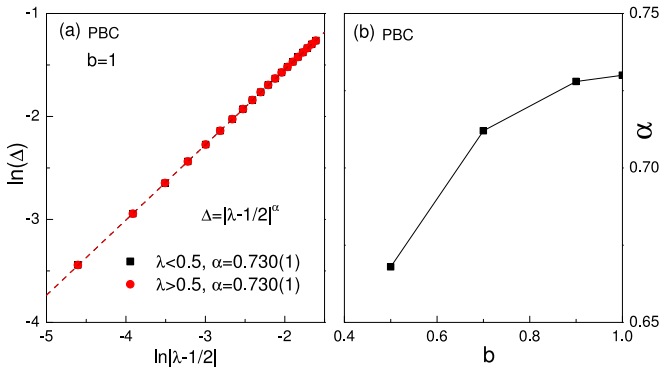

Figure 2.9: (Color online) (a) $\ln \Delta$ versus $\ln|\lambda - 1/2|$ for $b = 1$ under periodic boundary condition. Linearity implies $\Delta \sim |\lambda - 1/2|^{\alpha}$. (b) Gap exponent α for several values of b Note that while $c = 1$ for all these b values the gap exponent varies.

Here $\sigma_1, \ldots, \sigma_6$ designate the Ising variables on the six neighbours of i as depicted in Fig. A.1(b), and the product $\Pi_{<j,k>}$ is performed over the six links connecting site i and its six nearest neighbors. The non-trivial element of the Z_2^T transformation is given by

$$S_{-1} = \prod_{\Delta} (-1)^{(\frac{1-\sigma_1}{2})(\frac{1+\sigma_2}{2})(\frac{1-\sigma_3}{2})} K \tag{2.17}$$

where $\sigma_1, \sigma_2, \sigma_3$ are the ordered vertices on each triangle Δ. Again $S_{-1} H_0 S_{-1}^{-1} = H_1$ and $S_{-1} H_1 S_{-1}^{-1} = H_0$.

We construct the hamiltonian to study the phase transition in exactly the same way as in Equation (2.4). $H(\lambda)$ is solvable for $\lambda = 0$ and 1. For intermediate value of λ it was suggested[12] numerically that there is a first-order transition at $\lambda = 1/2$. Thus scenario (2) in Fig. 2.1 is realized.

Phase transition between trivial and non-trivial phases of 1D integer spin chain

For integer spin chains $G = SO(3)$. The SPT phases are classified by Z_2, i.e., there is a trivial and a non-trivial SPT. For spin-1 chain, the non-trivial phase is also known as the Haldane[23] or the AKLT phase[24]. The continuum field theory describing the trivial and non-trivial phases is given by the following $O(3)$-non linear sigma model(NLSM) with $\Theta = 0$ and 2π, respectively

$$S = \frac{1}{2g} \int dxdt (\partial_\mu \hat{n})^2 + i \frac{\Theta}{4\pi} \int dxdt \; \hat{n} \cdot \partial_x \hat{n} \times \partial_t \hat{n}. \tag{2.18}$$

Here $\hat{n}$ is a 3-component unit vector. The critical point between the trivial and the non-trivial SPT is described by the $SU(2)_1$ Wess-Zumino-Witten(WZW) theory in 1+1 dimensions[25]:

$$\begin{aligned} S &= \frac{1}{2\tilde{g}} \int dxdt (\partial_\mu \hat{\Omega})^2 \\ &+ \frac{i}{\pi} \int dxdt \int_0^1 du\ \epsilon^{abcd} \Omega_a \partial_x \Omega_b \partial_t \Omega_c \partial_u \Omega_d. \end{aligned} \tag{2.19}$$

Here $\hat{\Omega} \in S^3$ is a 4-component unit vector, and u is an extension paramater such that $\hat{\Omega}(u = 0, x, t) = (0, 0, 0, 1)$, and $\hat{\Omega}(u = 1, x, t)$ is the physical $\hat{\Omega}(x, t)$. If the extra term $-\lambda \int dxdt \Omega_4(x, t)$ is added to Equation (2.19), upon renormalization the low energy and long wavelength effective action flows to Equation (2.18) with $\Theta = 0$ or 2π depending on the sign of λ. Hence λ tunes the phase transition between the two SPTs. The emergent Z_2^T symmetry discussed in this chapter corresponds to reversing the sign of Ω_4 followed by complex conjugation[26]. This symmetry is broken by the term $-\lambda \int dxdt \Omega_4(x, t)$. When Z_2^T and $SO(3)$(which rotates Ω_1,Ω_2,Ω_3) symmetries are preserved, the 1+1d boundary will either be gapless or degenerate[27].

2.6 Conclusion and Discussion

In this chapter we focus on the quantum phase transition between trivial and non-trivial symmetry protected topological states (SPTs) in d dimensions. We prove that if the non-trivial SPT satisfies the "non double stacking condition" (see the theorem) all phase transition scenarios between them are captured by the boundary of a d+1 dimensional $G \times Z_2^T$ symmetric SPT in the presence of Z_2^T symmetry breaking field. This result proves that at the critical point of the topological phase transition in question there is always emergent non-local symmetry. Moreover the symmetry operation associated with this non-local symmetry transforms one SPT phase into another. In addition our results provide explicit recipes for constructing d- dimensional lattice hamiltonians describing different phase transition scenarios. As a byproduct we prove the conjecture made in Ref.[6], namely, the gapless excitations at the critical point between a trivial and non-trivial SPT consists of delocalized (or dynamically percolated) gapless boundary states of the non-trivial SPT. For future studies, we shall study how to describe phase transition between SPTs which do not satisfy the non double staking condition. We will also consider the ramification of the interesting recent works which show the boundary of a three dimensional SPT can exhibit topological order[14;15;16;17;18;19;20;21]. We ask what is the implication of this possibility on transitions between SPTs. Of course we are also interested in generating simple lattice models, especially in $d > 1$, describing the phase transition between SPTs, and in generalizing the approach here to the fermionic case.

Chapter 3

Which CFTs can describe phase transitions between bosonic SPTs?

3.1 Introduction and the outline

Having understood quanlitatively that the physical picture that the critical point at a topological phase transition is a proliferated boundary states, we would like to make a more quantitative statement about the nature of the critical point. Our goal is to understand the difference (if any) between the traditional Landau type and this new kind of "topological" phase transitions.

Because the Landau-type phase transitions are triggered by the fluctuations of bosonic order parameters over space-time, to minimize the obvious difference we focus on the phase transitions between bosonic SPT phases[5]. Hence we do not address the phase transition between fermionic topological insulators or superconductors[3;4]. Moreover, to make everything as concrete as possible we shall focus on one space dimension and to topological phase transitions which have dynamical exponent equal to one (hence can be described by conformal field theories (CFTs)).

We spend most of the space describing the study of a specific class of such phase transitions – the phase transition between bosonic SPTs protected by $Z_n \times Z_n$. Here we combine a blend of analytic and numerical methods to arrive at a rather complete picture for such critical points. From studying these phase transitions we observe an interesting fact, namely whenever the transition is *direct* (i.e., when there are no intervening phases) and *continuous* the central charge (c) of the CFT is always greater or equal to one. Near the end of the chapter, we obtain a constraint on the central charge for CFTs describing bosonic SPT phase transitions: namely, $c \geq 1$. Therefore, none of the best known "minimal models[28]" can be the CFT for bosonic SPT phase transitions!

According to the group cohomology classification[5], in one space dimension, the group $Z_n \times Z_n$ protects n different topological classes of SPTs. If we "stack" a pair of SPTs (which

can belong to either the same or different topological class) on top of each other and turn on all symmetry allowed interactions, a new SPT will emerge to describe the combined system. An abelian (cohomology) group $H^2(Z_n \times Z_n, U(1)) = Z_n$ (here the superscript "2" refers to the space-time dimension) classifies the SPT phases and describes the stacking operation. Here each topological class is represented by an element (i.e., $0, ..., n-1$) of $H^2(Z_n \times Z_n, U(1)) = Z_n$ and the "stacking" operation is isomorphic to the $mod(n)$ addition of these elements.

To understand the phase transitions between different classes of SPTs it is sufficient to focus on the transition between the trivial state (which corresponds to the "0" of Z_n) and the non-trivial SPT corresponding to the "1" of Z_n. The transition between phases correspond to other adjacent elements of Z_n, e.g., $(m, m+1)$, will be in the same universality class as that between $(0, 1)$. Transitions between "non-adjacent" topological classes will generically spit into successive transitions between adjacent classes.

There are 11 sections in the main text. In these sections we restrain from heavy mathematics, i.e., we simply state the main results and provide simple arguments. There are 6 appendices where mathematical details can be found. The outline of this chapter is the follows. In section 3.2 we present the exactly solvable fixed point hamiltonians for the trivial and non-trivial $Z_n \times Z_n$ protected SPT phases. In section 3.3 we present a hamiltonian that interpolates between the fixed point hamiltonians in section 3.2. A single parameter tunes this hamiltonian through the SPT phase transition. Section 3.4 introduces a non-local transformation that maps the hamiltonian in section 3.3 to that of two n-state clock models with spatially twisted boundary condition and Hilbert space constraint. In particular, at criticality, we show that the partition function of the transformed hamiltonian corresponds to an "orbifolded" $Z_n \times Z_n$ clock model. In section 3.5 we discuss the effects of orbifolding on the phases of the clock model and show the results are consistent with what one expect for the SPT phases. Section 3.6 gives the phase diagram of the hamiltonian given in section 3.3. In section 3.7 we show that from the point of view of the orbifolded clock model the SPT transition corresponds to a Landau forbidden transition. In section 3.8 we present the conformal field theories for the SPT phase transitions discussed up to that point. Section 3.9 presents our numerical density matrix renormalization group results. We compare these results with the prediction of section 3.8. Section 3.10 presents the argument that the central charge of the CFTs that describe SPT phase transitions must be greater or equal to one. Finally, section 3.11 is the conclusion.

In appendix B.1, we provide a brief review of the key ingredients of the $1+1$D group cohomology, namely, the notions of cocycles and projective representations. After that, we show how to use cocycles to construct solvable fixed point SPT hamiltonians. Appendix B.2 summarizes the non-local transformation that maps the hamiltonian in section 3.3 of the main text to that of two n-state clock models with spatially twisted boundary condition and Hilbert space constraint. In appendix B.3 we show that the partition function associated

with the hamiltonian in appendix B.2 (and section 3.3 of the main text) corresponds to that of "orbifolded" $Z_n \times Z_n$ clock model. Appendices B.4,B.5,B.6 present the modular invariant partition functions of the orbifold $Z_2 \times Z_2$, $Z_3 \times Z_3$ and $Z_4 \times Z_4$ clock models, respectively. In these appendices, we examine the primary scaling operator content of the modular invariant conformal field theory. In addition, we study the symmetry transformation properties of various Verma modules and the scaling dimension of primary scaling operators, particularly that of the gap opening operator. Appendix B.7 summarizes the details of the density matrix renormalization group calculation. Finally, in appendix B.8 we briefly review the symmetry of the minimal model conformal field theories.

3.2 Exactly solvable "fixed point" Hamiltonians for the SPTs

Each SPT phase is characterized by an exactly solvable "fixed point" Hamiltonian. In appendix B.1 we briefly review the construction of these Hamiltonians using the "cocycles" associated with the cohomology group[29;30]. For the case relevant to our discussion the following lattice Hamiltonians can be derived[31] so that its ground state belong to the "0" and "1" topological classes of $H^2(Z_n \times Z_n, U(1)) = Z_n$

$$\begin{aligned} H_0 &= -\sum_{i=1}^{N}(M_{2i-1} + M_{2i} + h.c.) \\ H_1 &= -\sum_{i=1}^{N}(R^\dagger_{2i-2} M_{2i-1} R_{2i} + R_{2i-1} M_{2i} R^\dagger_{2i+1} + h.c.) \end{aligned} \tag{3.1}$$

These Hamiltonians are defined on 1D rings consisting of N sites. For each site labeled by i the local Hilbert space is spanned by $|g_{2i-1}, g_{2i}\rangle := |g_{2i-1}\rangle \otimes |g_{2i}\rangle$ where $(g_{2i-1}, g_{2i}) \in Z_n \times Z_n$ with $g_{2i-1}, g_{2i} = 0, 1, ..., n-1$. The total Hilbert space is the tensor product of the local Hilbert space for each site. For the convenience of future discussions from now on we shall refer to $(2i-1, 2i)$ as defining a "cell", and call $|g_{2i-1}\rangle$ and $|g_{2i}\rangle$ as basis states defined for "site" $2i-1$ and $2i$. The operators M_j and R_j in Equation (3.1) are defined by

$$\begin{aligned} &M_j|g_j\rangle := |g_j + 1\rangle \mod n, \text{ and} \\ &R_j|g_j\rangle := \eta_n^{g_j}|g_j\rangle \text{ where } \eta_n = e^{i2\pi/n}. \end{aligned} \tag{3.2}$$

From Equation (3.2) we deduce the following commutation relation between M and R:

$$\begin{aligned} R_j R_k &= R_k R_j \\ M_j M_k &= M_k M_j \\ R_j M_k &= \eta_n^{\delta_{jk}} M_k R_j. \end{aligned} \tag{3.3}$$

Due to this commutation relation, it can be checked that the $n \times n$ matrices associated with M_j and R_j form a *projective* representation of the $Z_n \times Z_n$ group multiplication law (see appendix B.1 for the definition of projective representations). Finally periodic boundary condition is imposed on Equation (3.1) which requires

$$g_{2N+1} = g_1, \quad \text{and} \quad g_{2N+2} = g_2. \tag{3.4}$$

Under these definitions Equation (3.1) is invariant under the global $Z_n \times Z_n$ group generated by

$$\prod_{i=1}^{N} M_{2i-1} \quad \text{and} \quad \prod_{i=1}^{N} M_{2i}. \tag{3.5}$$

The form of Hamiltonians given in Equation (3.1) is quite asymmetric between M and R. We can make it more symmetric by performing the following unitary transformation on the local cell basis as follow

$$|g_{2i-1}, g_{2i}\rangle \to U|g_{2i-1}, g_{2i}\rangle = \frac{1}{\sqrt{n}} \sum_{g'_{2i}=0}^{n-1} \eta_n^{(g_{2i-1}-g_{2i})g'_{2i}} |g_{2i-1}, g'_{2i}\rangle.$$

This results in the following transformations of the operators in Equation (3.1)

$$\begin{aligned} U^\dagger M_{2i-1} U &= M_{2i-1} M_{2i} \\ U^\dagger M_{2i} U &= R^\dagger_{2i-1} R_{2i} \\ U^\dagger R_{2i-1} U &= R_{2i-1} \\ U^\dagger R_{2i} U &= M^\dagger_{2i}. \end{aligned} \tag{3.6}$$

It is straightforward to show that after these transformations the new operators obey the same commutation relation as Equation (3.3). Moreover, it can also be shown that R obeys the same boundary condition, namely, $R_{2N+1} = R_1$ and $R_{2N+2} = R_2$. In addition, it is also straightforward to show that under Equation (3.6) the generators of the $Z_n \times Z_n$ group become

$$U^\dagger \left(\prod_{i=1}^{N} M_{2i-1} \right) U = \prod_{j=1}^{2N} M_j \quad \text{and} \quad U^\dagger \left(\prod_{i=1}^{N} M_{2i} \right) U = \prod_{j=1}^{2N} R_j^{(-1)^j}. \tag{3.7}$$

Thus alternating "site" carries the projective and anti-projective representation of $Z_n \times Z_n$.

Under Equation (3.6) the Hamiltonian H_0 and H_1 become

$$\begin{aligned} H_0 &= -\sum_{i=1}^{N} (M_{2i-1} M_{2i} + R_{2i-1} R^\dagger_{2i} + h.c.) \\ H_1 &= -\sum_{i=1}^{N} (M_{2i} M_{2i+1} + R_{2i} R^\dagger_{2i+1} + h.c.) \end{aligned} \tag{3.8}$$

These Hamiltonians are pictorially depicted in Fig. 3.1(a,b). Note that while H_0 (Fig. 3.1(a)) couples sites within the same cell, H_1 couples sites belong to adjacent cells (Fig. 3.1(b)). Because both H_0 and H_1 consist of decoupled pairs of sites (the coupling terms associated with different pairs commute with one another) they can be exactly diagonalized. The result shows a unique ground state with a fully gapped spectrum for both H_0 and H_1. Using Equation (3.7) it is simple to show that the ground states are invariant under $Z_n \times Z_n$.

The fact that H_0 and H_1 describe inequivalent SPTs can be inferred by forming an interface of H_0 and H_1 as shown in Fig. 3.1(c). A decoupled site (red) emerges. Localizing on this site there are degenerate gapless excitations carrying a projective representation of the $Z_n \times Z_n$ [32]. The fact that gapless excitations must exist at the interface between the ground states of H_0 and H_1 attests to that fact that these states belong to inequivalent topological classes of $H^2(Z_n \times Z_n, U(1)) = Z_n$.

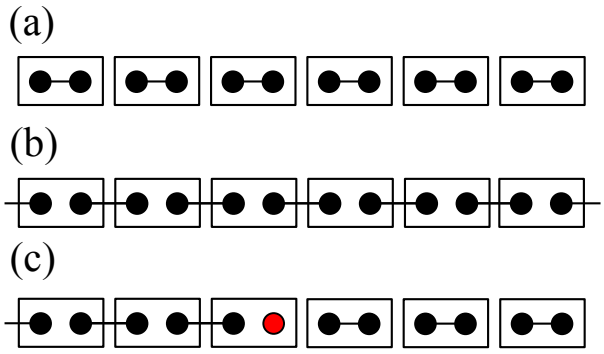

Figure 3.1: (Color online) (a) H_0 couples states associated with the same cell (each cell is represented by the rectangular box). (b) H_1 couples states associated with adjacent cells. Each pair of black dots in a rectangle represents the sites in each cell. They carry states $|g_{2i-1}\rangle$ and $|g_{2i}\rangle$ which form a projective representation of $Z_n \times Z_n$. Each link represents a coupling term in the Hamiltonian (3.8). (c) Hamiltonian describing the interface between the two SPTs each being the ground state of H_0 and H_1. It is seen that there is a leftover site (highlighted in red) transforming projectively at the interface.

3.3 An interpolating Hamiltonian describing the phase transition between $Z_n \times Z_n$ SPTs

To study the phase transition between the ground state of H_0 and the ground state of H_1 we construct the following Hamiltonian which interpolates between H_0 and H_1 as follows

$$\begin{aligned} &H_{01}(\lambda) = (1-\lambda)H_0 + \lambda H_1 \\ &= -(1-\lambda)\sum_{i=1}^{N}(M_{2i-1}M_{2i} + R_{2i-1}R_{2i}^\dagger) - \lambda\sum_{i=1}^{N}(M_{2i}M_{2i+1} + R_{2i}R_{2i+1}^\dagger) \\ &+h.c. \end{aligned} \tag{3.9}$$

With both H_0 and H_1 present the Hamiltonian given in Equation (3.9) is no longer easily solvable. However, in the following, we present analytic results showing (1) for $2 \leq n \leq 4$ the phase transition occurs at $\lambda = 1/2$, (2) the central charge, the conformal field theory and its associated primary scaling operators at the phase transitions. For $n \geq 5$ there is a gapless phase centered around $\lambda = 1/2$ hence the phase transition is not direct. Moreover for the interesting case of $n = 3$ we will present the numerical density matrix renormalization group results which confirm our analytic solution.

3.4 Mapping to "orbifold" $Z_n \times Z_n$ clock chains

In appendix B.2 we show that Equation (3.9) can be mapped onto a $Z_n \times Z_n$ clock model with spatially twisted boundary condition and a Hilbert space constraint. In appendix B.3 we further show that these amount to "orbifolding",

The mapping is reminiscent of the duality transformation in a single Z_n clock model. The mapping is achieved via the following transformations:

$$\begin{aligned} &R_{j-1}^\dagger R_j = \widetilde{M}_j \quad \text{for} \quad j = 2...2N, \quad R_{2N}^\dagger R_1 = \widetilde{M}_1 \\ &\text{and} \quad M_j = \widetilde{R}_j^\dagger \widetilde{R}_{j+1} \text{ for all } j. \end{aligned} \tag{3.10}$$

After the mapping, the Hamiltonian in Equation (3.9) is transformed to

$$\begin{aligned} &H_{01}(\lambda) = H_{\text{even}}(\lambda) + H_{\text{odd}}(\lambda) \\ &H_{\text{even}}(\lambda) = -\sum_{i=1}^{N}\left[(1-\lambda)\widetilde{M}_{2i} + \lambda\widetilde{R}_{2i}^\dagger\widetilde{R}_{2i+2}\right] + h.c. \\ &H_{\text{odd}}(\lambda) = -\sum_{i=1}^{N}\left[\lambda\widetilde{M}_{2i-1} + (1-\lambda)\widetilde{R}_{2i-1}^\dagger\widetilde{R}_{2i+1}\right] + h.c. \end{aligned} \tag{3.11}$$

Here $\widetilde{M}$ and $\widetilde{R}$ obey the same commutation relations as M and R in Equation (3.3).

Equation (3.11) is the quantum Hamiltonian for two Z_n clock models[33], one defined on the even and one on the odd sites, respectively. However, generated by the mapping, Equation (3.11) is supplemented with a twisted spatial boundary condition and a constraint:

$$\text{Boundary condition: } \widetilde{R}_{2N+1} := \widetilde{B}\widetilde{R}_1 \text{ and } \widetilde{R}_{2N+2} := \widetilde{B}\widetilde{R}_2, \tag{3.12}$$

$$\text{Constraint: } \prod_{i=1}^{2N} \widetilde{M}_i = 1. \tag{3.13}$$

Here $\widetilde{B}$ is an operator that commutes with all the $\widetilde{R}$s and $\widetilde{M}$s. The eigenvalues of $\widetilde{B}$ are $\tilde{b} = 1, \eta_n, ..., \eta_n^{n-1}$ (recall that $\eta_n = e^{i2\pi/n}$). In terms of the transformed variables, the generators of the original $Z_n \times Z_n$ group are given by

$$\widetilde{B} \text{ and } \prod_{j=1}^{N} \widetilde{M}_{2j}. \tag{3.14}$$

The spatially twisted boundary condition Equation (3.12) and the constraint Equation (3.13) (which turns into a time direction boundary condition twist in the path integral representation of the partition function) execute the "orbifolding" (see later).

By swapping the even and odd chains Equation (3.11) exhibit the

$$\lambda \leftrightarrow (1 - \lambda)$$

duality. This implies the self-dual point at $\lambda = 1/2$ is special. In particular, *if* there is a single critical point as a function of λ, it must occur at $\lambda = 1/2$. Incidentally, if we put aside Equation (3.12) and Equation (3.13), $\lambda = 1/2$ is where each of the clock chains in Equation (3.11) becomes critical.

As we will show later the effects of Equation (3.12) and Equation (3.13) (i.e., orbifold) is to change the primary scaling operator content of the critical CFT from that of the direct product of two Z_n clock models. However they do not jeopardize the criticality, nor do they change the central charge. We shall return to these more technical points later. At the meantime let's first study the effects of Equation (3.12) and Equation (3.13) on the phases.

3.5 The effect of orbifold on the phases

Knowing the behavior of the single Z_n clock chain, Equation (3.11) suggests for $\lambda < 1/2$ the odd-site chain will spontaneously break the Z_n symmetry while the even chain remains disordered. The ground state will lie in the $\tilde{b}$ (the eigenvalue of $\tilde{B}$) $= 1$ sector on account

of the twisted boundary condition. For $\lambda > 1/2$ the behaviors of the even and odd chains exchange, and the ground state remains in the $\tilde{b} = 1$ sector. On the surface, such symmetry breaking should lead to ground state degeneracy which is inconsistent with the fact that both SPTs (for $\lambda < 1/2$ and $\lambda > 1/2$) should have unique groundstate.

This paradox is resolved if we take into account of the constraint in Equation (3.13). For simplicity let's look at the limiting cases. For $\lambda = 0$ the ground state of Equation (3.11) is

$$|g, g, ..., g\rangle_{\text{odd}} \otimes |p, p, ..., p\rangle_{\text{even}} \otimes |\tilde{b} = 1\rangle \tag{3.15}$$

where $g = 0, ..., n-1$. Here the "paramagnet state" $|p\rangle$ for each site is defined as

$$|p\rangle := \frac{1}{\sqrt{n}} \left(|0\rangle + |1\rangle + ... + |n-1\rangle\right). \tag{3.16}$$

As expected, such ground state is n-fold degenerate and it does not satisfy the constraint of Equation (3.13). However, if we form the symmetric superposition of the odd-site symmetry breaking states

$$\left(\frac{1}{\sqrt{n}} \sum_{g=0}^{n-1} |g, g, ..., g\rangle_{\text{odd}}\right) \otimes |p, p, ..., p\rangle_{\text{even}} \otimes |\tilde{b} = 1\rangle \tag{3.17}$$

the constraint is satisfied and the state is non-degenerate. Obviously, Equation (3.17) is invariant under the $Z_n \times Z_n$ generated by Equation (3.14). Although Equation (3.17) is non-degenerate, the two-point correlation function $\langle \widetilde{R}_{2j+1} \widetilde{R}^{\dagger}_{2k+1} \rangle$ still shows long-range order. Almost exactly the same arguments, with odd and even switched, apply to the $\lambda = 1$ limit. The only difference is instead of observing $|p, p, ..., p\rangle_{\text{even}}$ being invariant under the action of $\prod_{j=1}^{N} \widetilde{M}_{2j}$ we need to observe that $\left(\frac{1}{\sqrt{n}} \sum_{g=0}^{n-1} |g, g, ..., g\rangle_{\text{even}}\right)$ is invariant. As λ deviates from the limiting values, so long as it does not cross any phase transition the above argument should remain qualitatively unchanged. In this way we understand the effects of Equation (3.12) and Equation (3.13) on the phases.

3.6 The phase diagram

Since upon orbifolding the phases of the decoupled $Z_n \times Z_n$ clock models seamlessly evolve into the SPT phases we shall construct that phase diagram using what's know about the phase structure of the clock model. It is known that a single Z_n clock chain shows an order-disorder phase transition at a single critical point for $n \leq 4$, while there is an intermediate gapless phase for $n \geq 5$ we conclude the phase diagram is shown in Fig. 3.2(a,b). Since our goal is to study the continuous phase transition between SPTs we focus on $n \leq 4$.

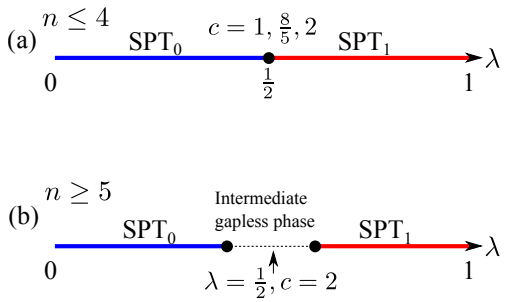

Figure 3.2: (Color online) Phase diagram for (3.9), which linearly interpolates between the fixed point hamiltonians of $Z_n \times Z_n$ SPT phases. Red and blue mark the non-trivial and trivial SPTs respectively. (a) For $n \leq 4$, a second-order transition occurs between the two SPT phases, and the central charge takes values of 1, $\frac{8}{5}$ and 2 for $n = 2, 3, 4$, respectively. (b) For $n \geq 5$, a gapless phase intervenes between the two SPT phases. The entire gapless phase has central charge $c = 2$.

3.7 SPT transitions as "Landau-forbidden" phase transitions

According to Landau's rule, transitions between phases whose symmetry groups do not have subgroup relationship should generically be first order. *Continuous* phase transitions between such phases are regarded as "Landau forbidden" in the literature.

As discussed earlier, in terms of the orbifolded $Z_n \times Z_n$ clock chains, the two phases on either side of the SPT phase transition correspond to the breaking of the Z_n symmetry in one of the clock chain but not the other. In the following, we elaborate on this statement.

For $\lambda < 1/2$ although the ground state in Equation (3.17) is non-degenerate, the two-point correlation function $\langle \widetilde{R}_{2j+1} \widetilde{R}^{\dagger}_{2k+1} \rangle$ shows long-range order. When the odd and even chains are switched the same argument applies to the $\lambda > 1/2$ limit. If we define

$$Q_{\text{even}} = \prod_{j=1}^{N} \widetilde{M}_{2j} \text{ and } Q_{\text{odd}} = \prod_{j=1}^{N} \widetilde{M}_{2j-1} \tag{3.18}$$

it is easy to show that equations (3.11), (3.12) and (3.13) commute with them, hence the $Z'_n \times Z'_n$ group they generate are also the symmetry of the problem. However it is important not to confuse $Z'_n \times Z'_n$ with the original $Z_n \times Z_n$ group (which is generated by Equation (3.14)).

Symmetry group	Central charge
$Z_2 \times Z_2$	1
$Z_3 \times Z_3$	8/5
$Z_4 \times Z_4$	2

Table 3.1: The central charges associated with the critical point of the $Z_n \times Z_n$ SPT phase transitions for $n = 2, 3, 4$.

With respect to the $Z'_n \times Z'_n$ symmetry the two phases (realized for $\lambda < 1/2$ and $\lambda > 1/2$) breaks two different Z'_n factors, hence the symmetry groups of the two phases have no subgroup relationship, thus if a continuous phase transition between them exists it is a Landau forbidden transition. In fact, it is the original $Z_n \times Z_n$ symmetry that "fine tunes" the system to realize such non-generic continuous phase transition.

3.8 The CFT at the SPT phase transition for $n = 2, 3, 4$

It is known that the central charge of the CFT describing the criticality of a *single* Z_n clock chain is $c = 1/2, 4/5, 1$ for $n = 2, 3, 4$. Thus the central charge of the CFT describing the simultaneous criticality of two decoupled Z_n clock chains should be $c = 1, 8/5, 2$ for $Z_2 \times Z_2$, $Z_3 \times Z_3$ and $Z_4 \times Z_4$. This is summarized in Table 3.1.

Of course, we do not have two decoupled clock chains. The spatial boundary condition twist (Equation (3.12)) and the constraint (Equation (3.13)), namely the orbifolding, couples the two chains together. The purpose of this section is to address the effects of orbifolding on the criticality of the two decoupled chains.

Let's start with the conformal field theory of a single Z_n clock chain. The partition function of such CFT on a torus is given by

$$Z(q) = \sum_{a,b} \chi_a(q) M_{ab} \bar{\chi}_b(\bar{q}). \tag{3.19}$$

Here the indices a, b labels the Verma modules. Each Verma module is spanned by states associated with a primary scaling operator and its descendants through the operator-state correspondence. Each Verma module carries an irreducible representation of the conformal group. The parameter q in Equation (3.19) is equal to $e^{2\pi i \tau}$, where τ is the modular parameter of the spacetime torus (see Fig. B.2). $\chi_a(q)$ and $\bar{\chi}_b(\bar{q})$ are, respectively, the partition function associated with the holomorphic Verma module a and antiholomorphic Verma module b. The matrix M_{ab} has non-negative integer entries.

The partition function of the two decoupled Z_n clock chains that are simultaneously critical is given by

$$Z(q) \times Z(q) = \sum_{a,b,c,d} \chi_a(q)\chi_c(q)(M_{ab}M_{cd})\bar{\chi}_b(\bar{q})\bar{\chi}_d(\bar{q}). \tag{3.20}$$

It turns out that the effect of orbifold is to change

$$M_{ab}M_{cd} \to N_{(a,c);(b,d)} \tag{3.21}$$

($N_{(a,c);(b,d)}$ is a different non-negative integer matrix) so that

$$Z_{\text{orbifold}}(q) = \sum_{a,b,c,d} \chi_a(q)\chi_c(q)N_{(a,c);(b,d)}\bar{\chi}_b(\bar{q})\bar{\chi}_d(\bar{q}). \tag{3.22}$$

In particular, $N_{(1,1);(1,1)} = 1$, i.e., the tensor product of the ground state of the two clock chains is also the ground state of the orbifold model. Moreover, for those $N_{(a,c);(b,d)} > 0$ the scaling dimension of the holomorphic primary operator (a, c) is $h_{(a,c)} = h_a + h_c$ and that of the antiholomorphic primary operator (b, d) is $\bar{h}_{(b,d)} = \bar{h}_b + \bar{h}_d$. The fact that the ground state of the orbifold model remain the same as the tensor product of the ground states of the decoupled clock chains implies

$$c_{\text{orbifold}} = c_{\text{decoupled clock chains}}. \tag{3.23}$$

The latter identity can be seen from the fact that the central charge can be computed from the entanglement entropy, which is a pure ground state property. Thus, after the orbifold, the system is still conformal invariant (i.e. quantum critical) and the central charge is unaffected by the orbifold. This argument allows us to conclude that the central charge of the $Z_n \times Z_n$ ($n = 2, 3, 4$) SPT phase transition is indeed given in table 3.1.

In appendices B.4,B.5 and B.6 we go through the details of obtaining the modular invariant partition function for the orbifold $Z_n \times Z_n$ ($n = 2, 3, 4$) clock chains. We examine the primary scaling operator content of the modular invariant conformal field theory. In addition, we study the symmetry transformation properties of various Verma modules and the scaling dimension of primary scaling operators, in particular, that of the gap opening operator. In Table 3.2 we list the first few most relevant scaling operators and their scaling dimension for $n = 2, 3, 4$. Entries in blue are invariant under $Z_n \times Z_n$.

3.9 Numerical DMRG study of the $Z_3 \times Z_3$ SPT phase transition

In this section, we report the results of numerical density matrix renormalization group calculation for the $Z_3 \times Z_3$ transition. The purpose is to check our analytic predictions in the

Table 3.2: (Color online) The first few primary operators, with the lowest scaling dimensions $(h+\bar{h})$, of the orbifold $Z_n \times Z_n$ CFT for $n = 2, 3, 4$. The momentum quantum numbers of these operators are equal to $(h-\bar{h}) \times 2\pi/N$. Entries in blue are invariant under $Z_n \times Z_n$.

n	$h+\bar{h}$	$h-\bar{h}$	Multiplicity
2	0	0	1
	1/4	0	2
	1	0	2+2
	1	± 1	2
	5/4	± 1	8
3	0	0	1
	4/15	0	4
	4/5	0	2
	14/15	0	4
	17/15	± 1	8
	19/15	± 1	16
	4/3	0	4
	22/15	0	8
	8/5	0	1
4	0	0	1
	1/4	0	4
	1/2	0	2
	5/8	0	4
	1	0	2
	9/8	± 1	8
	5/4	0	20
	5/4	± 1	12
	5/4	± 1	16
	3/2	± 1	8
	13/8	0	4
	13/8	± 1	16

last section. The details of the numerical calculations are presented in appendix B.7.

First, we demonstrate that $\lambda = 1/2$ in Equation (3.9) is indeed a critical point. Let's look at the second derivative of the ground state energy with respect to λ for both open and periodic boundary conditions with different system sizes (Fig. 3.3). The results clearly suggest a second-order phase transition at $\lambda_c = 1/2$ where the second order energy derivative diverges.

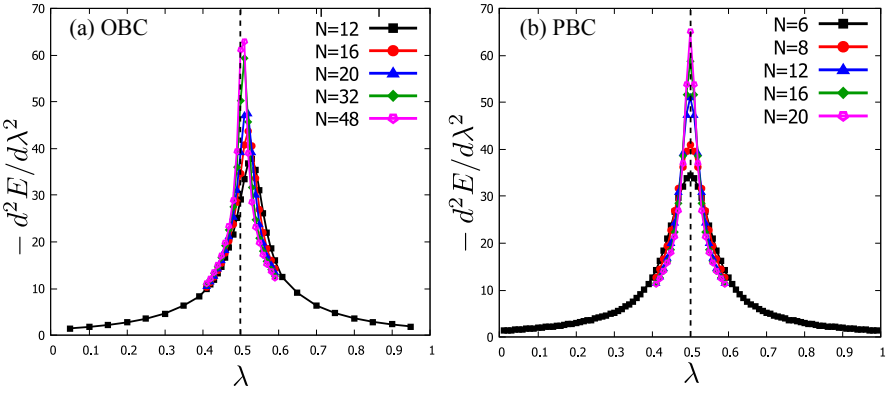

Figure 3.3: (Color online) Second order derivative of the ground state energy with respect to λ for both open (OBC) and periodic (PBC) boundary conditions and different values of N. The results suggest a divergent $-\mathrm{d}^2E/\mathrm{d}\lambda^2$ as $\lambda \to 1/2$ and $N \to \infty$. Hence it signifies a second-order phase transition. As expected, we note that finite size effect is significantly stronger for open as compared to periodic boundary condition.

Next, we compute the central charge at $\lambda = 1/2$. This is done by computing the entanglement entropy, which is calculated from the reduced density matrix by tracing out the degrees of freedom associated with $N - l$ sites in a system with total N sites. In Fig. 3.4 we plot the von Neumann entanglement entropy S against $x = \frac{N}{\pi}\sin(\pi l/N)$ where l is the number of sites that are not traced out. CFT predicts $S = \frac{c}{6}\ln(x) + const$ for the open boundary condition and $S = \frac{c}{3}\ln(x) + const$ for periodic boundary condition[34]. From the numerics we find $c = 1.599(9)$. This result is in nearly perfect agreement with our analytic prediction $c = 8/5$.

In addition to the above results, we have also calculated the gap as a function of λ. In fitting the result to

$$\Delta \sim |\lambda - \lambda_c|^{\alpha} \tag{3.24}$$

we estimate the gap exponent to be $\alpha = 0.855(1)$ for open boundary condition (Fig. 3.5) and $\alpha = 0.847(1)$ for periodic boundary condition (Fig. 3.6). These results are in good agreement with the analytic prediction $\alpha = 5/6$ (see appendix B.5).

3.10 The constraint on the central charge

After an examination of Table I it is easy to notice that $c \geq 1$ for all $Z_n \times Z_n$ SPT phase transitions. Moreover, for all the cases we know, including SPTs protected by continuous

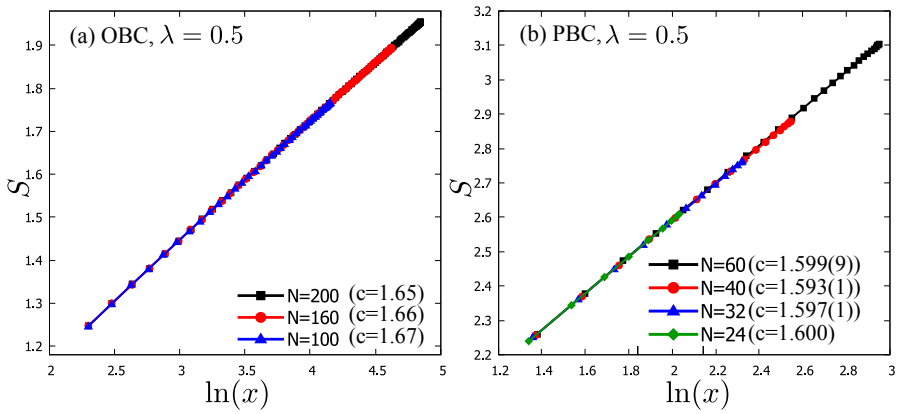

Figure 3.4: (Color online) Entanglement entropy is plotted against $\ln(x)$, (where $x = \frac{N}{\pi}\sin(\pi l/N)$ and l is the size of the subsystem which is not traced over) for a few different total system length N. (a) For open boundary condition (OBC) the maximum N is 200. (b) For periodic boundary condition (PBC) the maximum N is 60. Combining these results we estimate $c = 1.62 \pm 0.03$.

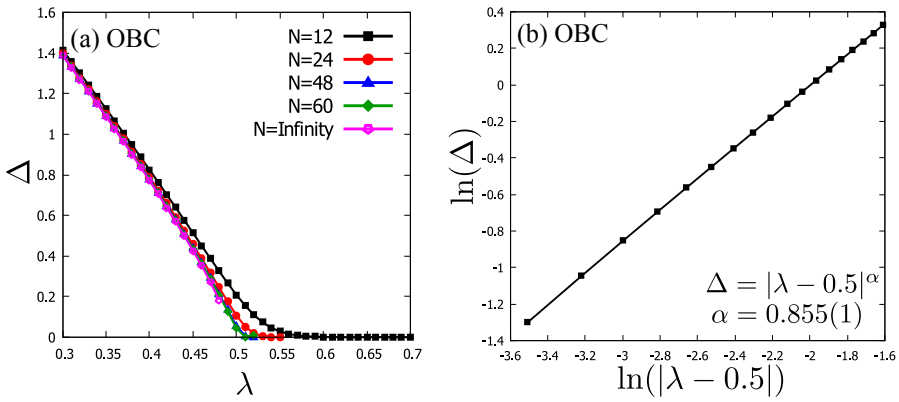

Figure 3.5: (Color online) The energy gap Δ as a function of λ for open boundary condition. (a) The gap closes for $\lambda > 1/2$ because of the presence of edge modes associated with the non-trivial SPT. (b) The gap exponent is extracted by approaching λ_c from the $\lambda < 1/2$ side. The value of α is found to be 0.855(1).

groups, all 1D ($z = 1$) bosonic SPT phase transitions are described by CFT with $c \geq 1$. In the following present an argument that *the CFT of all 1D bosonic SPT phase transition must have* $c \geq 1$.

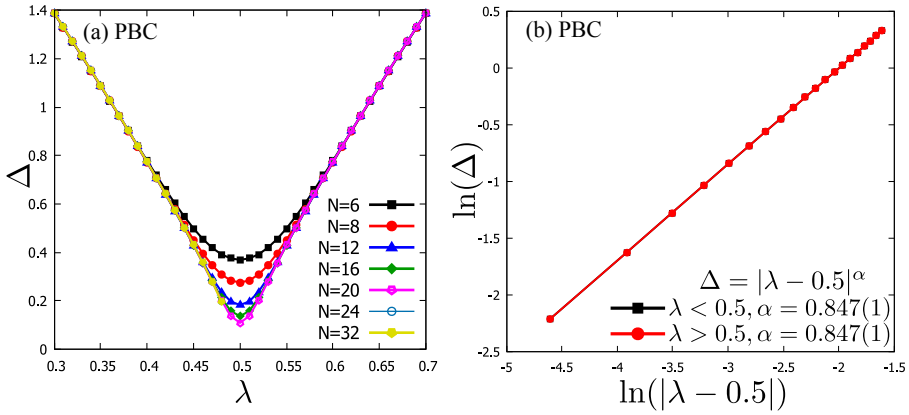

Figure 3.6: (Color online) The energy gap Δ as a function of λ for periodic boundary condition. (a) Now there is a non-zero gap for both $\lambda > 1/2$ and $\lambda < 1/2$. (b) The gap exponent is extracted and found to be $\alpha = 0.847(1)$.

We proceed by showing that the $c < 1$ CFTs cannot be the critical theory for bosonic SPT transitions. The 1D CFTs that are *unitary* and have $c < 1$ are the so-called minimal models. In appendix B.8 we summarize the argument in Ref.[35] where it is shown that the *maximum* on-site internal symmetry ("on-site" symmetries are the ones consisting of product over local transformations that act on the local, e.g. site or group of sites, Hilbert space.) that these CFTs can possess are either Z_2 or S_3. Since the critical point of the bosonic SPT phase transitions must possess the same on-site symmetry as the phases on either side, and neither Z_2 nor S_3 can protect non-trivial bosonic SPTs in 1D (i.e., $H^2(Z_2, U(1)) = H^2(S_3, U(1)) = Z_1$), we conclude that the CFTs corresponding to the minimal model cannot possibly be the critical theory for bosonic SPT phase transitions. This leaves the $c \geq 1$ CFTs the only possible candidates as the critical theory for bosonic SPT phase transitions.

3.11 Conclusions

In this chapter, we present an analytic theory for the phase transition between symmetry protected topological states protected by the $Z_n \times Z_n$ symmetry group. We have shown that for $2 \leq n \leq 4$ a direct, continuous, topological phase transition exists. In contrast for $n \geq 5$ the transition from the topological trivial to non-trivial SPTs is intervened by an intermediate gapless phase. Our theory predicts that for $n = 2, 3, 4$ the central charge of the CFT describing the SPT phase transitions are $c = 1, 8/5$ and 2, respectively. We perform explicit numerical density matrix renormalization group calculations for the interesting case of $n = 3$ to confirm our analytic predictions.

We expect treatment analogous to what's outlined in this chapter can be generalized to the phase transitions between SPTs protected by symmetry group $Z_{n_1} \times Z_{n_2} \times ....$ In addition, we provide the proof for a conjectured put forward in a previous unpublished preprint [36] that the central charge of the CFTs describing bosonic SPT transitions must be greater or equal to 1. Thus all $c < 1$ CFTs cannot be the critical theory for bosonic phase transitions. However, we have not yet answered the question "are all CFTs with $c \geq 1$ capable of describing topological phase transitions."

Of course upon non-local transformation the $c < 1$ minimal models can be viewed as the critical theory for *parafermion* SPT transitions. Indeed, the $c = 1/2$ Ising conformal field theory describes the critical Majorana chain. The $c = 4/5$ three-state Potts model CFT describes the critical point of Z_3 parafermion chain. We suspect that the parafermion models escape the classification of either the K theory or the cohomology group because of its non-local commutation relation.

In space dimension greater than one, we do not know a model which *definitively* exhibits a continuous phase transition between bosonic SPTs. This is due partly to the likelihood of spontaneous breaking of the discrete protection symmetry when $d \geq 2$. In addition, even if the continuous phase transition exists, it is more difficult to study these phase transitions, even numerically. However a "holograpic theory" was developed for phase transitions between SPT phases which satisfy the "no double-stacking constraint" [30]. That theory predicts the critical point should exhibit "delocalized boundary excitations" of the non-trivial SPT, which are extended "string" or "membrane" like objects with gapless excitation residing on them. We expect this kind of critical point to be fundamentally different from the Landau-like critical point. Clearly many future studies are warranted for the understanding of these interesting phase transitions.

A

Appendix for Chapter 2

A.1 The ground state wavefunction and exactly solvable bulk Hamiltonians from cocycles

We review the construction of bulk hamiltonians and wavefunctions from cocycles[5;29]. In this section we focus on lattices residing on *closed* d-dimensional manifolds. A n-cochain with symmetry $\mathcal{G}$ is a map $c_n(g_0, g_1, \ldots, g_n) : \mathcal{G}^{n+1} \to U(1)$ which satisfies $c_n(gg_0, \ldots, gg_n) = c_n(g_0, \ldots, g_n)^\epsilon$, where $\epsilon = -1$ if g is antiunitary and $+1$ for unitary g. A n-cocycle ν_n is a n-cochain which also satisfies the cocycle condition: $\partial\nu_n = 1$, where

$$(\partial\nu_n)(g_0, \ldots, g_{n+1}) = \prod_{i=0}^{n+1} \nu_n(g_0, \ldots, \hat{g}_i, \ldots, g_{n+1})^{(-1)^i}. \tag{A.1}$$

(Here $\hat{g}_i$ means g_i is deleted). If $\nu_n = \partial c_{n-1}$ for some $n-1$-cochain c_{n-1} we say it is a coboundary. It may be checked that a coboundary also satisfies the cocycle condition, namely $\partial^2 c_{n-1} = 1$. Two cocycles related by the *multiplication* of a coboundary are viewed as equivalent.

$$\nu_n \sim \nu_n' = \nu_n \cdot \partial c_{n-1}. \tag{A.2}$$

The equivalence classes of n-cocycles form $H^n(\mathcal{G}, U(1))$ – the n^{th} cohomology group. In Ref.[5] it is proposed that bosonic $\mathcal{G}$-symmetric SPTs in d space dimensions are "classified" by $H^{d+1}(\mathcal{G}, U(1))$, i.e., each SPT is in one to one correspondence with a equivalence class of $d+1$-cocycles.

Suppose we have a triangulated d-dimensional *closed manifold* where vertices are the lattice sites. The Hilbert space for each site is spanned by $\{|g_i\rangle\}$ where $g_i \in \mathcal{G}$, and the total Hilbert space is spanned by the tensor product of the site basis, i.e., $|\{g_i\}\rangle = \prod_i |g_i\rangle$. The "fixed point" form (which is a particular representative) of the SPT states associated with

the equivalence class of ν_{d+1} is equal to (Ref.[5] Section IX)

$$|\psi_0\rangle = \sum_{\{g_i\}} \phi(\{g_i\}) \; |\{g_i\}\rangle$$
$$\phi(\{g_i\}) = \prod_{\Delta} [\nu_{d+1}(e, \{g_i\}_\Delta)]^{\sigma(\Delta)}. \tag{A.3}$$

Here e is the identity element, $\prod_\Delta$ is the product over the simplices of the triangulation, $\{g_i\}_\Delta$ is a shorthand for the $d+1$ elements of $\mathcal{G}$ assigned to the ordered vertices of simplex Δ, and $\sigma(\Delta) = \pm 1$ depending on the orientation of the simplex.

The Hamiltonian whose exact ground state is Equation (A.3) is

$$H = -J \sum_i B_i, \tag{A.4}$$

where $J > 0$. The operator B_i only affect the state on site i and

$$\langle \{g'_k\} | B_i | \{g_k\} \rangle = \left(\prod_{k \neq i} \delta_{g'_k, g_k} \right) \frac{\phi(\{g'_k\})}{\phi(\{g_k\})}. \tag{A.5}$$

From Eqs A.3, A.4 and A.5 it is straightforward to show B_i is a projection operator, $\mathrm{Tr}(B_i) = 1$ and $B_i|\psi_0\rangle = |\psi_0\rangle$. In addition using the cocycle condition it can be shown that $[B_i, B_j] = 0 \; \forall \; i, j$. So $|\psi_0\rangle$ is the unique gapped groundstate of H. In addition using the cocycle condition $\phi(g_1, ..., g'_i, ...g_N)/\phi(g_1, ..., g_i, ...g_N)$ can be shown to depend on the g's in the neighborhood of site i, hence the hamiltonian is local. Examples for 1D and 2D are given below.

In 1D $\phi(\{g'_i\})/\phi(\{g_i\})$ can be reduced via the cocycle condition into (Fig. A.1 (a)):

$$\frac{\nu_2(g_{i-1}, g_i, g'_i)}{\nu_2(g_i, g'_i, g_{i+1})}$$

In 2D, suppose we have a triangular lattice, each site has six neighbors 1,...,6. In this case $\phi(\{g'_i\})/\phi(\{g_i\})$ involves the g's on six tetrahedrons (Fig. A.1 (b)):

$$\frac{\nu_3(g_3, g_4, g_i, g'_i)\nu_3(g_4, g_i, g'_i, g_5)\nu_3(g_i, g'_i, g_5, g_6)}{\nu_3(g_3, g_2, g_i, g'_i)\nu_3(g_2, g_i, g'_i, g_1)\nu_3(g_i, g'_i, g_1, g_6)}$$

A.2 Boundary basis and their symmetry transformations

In this section we consider lattices on *open* d+1-dimensional manifolds. In general, a ground-state wavefunction on an open manifold is defined subject to fixed boundary site configurations. Then the wavefunction is given by (A.3) summed over all bulk site configurations

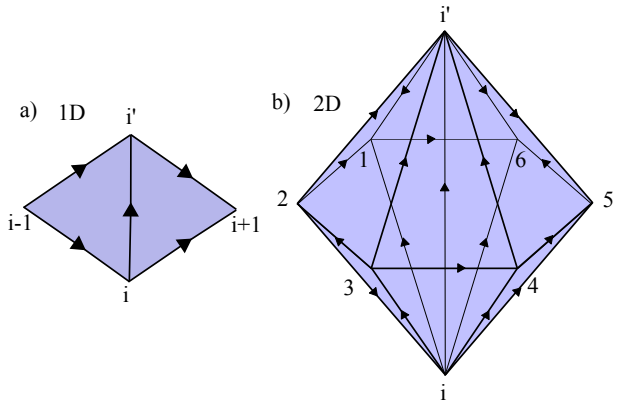

Figure A.1: (Color online) The construction of the exactly solvable bulk SPT hamiltonians from cocycles. B_i updates g_i to g_i'. a) For d=1 the phase $\langle\{g_i'\}|B_i|\{g_i\}\rangle$ involves the cocycles associated with two triangles. b) For d=2 the phase $\langle\{g_i'\}|B_i|\{g_i\}\rangle$ involves the cocycles associated with six tetrahedrons.

with the product carried out over simplices within the open manifold. In this way, if we have two open manifolds with the same boundary, we may take the direct product of their wavefunctions, identify their boundary sites and sum over all the possible boundary site configurations to recover the wavefunction on a closed manifold.

Let the vertices (sites) of the triangulated d-dimensional boundary be labeled by Greek index μ, and let there be a single "bulk site" labeled by "0". Together with the boundary sites they triangulate a $d+1$ dimensional open manifold. Our convention for vertex ordering is that all arrows point from 0 to μ (see Fig. A.2). Note that the assumption of having a single bulk site is purely for ease of manipulation, and does not put constraint on the topology of the manifold considered. It can be checked that our final result, the boundary transformation (A.11) remains unchanged even when more sites are added in the bulk.

The total Hilbert space is spanned by $\{|g_0, \{g_\mu\}\rangle\}$, and using Equation (A.3) (except the spatial dimension is $d+1$ rather than d) we write down the expression for the ground state subject to boundary conditions $\{g_\mu\}$ as discussed before

$$|\{g_\mu\}\rangle_B = \sum_{g_0} \prod_{\Delta} [\nu_{d+2}(e, g_0, \{g_\mu\}_\Delta)]^{\sigma(\Delta)} |g_0, \{g_\mu\}\rangle \tag{A.6}$$

Upon the action of the global symmetry group both the bulk and boundary states are transformed. Let S_g be the representation of the symmetry operation $g \in G$, we have

$$S_g |g_0, \{g_\mu\}\rangle = |g g_0, \{g g_\mu\}\rangle, \tag{A.7}$$

and

$$\begin{aligned} & S_g|\{g_\mu\}\rangle_B \\ &= \sum_{g_0}\prod_{\Delta}[\nu_{d+2}(e,g_0,\{g_\mu\}_\Delta)]^{\epsilon\sigma(\Delta)}|gg_0,\{gg_\mu\}\rangle \\ &= \sum_{g_0}\prod_{\Delta}[\nu_{d+2}(g,gg_0,\{gg_\mu\}_\Delta)]^{\sigma(\Delta)}|gg_0,\{gg_\mu\}\rangle \\ &= \sum_{g_0}\prod_{\Delta}[\nu_{d+2}(g,g_0,\{gg_\mu\}_\Delta)]^{\sigma(\Delta)}|g_0,\{gg_\mu\}\rangle \end{aligned} \tag{A.8}$$

Using the cocycle condition

$$\partial\nu_{d+2}(g,e,g_0,\{gg_\mu\}_\Delta)=1 \tag{A.9}$$

the last line of Equation (A.8) can be equated with

$$\begin{aligned} & \sum_{g_0}\prod_{\Delta}\Big\{\nu_{d+2}(g,e,\{gg_\mu\}_\Delta)^{\sigma(\Delta)} \\ & \times\left[\prod_{i=0}^{d}\nu_{d+2}(g,e,g_0,\{gg_\mu\}_{\Delta_i})^{(-1)^{i+1}\sigma(\Delta)}\right] \\ & \times\nu_{d+2}(e,g_0,\{gg_\mu\}_\Delta)^{\sigma(\Delta)}\Big\}|g_0,\{gg_\mu\}\rangle \\ &= \left[\prod_{\Delta}\nu_{d+2}(g,e,\{gg_\mu\}_\Delta)^{\sigma(\Delta)}\right]|\{gg_\mu\}\rangle_B \end{aligned} \tag{A.10}$$

In the second line Δ_i is the shorthand for the $d-1$-dimensional simplex which is a face of Δ obtained by removing its i^{th} vertex. In the last step we have used the fact that each $d-1$-dimensional simplex is the face to two opposite orientation d dimensional simplices Δ's, hence their contributions cancel in the product. Therefore

$$S_g|\{g_\mu\}\rangle_B=\left[\prod_{\Delta}\nu_{d+2}(g,e,\{gg_\mu\}_\Delta)^{\sigma(\Delta)}\right]|\{gg_\mu\}\rangle_B \tag{A.11}$$

For example when $d=0$, the edge of the 1D SPT are two points g_L, g_R. Under g they transform as

$$S_g|g_L,g_R\rangle_B=\frac{\nu_2(g,e,gg_R)}{\nu_2(g,e,gg_L)}|gg_L,gg_R\rangle_B \tag{A.12}$$

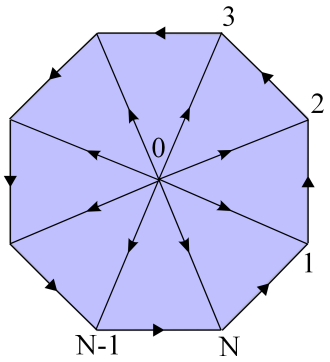

Figure A.2: (Color online) A single site 0 represents all the bulk degrees of freedom. We use a convention where arrows point from the bulk to the boundary.

The phase $\frac{\nu_2(g,e,gg_R)}{\nu_2(g,e,gg_L)}$ is interpreted as the edge states being carrying the projective representation of the symmetry group. For $d = 1$, the edge forms a ring labeled by $\mu = 1, \ldots N$. In this case

$$S_g|\{g_\mu\}\rangle_B = \prod_{\mu=1}^{N} \nu_3(g, e, gg_\mu, gg_{\mu+1})|\{gg_\mu\}\rangle_B \tag{A.13}$$

In Ref.[37], this transformation with $G = Z_2$ is an example of "Matrix Product Unitary Operator". They also show that if ν_3 is non-trivial, then the edge states made up of linear combination of $|\{g_\mu\}\rangle_B$ cannot be a short ranged entangled state.

A.3 Construction and the physical interpretation of $G \times Z_2^T$ SPTs

The special subset of cocycles

In this section we use a particular cocycle of $H^{d+2}(G \times Z_2^T, U(1))$ to construct the SPT in $d+1$ dimensions. This cocycle is given by

$$\begin{aligned} &\nu_{d+2}(\rho_0 g_0, \rho_1 g_1, \ldots, \rho_{d+2} g_{d+2}) \\ &= [\nu_{d+1}(g_1, \ldots, g_{d+2})]^{\frac{\rho_1 - \rho_0}{2}}, \end{aligned} \tag{A.14}$$

where $g_i \in G$, $\rho_i = \pm 1 \in Z_2^T$ and ν_{d+1} is a non-trivial cocycle of $H^{d+1}(G, U(1))$. It is straightforward to verify that ν_{d+2} indeed satisfies the cocycle condition.

The non double stacking condition on the ν_{d+1} in Equation (A.14)

In the following we prove that so long as ν_{d+1} can not be written as the square of another d+1 cocycle, say, $\tilde{\nu}_{d+1}$, the ν_{d+2} given by Equation (A.14) is a non-trivial cocycle of $H^{d+2}(G \times Z_2^T, U(1))$. More precisely we will show ν_{d+2} is trivial if and only if $\nu_{d+1} = (\tilde{\nu}_{d+1})^2 \cdot \partial c'_d$ for some (not necessarily trivial) G-symmetric cocycle $\tilde{\nu}_{d+1}$ and cochain c'_d. Thus the higher dimensional SPT constructed using Equation (A.14) is trivial if and only if ν_{d+1} is a double-stacking of another $\tilde{\nu}_{d+1}$.

To prove the "if" part, suppose $\nu_{d+1} = (\tilde{\nu}_{d+1})^2 \cdot \partial c'_d$. Substitute this into Equation (A.14) we obtain

$$\begin{aligned}&\nu_{d+2}(\rho_0 g_0, \rho_1 g_1, \ldots, \rho_{d+2}, g_{d+2}) \\ &= \tilde{\nu}_{d+1}(g_1, \ldots, g_{d+2})^{\rho_1 - \rho_0} \partial c'_d(g_1, \ldots, g_{d+2})^{\frac{\rho_1 - \rho_0}{2}}\end{aligned}$$

If we define

$$\begin{aligned}&c_{d+1}(\rho_1 g_1, \ldots, \rho_{d+2} g_{d+2}) \\ &:= \tilde{\nu}_{d+1}(g_1, \ldots, g_{d+2})^{\rho_1} c'_d(g_2, \ldots, g_{d+2})^{\frac{\rho_1 - \rho_2}{2}}\end{aligned}$$

Then using the cocycle condition on $\tilde{\nu}_{d+1}$, it may be checked that c_{d+1} is a $G \times Z_2^T$ cochain (hence is symmetric under the action of the group) and $\partial c_{d+1} = \nu_{d+2}$. So ν_{d+2} is a trivial cocycle.

To prove the "only if" part, suppose $\nu_{d+2} = \partial c_{d+1}$ for some $G \times Z_2^T$ cochain c_{d+1}, *i.e.*

$$\begin{aligned}&\nu_{d+2}(\rho_0 g_0, \ldots, \rho_{d+2} g_{d+2}) \\ &= \partial c_{d+1}(\rho_0 g_0, \ldots, \rho_{d+2} g_{d+2}) \\ &= c_{d+1}(\rho_1 g_1, \ldots, \rho_{d+2} g_{d+2}) \\ &\times \prod_{k=1}^{d+2} c_{d+1}^{(-1)^k}(\rho_0 g_0, \rho_1 g_1, \ldots, \widehat{\rho_k g_k}, \ldots, \rho_{d+2} g_{d+2})\end{aligned} \tag{A.15}$$

We will prove the c_{d+1} in question must satisfy

$$\begin{aligned}\partial c_{d+1}(g_0, \ldots, g_{d+2}) &= \partial c_{d+1}(\rho_0 g_0, \ldots, \rho_{d+2} g_{d+2})\Big|_{\rho_i \to 1 \ \forall i} \\ &= 1,\end{aligned} \tag{A.16}$$

i.e., upon setting all $\rho_i = 1$ the c_{d+1} in question is a G-cocycle. In addition we shall prove that if $\nu_{d+2} = \partial c_{d+1}$ the ν_{d+1} in Equation (A.14) must satisfy

$$\nu_{d+1} = c_{d+1}^2\Big|_{\rho_i \to 1 \ \forall i} \cdot \partial c'_d \tag{A.17}$$

for certain G-coboundary $\partial c'_d$. (Assuming (A.16) and (A.17) hold, then we choose $\tilde{\nu}_{d+1} = c_{d+1}\Big|_{\rho_i \to 1 \ \forall i}$ to complete the proof.)

To show (A.16), we first note that by taking $\rho_0 = \rho_1 = 1$ in Equation (A.14) and the second line of Equation (A.15), we have

$$1 = \partial c_{d+1}(g_0, g_1, \rho_2 g_2, \ldots, \rho_{d+2} g_{d+2}) \tag{A.18}$$

Then (A.16) follows directly by further setting $\rho_i = 1$ for all i.

To show (A.17), we let $\rho_0 = -1$, $\rho_i = 1$ for $i \neq 0$ and $g_0 = g_1$ in (A.14) and (A.15). Then

$$\begin{aligned}
&\nu_{d+1}(g_1, \ldots, g_{d+2}) \\
&= c_{d+1}(g_1, \ldots, g_{d+2}) \\
&\times \prod_{k=1}^{d+2} c_{d+1}^{(-1)^k}(-g_1, g_1, \ldots, \widehat{g_k}, \ldots, g_{d+2}) \\
&= c_{d+1} \cdot \gamma_1
\end{aligned} \tag{A.19}$$

where γ_l is defined as follows. For $l = 1, \ldots, d+2$,

$$\begin{aligned}
&\gamma_l(g_1, \ldots, g_{d+2}) \\
&:= \prod_{k=l}^{d+2} c_{d+1}^{(-1)^{l-k+1}}(-g_1, \ldots, -g_l, g_l, \ldots, \widehat{g_k}, \ldots, g_{d+2})
\end{aligned}$$

It turns out that $\gamma_l \sim \gamma_{l+1}$, for $l = 1, \ldots, d+1$. The proof is as follows

$$\begin{aligned}
\gamma_l &= c_{d+1}^{-1}(-g_1, \ldots, -g_l, g_{l+1}, \ldots, g_{d+2}) \\
&\times \prod_{k=l+1}^{d+2} c_{d+1}^{(-1)^{l-k+1}}(-g_1, \ldots, -g_l, g_l, \ldots, \widehat{g_k}, \ldots, g_{d+2}) \\
&= c_{d+1}^{-1}(-g_1, \ldots, -g_l, g_{l+1}, \ldots, g_{d+2}) \\
&\times \prod_{k=1}^{l} c_{d+1}^{(-1)^{l-k}}(-g_1, \ldots, \widehat{-g_k}, \ldots, -g_{l+1}, g_{l+1}, \ldots, g_{d+2}) \\
&\times \partial c_d'^{(-1)^{l+1}}(g_1, \ldots, g_{d+2}) \\
&\sim \prod_{k=1}^{l+1} c_{d+1}^{(-1)^{l-k}}(-g_1, \ldots, \widehat{-g_k}, \ldots, -g_{l+1}, g_{l+1}, \ldots, g_{d+2}) \\
&= \prod_{k=l+1}^{d+2} c_{d+1}^{(-1)^{l-k}}(-g_1, \ldots, -g_{l+1}, g_{l+1}, \ldots, \widehat{g_k}, \ldots, g_{d+2}) \\
&\times \partial c_{d+1}^{(-1)^{l+1}}(-g_1, \ldots, -g_{l+1}, g_{l+1}, \ldots, g_{d+2}) \\
&= \gamma_{l+1}
\end{aligned}$$

where c'_d is a G-symmetric cochain defined by:

$$c'_d(\tilde{g}_1, \ldots, \tilde{g}_{d+1}) := c_{d+1}(-\tilde{g}_1, \ldots, -\tilde{g}_l, \tilde{g}_l, \ldots, \tilde{g}_{d+1})$$

and in the last line we used

$$\partial c_{d+1}(-g_1, \ldots, -g_{l+1}, g_{l+1}, \ldots, g_{d+2}) = 1$$

which follows from (A.18). Thus

$$\begin{aligned} &\gamma_1 \sim \gamma_{d+2} \\ &= c_{d+1}^{-1}(-g_1, \ldots, -g_{d+2}) = c_{d+1}(g_1, \ldots, g_{d+2}). \end{aligned} \tag{A.20}$$

In the last line we have used the fact that c_{d+1} is a $G \times Z_2^T$ symmetric cochain. Substituting Equation (B.21) into (A.19), (A.17) is proven.

Interpreting the wavefunction as decorated domain walls

The wavefunction,

$$\psi(\{\rho_i g_i\}) = \prod_{\Delta} [\nu_{d+2}(e, \{\rho_i g_i\}_\Delta)]^{\sigma(\Delta)}, \tag{A.21}$$

constructed from (A.14) can be viewed as having time-reversal domain walls decorated with lower dimensional SPT.

To demonstrate this, we first derive an alternative form for the groundstate wavefunction discussed in Appendix A.1 in general. In this subsection it is assumed the system is a closed manifold. Suppose we have a $\mathcal{G}$ protected SPT in d-dimensions with associated cocycle $H^{d+1}(\mathcal{G}, U(1))$. Applying the cocycle condition $\partial \nu_{d+1}(e, \{g_i\}_\Delta, e) = 1$ on the ground state wavefunction (A.3), we obtain

$$\begin{aligned} \phi(\{g_i\}) &= \prod_{\Delta} [\nu_{d+1}(e, \{g_i\}_\Delta)]^{\sigma(\Delta)} \\ &= \prod_{\Delta} [\nu_{d+1}^{(-1)^{d+1}}(\{g_i\}_\Delta, e)]^{\sigma(\Delta)} \\ &\times \left(\prod_{j=0}^{d} \nu_{d+1}^{(-1)^{d+j}}(e, \{g_i\}_{\Delta_j}, e) \right)^{\sigma(\Delta)} \end{aligned} \tag{A.22}$$

The last factor is identity because each simplex Δ_i is the face to two simpices Δ whose contribtions cancel. Therefore we may alternatively write the groundstate wavefunction as

$$\phi(\{g_i\}) = \prod_{\Delta} \underbrace{[\nu_{d+1}(\{g_i\}_\Delta, e)]^{\sigma(\Delta)(-1)^{d+1}}}_{:=\phi_\Delta(\{g_i\})^{\sigma(\Delta)}} \tag{A.23}$$

Now with $\mathcal{G} = G \times Z_2^T$ and using Equation (A.21), we have

$$\begin{aligned}\psi(\{\rho_i g_i\}) &= \prod_{\Delta} [\nu_{d+1}(\{g_i\}_{\Delta_0}, e)]^{\frac{\rho_{1(\Delta)} - \rho_{0(\Delta)}}{2} \sigma(\Delta)(-1)^{d+2}} \\ &= \prod_{\Delta} [\phi_{\Delta_0}(\{g_i\})]^{\sigma(\Delta)(\frac{\rho_{1(\Delta)} - \rho_{0(\Delta)}}{2})} \end{aligned} \tag{A.24}$$

Here Δ_0 is the simplex Δ with the first of its ordered vertices deleted, and $0(\Delta), 1(\Delta)$ stand for the integers labeling the first and second vertices of the simplex Δ.

We now assume the system is on a $(n = d+1)$-dimensional torus T^n with a specific triangulation defined as follows. Let the vertices form a simple hypercubic structure on T^n. Each hypercube is identified with the region $\{(x_1, \ldots, x_n) : 1 \geq x_i \geq 0\}$. Now cut the hypercube into $n!$ simplices $\Delta(P)$, each labelled by a permutation P of $(1, \ldots, n)$. The simplex $\Delta(P)$ occupies the region with $1 \geq x_{P(1)} \geq \cdots \geq x_{P(n)} \geq 0$. There are 2^n vertices in the hypercube, each has all its coordinates equal to 0 or 1. For each vertex v, let $\mathcal{N}(v)$ be the number of 1's in its coordinate. The arrows defining the ordering of the vertices run from a vertex with a smaller $\mathcal{N}$ to a vertex with larger $\mathcal{N}$. In each simplex, there are exactly one vertex with any given $\mathcal{N}$, which ranges from 0 to n. One may check that such ordering of vertices is consistent on faces shared by two hypercubes. For every simplex, the lowest vertex is the origin v_0 with all coordinates zero. The second lowest vertex has exact one 1 in its coordinates, which we label v_k such that its j-th component is δ_{kj}. We also let F_k to be the face on the hypercube whose vertices gas all their k-th coordinate = 1. F_k is itself a $n-1$-dimensional hypercube. A domain wall between v_0 and v_k lives in the hyperplane equidistant from v_0 and v_k, which we associate to F_k via a translation of $(\frac{1}{2}, \ldots, \frac{1}{2})$.

The orientation of simplex $\sigma(\Delta(P))$ is given by $\mathrm{sgn}(P)$. This induces an orientation on the face $\Delta(P)_0$ given by $\sigma(\Delta(P)_0) = \sigma(\Delta(P))$. Now the interpretation of (A.24) is that, if there is a domain wall between v_0 and v_k, then on F_k there will live a lower dimensional SPT with ground state wavefunction given by Equation (A.23) or its complex conjugate depending on whether the orientation of F_k points from the $\rho = +1$ vertex to the $\rho = -1$ vertex or vice versa.

An example is given in Fig. A.3. for the case where $d+1 = 2$. Here the dashed red line is the actual domain wall and the solid red line is where the d dimensional G-symmetric SPT resides. The wavefunction with Z_2^T variables fixed as in Fig. A.3 is

$$\begin{aligned}\psi(\{g_i\}) &= \textstyle\prod_{j=0}^{3} [\nu_2(g_{3j}, g_{3(j+1)}, e)] \\ &= \textstyle\prod_{j=0}^{3} [\nu_2(e, g_{3j}, g_{3(j+1)})] \end{aligned}$$

Thus the SPT wavefunctions constructed using cocycles satisfying Equation (A.14) are indeed decorated domain wall wavefunctions.

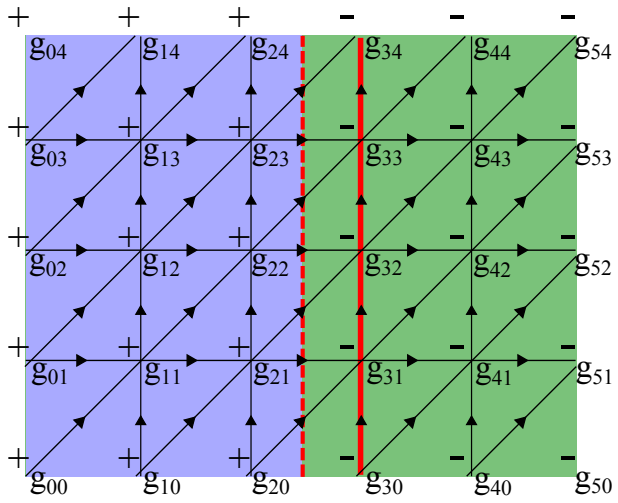

Figure A.3: (Color online) The wavefunction for the 2-D $G\times Z_2^T$-symmetric SPT (constructed from Equation (A.24)) with frozen configuration of the Z_2^T variable (denoted by + (blue) and - (green) on each site). Upon examining the dependence of such wavefunction on the unfrozen $g_i \in G$ on each site it is noted that the value is the same as the wavefunction of a 1-D G-symmetric SPT living on the solid red line, which is the domain wall (dashed red line) slightly displaced. Here the top and bottom edges are identified by the periodic boundary condition.

A.4 A $G \times Z_2^T$ invariant boundary subspace of the $d+1$ dimensional $G \times Z_2^T$ symmetric SPT that is transplantable to d dimension.

According to Equation (A.6) and Equation (A.14)

$$\begin{aligned}
|\rho_\mu g_\mu\rangle_B &= \sum_{\rho_0,g_0}\prod_{\Delta}[\nu_{d+2}(e,\rho_0 g_0,\{\rho_\mu g_\mu\}_\Delta)]^{\sigma(\Delta)}|\rho_0 g_0,\{\rho_\mu g_\mu\}\rangle \\
&= \sum_{\rho_0,g_0}\prod_{\Delta}\left\{[\nu_{d+1}(g_0,\{g_\mu\}_\Delta)]^{(\rho_0-1)/2}\right\}^{\sigma(\Delta)}|\rho_0 g_0,\{\rho_\mu g_\mu\}\rangle \\
&:= \sum_{\rho_0,g_0}\chi(\rho_0,g_0,\{g_\mu\})|\rho_0 g_0,\{\rho_\mu g_\mu\}\rangle
\end{aligned} \tag{A.25}$$

It is important to note

$$\chi(\rho_0,g_0,\{g_\mu\}) = \prod_{\Delta}\left\{[\nu_{d+1}(g_0,\{g_\mu\}_\Delta)]^{(\rho_0-1)/2}\right\}^{\sigma(\Delta)}$$

is independent of $\{\rho_\mu\}$. Therefore

$$|\{g_\mu\}\rangle_B := \frac{1}{(2|G|)^{1/2}} \frac{1}{2^{N/2}} \sum_{\{\rho_\mu\}} |\{\rho_\mu g_\mu\}\rangle_B, \tag{A.26}$$

where N is the number of boundary sites, form an orthonormal basis

$${}_B\langle\{g'_\mu\}|\{g_\mu\}\rangle_B = \prod_\mu \delta_{g'_\mu, g_\mu} \tag{A.27}$$

for the sub-Hilbert space spanned by

$$|\rho_0\rangle|g_0\rangle \prod_\mu \left(\frac{|\rho_\mu = +1\rangle + |\rho_\mu = -1\rangle}{\sqrt{2}} \right) |g_\mu\rangle$$

.

The subspace spanned by $\{|\{g_\mu\}\rangle_B\}$ is isomorphic to that spanned by the usual site basis $\{|\{g_\mu\}\rangle\}$ for G-symmetric SPTs in one dimension lower (d dimensions).

Since

$$\begin{aligned} &\nu_{d+2}(g, e, g\rho_2 g_2, \ldots, g\rho_{d+2} g_{d+2}) \\ &= \nu_{d+1}(e, gg_2, \ldots, gg_{d+2})^0 = 1 \end{aligned} \tag{A.28}$$

for $g \in G$, Equation (A.11) implies

$$S_g|\{g_\mu\}\rangle_B = |\{gg_\mu\}\rangle_B, \tag{A.29}$$

i.e., the boundary basis $\{|\{g_\mu\}\rangle_B\}$ transform in exactly the same way as the usual site basis under group G. However the $Z_2^T := \{+1, -1\}$ group transforms the boundary basis differently:

$$\begin{aligned} &S_{+1}|\{g_\mu\}\rangle_B = |\{g_\mu\}\rangle_B \\ &S_{-1}|\{g_\mu\}\rangle_B = \phi(\{g_\mu\})K|\{g_\mu\}\rangle_B, \quad \text{where} \\ &K = \text{complex conjugation and} \\ &\phi(\{g_\mu\}) = \prod_\Delta [\nu_{d+1}(e, \{g_\mu\}_\Delta)]^{\sigma(\Delta)}. \end{aligned} \tag{A.30}$$

Because ν_{d+1} is a pure phase

$$|\phi(\{g_\mu\})|^2 = 1 \tag{A.31}$$

Eqs.A.29 and A.30 are the basic transformation laws of the boundary basis.

Breaking the Z_2^T symmetry and the resulting G- symmetric SPT

Let's come back to the basis defined by Equation (A.26) and their transformation law, Equation (A.30), under $G \times Z_2^T$. Now consider the following G-symmetric boundary Hamiltonian

$$H_0 = -J \sum_{\mu} \sum_{g_\mu, g'_\mu} |\{g'_\mu\}\rangle_B \ {}_B\langle\{g_\mu\}|, \tag{A.32}$$

where $J > 0$ (and can be taken to very large values). Under the action of S_g

$$S_g H_0 S_g^{-1} = H_0 \tag{A.33}$$

while under the action of Z_2^T transformation it becomes

$$S_{-1} H_0 S_{-1}^{-1} = -J \sum_{\mu} \sum_{g_\mu, g'_\mu} \frac{\phi(\{g'_\mu\})}{\phi(\{g_\mu\})} \overline{|\{g'_\mu\}\rangle_B} \ \overline{{}_B\langle\{g_\mu\}|} := H_1 \tag{A.34}$$

where $\overline{|\ \rangle}_B$ stands for the complex conjugate. Equation (A.34) has exactly the form of(A.4), namely the Hamiltonian for the d-dimensional non-trivial (assuming ν_{d+1} is non-trivial and can not be expressed as the square of another $d+1$ cocycle) G-symmetric SPT. We note that H_1 is also invariant under the action of S_g, i.e.,

$$S_g H_1 S_g^{-1} = H_1. \tag{A.35}$$

Moreover due to Equation (A.31)

$$S_{-1} H_1 S_{-1}^{-1} = H_0. \tag{A.36}$$

The Hamiltonian $(H_0 + H_1)/2$ is symmetric under $G \times Z_2^T$, then based on the theorem of Appendix A.5 we conclude that either its spectrum is gapless or the $G \times Z_2^T$ symmetry is spontaneously broken. In the Appendix A.6 we give an example where $(H_0+H_1)/2$ is gapless.

A.5 A Lieb-Schultz-Mattis type theorem

In this section we present a proof stating that a d dimensional system with $G \times Z_2^T$ symmetry (where Z_2^T acts according to Equation (A.30) can not be gapped without degeneracy.

Proposition: Let $|\{g_i\}\rangle$ ($g_i \in G$) be the site basis of a d-dimensional lattice problem, and under the group G they transform as

$$S_g |\{g_i\}\rangle = |\{g g_i\}\rangle. \tag{A.37}$$

Let there be an additional group $Z_2^T = \{+1, -1\}$ which acts on the basis as

$$\begin{aligned} S_{+1}|\{g_i\}\rangle &= |\{g_i\}\rangle \\ S_{-1}|\{g_i\}\rangle &= \phi(\{g_i\})K|\{g_i\}\rangle. \end{aligned} \tag{A.38}$$

In addition we assume $\phi(\{g_i\})$ is the ground state wavefunction of a d-dimensional SPT constructed out of cocycle ν_{d+1} which can not be expressed as the square of another cocycle, i.e.,

$$\phi(\{g_i\}) = \prod_{\triangle} \nu_{d+1}(e, \{g_i\}_{\triangle})^{\sigma(\triangle)}. \tag{A.39}$$

Then it follows that it is impossible to find a local $G \times Z_2^T$-symmetric Hamiltonian which possesses an unique gapped ground state without breaking any symmetry.

The situation described above arises naturally at the boundary of a $d+1$ dimensional $G \times Z_2^T$ symmetric SPT. It can also be regarded as a d-dimensional problem with a G symmetry as well as a non-local Z_2^T symmetry. In either case the Z_2^T symmetry ensures the impossibility to have a totally symmetric gapped ground state without breaking any symmetry. This theorem is similar to the Lieb-Schultz-Mattis theorem [38;39;40] for translationally invariant spin 1/2 chain. The difference is the group $G \times Z_2^T$ can be discrete.

We prove the above proposition by reductio ad absurdum. Let's assume it is possible to find an unique $G \times Z_2^T$ symmetric ground state that is separated from all excited states by an energy gap. Let $|\psi\rangle$ be such a ground state:

$$|\psi\rangle = \sum_{\{g_i\}} \chi(\{g_i\})|\{g_i\}\rangle. \tag{A.40}$$

Since $|\psi\rangle$ is symmetric under G it must lie in certain equivalent class of a G-symmetric SPT having the fixed point form for χ

$$\chi(\{g_i\}) = \prod_{\triangle} \tilde{\nu}_{d+1}(e, \{g_i\}_{\triangle})^{\sigma(\triangle)}. \tag{A.41}$$

Since $|\psi\rangle$ is also invariant under S_{-1}

$$\begin{aligned} S_{-1}|\psi\rangle \quad &= \sum_{\{g_i\}} \chi^*(\{g_i\})\phi(\{g_i\})|\{g_i\}\rangle \\ &= |\psi\rangle = \sum_{\{g_i\}} \chi(\{g_i\})|\{g_i\}\rangle. \end{aligned} \tag{A.42}$$

Since $\{g_i\}$ is an orthonormal set we must have

$$\chi^*(\{g_i\})\phi(\{g_i\}) = \chi(\{g_i\}), \tag{A.43}$$

or

$$\phi(\{g_i\}) = \chi(\{g_i\})^2 = \prod_{\triangle} \left[\tilde{\nu}_{d+1}(e, \{g_i\}_{\triangle})^2\right]^{\sigma(\triangle)}. \tag{A.44}$$

This contradicts the assumption that ϕ in Equation (A.39) can not be constructed from the square of another cocycle. Therefore this d-dimensional problem must be either gapless or it spontaneously break the $G \times Z_2^T$ symmetry.

A.6 Gapless $Z_2 \times Z_2 \times Z_2^T$ symmetric hamiltonian in 1D and the transition between the $Z_2 \times Z_2$ SPTs

The $Z_2 \times Z_2$-symmetric SPTs in 1D is classified by $H^2(Z_2 \times Z_2, U(1)) = Z_2$. Let $g = (\sigma, \tau) \in Z_2 \times Z_2$ where $\sigma = \pm 1$, $\tau = \pm 1$. Following Appendix A.1, the bulk Hamiltonian is

$$H_1 = -J \sum_i B_i, \tag{A.45}$$

where

$$\langle \{g_k'\} | B_i | \{g_k\} \rangle = \frac{\nu_2(g_{i-1}, g_i, g_i')}{\nu_2(g_i, g_i', g_{i+1})} \prod_{k \neq i} \delta_{g_k', g_k}. \tag{A.46}$$

The trivial cocycle is $\nu_2 \equiv 1$, hence the Hamiltonian associated with the trivial SPT is

$$H_0 \ = -J \textstyle\sum_i (\sigma_i^x + \tau_i^x). \tag{A.47}$$

The nontrivial cocycle is

$$\nu_2(e, \sigma_1\tau_1, \sigma_2\tau_2) = \tau_1^{(1-\sigma_1\sigma_2)/2}, \tag{A.48}$$

hence

$$\begin{aligned} &\frac{\nu_2(g_{i-1}, g_i, g_i')}{\nu_2(g_i, g_i', g_{i+1})} \\ &= (\tau_{i-1}\tau_i)^{(\frac{1-\sigma_i\sigma_i'}{2})} (\tau_i\tau_i')^{(\frac{1-\sigma_i'\sigma_{i+1}}{2})} \\ &= \begin{cases} 1 & \text{if } (\sigma_i', \tau_i') = (\sigma_i, \tau_i) \\ \sigma_i\sigma_{i+1} & \text{if } (\sigma_i', \tau_i') = (\sigma_i, -\tau_i) \\ \tau_{i-1}\tau_i & \text{if } (\sigma_i', \tau_i') = (-\sigma_i, \tau_i) \\ \sigma_i\sigma_{i+1}\tau_{i-1}\tau_i & \text{if } (\sigma_i', \tau_i') = (-\sigma_i, -\tau_i) \end{cases} \end{aligned} \tag{A.49}$$

Therefore the Hamiltonian associated with the non-trivial SPT is

$$\begin{aligned} H_1 \quad &= -J\sum_i \Big[1+\tau^z_{i-1}\sigma^x_i\tau^z_i+\sigma^z_i\tau^x_i\sigma^z_{i+1} \\ &\quad +(\tau^z_{i-1}\sigma^x_i\tau^z_i)(\sigma^z_i\tau^x_i\sigma^z_{i+1})\Big]. \end{aligned} \tag{A.50}$$

Note that each term of the Hamiltonian commutes with all others. In fact because the fourth term is the product of the 2nd and 3rd terms we may drop the constant term and the fourth term without changing the ground state wavefunction or closing the gap. Thus H_0 and the simplified H_1 read

$$\begin{aligned} H_0 &= -J\sum_i(\sigma^x_i+\tau^x_i) \\ H_1 &= -J\sum_i(\tau^z_{i-1}\sigma^x_i\tau^z_i+\sigma^z_i\tau^x_i\sigma^z_{i+1}). \end{aligned} \tag{A.51}$$

Now enlarge the symmetry group to $Z_2\times Z_2\times Z_2^T$ and go through the steps in Appendix A.3 it is straightforward to show is given by

$$S_{-1}=\prod_i(\tau^z_i)^{(1-\sigma^z_i\sigma^z_{i+1})/2}\,K, \tag{A.52}$$

which transforms H_0 and H_1 into each another.

The critical Hamiltonian $(H_0+H_1)/2$ can be solved exactly by the Jordan-Wigner transformation

$$\begin{aligned} &\sigma^x_i=2n_{2i-1}-1,\quad \tau^x_i=2n_{2i}-1,\quad n_i=f^\dagger_i f_i \\ &\sigma^z_i=(f^\dagger_{2i-1}+f_{2i-1})e^{i\pi\sum_{j<2i-1}n_j} \\ &\tau^z_i=(f^\dagger_{2i}+f_{2i})e^{i\pi\sum_{j<2i}n_j}, \end{aligned} \tag{A.53}$$

where f_i are fermionic operators. The Hamiltonian is further simplified by introducing the Majorana fermion operators

$$c_{2j-1}=f^\dagger_j+f_j,\quad c_{2j}=(f_j-f^\dagger_j)/i. \tag{A.54}$$

In terms of the Majorana fermion operators

$$\begin{aligned} H_0 &= -J\sum_j ic_{2j-1}c_{2j} \\ H_1 &= -J\sum_j ic_{2j-2}c_{2j+1} \\ H_{\text{critical}} &= -\frac{J}{2}\sum_j\left[ic_{2i-1}c_{2i}+ic_{2i-2}c_{2i+1}\right]. \end{aligned} \tag{A.55}$$

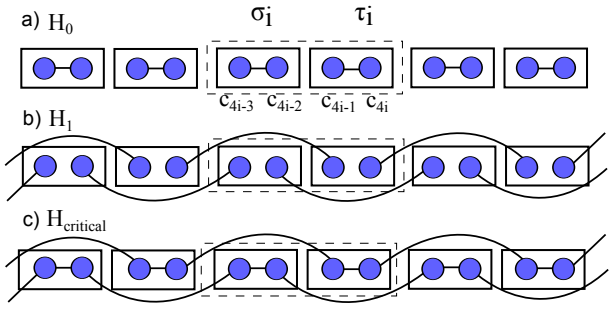

Figure A.4: (Color online) H_0 (a) and H_1 (b) in terms of Majorana fermions. Each bond represents a Majorana fermion hopping term. For panel (b) there are two uncoupled Majorana fermions on each of the right and left end, leading to a $2^2 = 4$ fold degeneracy. (c) A graphical representation of $H_{critical} = \frac{1}{2}(H_0 + H_1)$. There are two independent Majorana chains each contributing 1/2 to the total central charge. The dashed lines enclose one unit cell. Each solid rectangle encloses a spin 1/2. The blue dots denote Majorana fermions.

The hopping patterns of these Hamiltonian are shown in Fig. A.4. Because the critical Hamiltonian describes two translational-invariant gapless Majorana chain each characterized by central charge 1/2, the total central charge of the critical Hamiltonian is 1.

Each site of the above problem can also be viewed as composing of two spin 1/2s each carrying a projective representation of $Z_2 \times Z_2$, or a linear representation of the quaternion group Q_8. The unitary transformation between the (σ, τ) basis discussed above and the spin 1/2 basis is $U = \prod_i \frac{1+i\tau_i^y}{\sqrt{2}}(\frac{1+\sigma_i^z}{2} - \frac{1-\sigma_i^z}{2}\tau_i^x)$. Under the new basis

$$\begin{aligned} H_0 &= \sum_i J(\sigma_i^x \tau_i^x + \sigma_i^z \tau_i^z) \\ H_1 &= \sum_i J(\tau_{i-1}^x \sigma_i^x + \tau_i^z \sigma_{i+1}^z) \\ S_\rho &= \prod_i (\frac{1+\sigma_i^z\sigma_{i+1}^z}{2} + \frac{1-\sigma_i^z\sigma_{i+1}^z}{2}\tau_i^x)K \end{aligned} \tag{A.56}$$

Upon renaming $\sigma_i \to \sigma_{2i-1}$, $\tau_i \to \sigma_{2i}$ and setting $J = 1$, we obtain (2.8), (2.9) of the main text.

A.7 Some details of the density matrix renormalization group calculations

We determine the ground state phase diagram and properties of the model Hamiltonian Eq.(2.13) by extensive and highly accurate density-matrix renormalization group(DMRG)

simulations. For the DMRG simulation, we consider both a periodic boundary condition (PBC) and open boundary condition (OBC). We study many system sizes for a more reliable extrapolation to the thermodynamic limit. We keep up to $m = 1024$ states in the DMRG block with around 10 sweeps to get converged results. The truncation error is of the order 10^{-8} or smaller.

For the a critical theory in one dimension, the central charge of the conformal field theory can easily be extracted by fitting the entanglement entropy to the analytical form [41]

$$S(x) = \frac{c}{3\eta}\ln(x) + O(1), \tag{A.57}$$

where $x = \frac{\eta N}{\pi}\sin(\frac{\pi l}{N})$ is the so-called chord distance for a cut dividing the chain into segments of length l and $N-l$, and periodic (open) boundary conditions are indicated by the parameter $\eta = 1$ or 2, respectively. Performing such a fit to the data in Fig.2.8 with different system sizes, we get the central charge $c = 1$.

A.8 Z_2 SPT in 2D

In this subsection we follow the framework set in previous sections to construct a lattice model describing phase transition between by 2D Z_2-symmetric SPTs. Because $H^3(Z_2, U(1)) = Z_2$, according to the cohomology group classfication there are two inequivalent Z_2-symmetric SPTs in 2D. The non-trivial cocycle is

$$\nu_3(\sigma_1, \sigma_2, \sigma_3, \sigma_4) = (-1)^{(\frac{1-\sigma_1\sigma_2}{2})(\frac{1-\sigma_2\sigma_3}{2})(\frac{1-\sigma_3\sigma_4}{2})} \tag{A.58}$$

To construct the lattice model we consider a triangular lattice. For each site i there is an Ising variable $\sigma_i := \sigma_i^z = \pm 1$. The trivial SPT hamiltonian is

$$H_0 = -J\sum_i \sigma_i^x. \tag{A.59}$$

The non-trivial SPT Hamiltonian is

$$H_1 = -J\sum_i B_i, \tag{A.60}$$

where

$$\langle\{\sigma_i'\}|B_i|\{\sigma_i\}\rangle = \prod_{k\neq i}\delta_{\sigma_k\sigma_k'}\times$$
$$\frac{\nu_3(\sigma_3,\sigma_4,\sigma_i,\sigma_i')\nu_3(\sigma_4,\sigma_i,\sigma_i',\sigma_5)\nu_3(\sigma_i,\sigma_i',\sigma_5,\sigma_6)}{\nu_3(\sigma_3,\sigma_2,\sigma_i,\sigma_i')\nu_3(\sigma_2,\sigma_i,\sigma_i',\sigma_1)\nu_3(\sigma_i,\sigma_i',\sigma_1,\sigma_6)}$$
$$= \prod_{k\neq i}\delta_{\sigma_k\sigma_k'}\times$$
$$\begin{cases} 1 & \text{if } \sigma_i' = \sigma_i \\ -\left[\Pi_{<j,k>} i^{\left(\frac{1-\sigma_j\sigma_k}{2}\right)}\right]\left[i^{(\sum_{j=1}^{6}\sigma_j)}\right] & \text{if } \sigma_i' = -\sigma_i \end{cases} \tag{A.61}$$

Here $\sigma_1,\ldots,\sigma_6$ designate the Ising variables on the six neighbors of i as depicted in Fig. A.1(b), and the product $\Pi_{<j,k>}$ is performed over the six links connecting site i and its six nearest neighbors. After dropping a constant term we obtain

$$H_1 = \sum_i \left[\Pi_{\langle j,k\rangle} i^{\left(\frac{1-\sigma_j\sigma_k}{2}\right)}\right]\left[i^{(\sum_{j=1}^{6}\sigma_j)}\right]\sigma_i^x. \tag{A.62}$$

It was shown in Appendix D of Ref.[29] that H_1 is related to the Levin-Gu[11] Hamiltonian $H_{LG} = \sum_i \left[\Pi_{\langle j,k\rangle} i^{\left(\frac{1-\sigma_j\sigma_k}{2}\right)}\right]\sigma_i^x$ by a local unitary transformation. The non-trivial element of the Z_2^T transformation is given by

$$S_{-1} = \prod_{\Delta}(-1)^{(\frac{1-\sigma_1}{2})(\frac{1+\sigma_2}{2})(\frac{1-\sigma_3}{2})}K \tag{A.63}$$

where $\sigma_1,\sigma_2,\sigma_3$ are the ordered vertices on each triangle Δ. Again $S_{-1}H_0S_{-1}^{-1} = H_1$ and $S_{-1}H_1S_{-1}^{-1} = H_0$.

We construct the hamiltonian to study the phase transition in exactly the same way as in Equation (2.4). $H(\lambda)$ is only solvable for $\lambda = 0$ and 1. For intermediate value of λ it was suggested[12] numerically that there is a first-order transition at $\lambda = 1/2$.

B

Appendix for Chapter 3

B.1 Construction of fixed point $Z_n \times Z_n$ SPT Hamiltonian in 1D

We briefly review the relation between of cocycles and projective representation, and recall a procedure[5;29] to construct fixed point SPT hamiltonians (3.1) that are relevant to this chapter.

Cohomology classification of 1D SPT

Recall from Appendix A.1 that bosonic G-symmetric SPTs in 1 space dimensions are "classified" by $H^2(G, U(1))$, i.e., each equivalent class of SPTs is in one to one correspondence with an element of the abelian group $H^2(G, U(1))$. The binary operation of the abelian group corresponds to the "stacking" operation, i.e., laying two SPTs on top of each other and turning on all symmetry allowed interactions. It turns out that in 1D, the cohomology group has the physical interpretation of projective representations of the boundary degrees of freedom.

Projective representation

In quantum mechanics, symmetry operators are usually realised as matrices $\mathcal{R}(g)$ acting on Hilbert space. Usually these matrices form a *linear* representation of the symmetry group, namely,

$$\mathcal{R}(g_1)\mathcal{R}(g_2) = \mathcal{R}(g_1 g_2). \tag{B.1}$$

However, two quantum states differ by an $U(1)$ phase are regarded as the same quantum mechanically. Thus, one should relax Equation (B.1) by allowing a phase ambiguity ω,

namely,

$$\mathcal{R}(g_1)\mathcal{R}(g_2) = \omega(g_1, g_2)\mathcal{R}(g_1 g_2). \tag{B.2}$$

When Equation (B.2) is satisfied we say that $\mathcal{R}(g)$ form a *projective* representation of the original symmetry group. Obviously, linear representation where $\omega(g_1, g_2) = 1$ is a special case of projective representation. In the literature linear representations are usually viewed as "trivial" projective representations. Associativity under group multiplication, namely,

$$[\mathcal{R}(g_1)\mathcal{R}(g_2)]\mathcal{R}(g_3) = \mathcal{R}(g_1)[\mathcal{R}(g_2)\mathcal{R}(g_3)] \tag{B.3}$$

requires

$$\omega(g_1, g_2g_3)\omega(g_2, g_3) = \omega(g_1, g_2)\omega(g_1g_2, g_3) \tag{B.4}$$

In addition the phase ambiguity of quantum states obviously allows one to multiply all $\mathcal{R}(g)$ by an $U(1)$ phase $\phi(g)$, namely,

$$\mathcal{R}(g) \to \phi(g)\mathcal{R}(g).$$

This phase transformation results in

$$\omega(g_1, g_2) \to \frac{\phi(g_2)\phi(g_1)}{\phi(g_1g_2)}\omega(g_1, g_2) \tag{B.5}$$

Consequently ωs related by Equation (B.5) should be regarded as equivalent.

To see how to interpret cocycles of group cohomology as projective representations, define $\omega(g_1, g_2)$ and $\phi(g_1)$ in terms of the cocycle ν and the coboundary c defined in sectionA.1, namely,

$$\begin{aligned}\omega(g_1, g_2) :=& \nu(e, g_1, g_1g_2)\\ \phi(g_1) :=& c(e, g_1).\end{aligned}$$

where e is the identity group element of G. In terms of ω the cocycle condition becomes

$$\begin{aligned}&(\partial\omega)(g_1, g_2, g_3) := (\partial\nu)(e, g_1, g_1g_2, g_1g_2g_3)\\ &= \frac{\nu(g_1, g_1g_2, g_1g_2g_3)}{\nu(e, g_1g_2, g_1g_2g_3)}\frac{\nu(e, g_1, g_1g_2g_3)}{\nu(e, g_1, g_1g_2)}\\ &= \frac{\omega(g_2, g_3)}{\omega(g_1g_2, g_3)}\frac{\omega(g_1, g_2g_3)}{\omega(g_1, g_2)} = 1\\ &\implies \omega(g_1, g_2g_3)\omega(g_2, g_3) = \omega(g_1, g_2)\omega(g_1g_2, g_3),\end{aligned} \tag{B.6}$$

namely Equation (B.4). In terms of c the coboundary equivalence relation becomes

$$\omega \sim \omega' \text{ if } \omega' = \omega \cdot \partial\phi, \tag{B.7}$$

where

$$\begin{aligned}(\partial\phi)(g_1, g_2) &:= (\partial c)(e, g_1, g_1 g_2) \\ &= \frac{c(g_1, g_1 g_2) c(e, g_1)}{c(e, g_1 g_2)} \\ &= \frac{\phi(g_2)\phi(g_1)}{\phi(g_1 g_2)},\end{aligned} \tag{B.8}$$

which is exactly the factor appearing in Equation (B.5).

Construction of Hamiltonian

Recall from Appendix A.1 that the groundstate wavefunction for an SPT is given in terms of the cocycles by

$$\begin{aligned}|\psi_0\rangle &= \sum_{\{g_i\}} \phi(\{g_i\})\ |\{g_i\}\rangle, \quad \text{where} \\ \phi(\{g_i\}) &= \prod_{i=1}^{L} [\nu(e, g_i, g_{i+1})]^{\sigma(0,i,i+1)}.\end{aligned} \tag{B.9}$$

Here e represents the identity element of G. It is attached to "0" site at the center of the ring as shown in Fig. B.1. $\sigma(i, i+1) = \pm 1$ depending on the orientation of the triangle $0, i, i+1$. The orientation of each link in the triangle is represented by an arrow pointing from the site labeled by a smaller site index to the site labeled by the bigger index. From the link orientation we determine the triangle orientation by following the majority of the link orientation and the right-hand rule). Finally periodic boundary condition requires $g_{N+1} = g_1$.

Recall from Appendix A.1, the Hamiltonian whose exact ground state is Equation (B.9) is

$$H = -J \sum_i B_i, \tag{B.10}$$

where $J > 0$. The operator B_i only changes the basis states on site i, and

$$\langle \{g'_k\} | B_i | \{g_k\} \rangle = \left(\prod_{k \neq i} \delta_{g'_k, g_k} \right) \frac{\nu(g_{i-1}, g_i, g'_i)}{\nu(g_i, g'_i, g_{i+1})}. \tag{B.11}$$

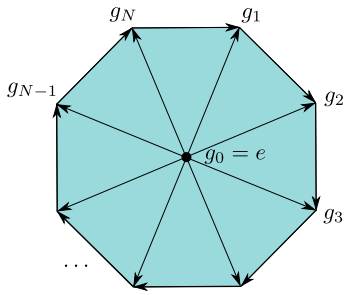

Figure B.1: (Color online) Construction of the 1D groundstate SPT wavefunction from the cocycle. Here the physical degrees of freedom labelled by $g_1, \ldots, g_N$ live on the boundary of the figure. At the center, there is an auxiliary "0" site to which we attach the identity group element e. A phase can be assigned to each triangle by evaluating the cocycle on the group elements on the vertices. The wavefunction is the product of the phases from all triangles.

For $G = Z_n \times Z_n$, there are n inequivalent SPT classes and $H^2(Z_n \times Z_n, U(1)) = Z_n$. Each equivalent class of $H^2(Z_n \times Z_n, U(1))$ is represented by a cocycle

$$\nu((e,e),(g_1,g_2),(g_3,g_4)) = \eta_n^{k g_2 g_3}, \quad \text{where} \quad \eta_n = e^{i2\pi/n}$$

In the above $(g_{2i-1}, g_{2i}) \in Z_n \times Z_n$ are the Z_n elements associated with site i, and $k \in \{0, 1, \ldots, n-1\}$ each correspond to a different element of Z_n ($H^2(Z_n \times Z_n, U(1))$). In the main text, we refer to $|g_{2i-1}, g_{2i}\rangle$ as the "cell basis" which is the tensor product of the "site basis" $|g_{2i-1}\rangle$ and $|g_{2i}\rangle$. The fixed point Hamiltonian constructed using the procedure discussed above is

$$H = -\sum_i (B_{2i-1} + B_{2i} + h.c.),$$

where B_{2i-1} changes the state $|g_{2i-1}\rangle$ and B_{2i} changes the state $|g_{2i}\rangle$. Explicitly calculating the matrix element (Equation (B.11)) for the cases, i.e., $k = 0$ and $k = 1$, relevant to our consideration (recall that we are interested in the quantum phase transition between SPTs correspond to the "0" and "1" elements of Z_n) it can be shown that

$$\begin{aligned} k = 0: &\quad B_{2i-1} = M_{2i-1}, && B_{2i} = M_{2i} \\ k = 1: &\quad B_{2i-1} = R_{2i-2}^\dagger M_{2i-1} R_{2i}, && B_{2i} = R_{2i-1} M_{2i} R_{2i+1}^\dagger, \end{aligned} \tag{B.12}$$

where M_j and R_j are defined by Equation (3.2) of the main text.

B.2 The mapping to $Z_n \times Z_n$ clock models with spatially twisted boundary condition and a Hilbert space constraint

In this section, we show that Equation (3.8) and Equation (3.9) of the main text can be mapped onto an "orbifold" $Z_n \times Z_n$ clock models. The mapping is similar to the "duality transformation" of the Z_n clock model. The mapping is given by

$$\begin{aligned} &R^\dagger_{j-1}R_j = \widetilde{M}_j, \text{ for } j = 2...2N, \text{ and } R^\dagger_{2N}R_1 = \widetilde{M}_1. \\ &M_j = \widetilde{R}^\dagger_j \widetilde{R}_{j+1} \text{ for all } j. \end{aligned} \tag{B.13}$$

Here the tilde operators obey the same commutation relation as the un-tilde ones. Due to the periodic boundary condition on R, namely, $R_{2N+1} = R_1$ and $R_{2N+2} = R_2$ the line of Equation (B.13)implies

$$\prod_{i=1}^{2N} \widetilde{M}_i = 1. \tag{B.14}$$

Moreover, if we also impose the periodic boundary condition on $\widetilde{R}_j$ a similar constraint on M_i, namely,

$$\prod_{i=1}^{2N} M_i = 1. \tag{B.15}$$

is obtained. Since there is no such constraint on M_i in the original problem we need to impose a "twisted" boundary condition on $\widetilde{R}_j$:

$$\begin{aligned} \widetilde{R}_{2N+1} &= \tilde{B}\widetilde{R}_1 \\ \widetilde{R}_{2N+2} &= \tilde{B}\widetilde{R}_2 \end{aligned} \tag{B.16}$$

where $\tilde{B}$ commutes with all $\tilde{R}_j$ and $\tilde{M}_j$. Moreover $\tilde{B}$ has eigenvalues $\tilde{b} = 1, \eta_n, ..., \eta_n^{n-1}$, i.e.,

$$\tilde{B}|\tilde{b}\rangle = \tilde{b}|\tilde{b}\rangle.$$

Substituting Equation (B.13) into Equation (3.8) and Equation (3.9) of the main text we obtain the following expression of the transformed Hamiltonian

$$\begin{aligned} &H_{01}(\lambda) = H_{01}^{\text{even}}(\lambda) + H_{01}^{\text{odd}}(\lambda) \text{ where} \\ &H_{01}^{\text{even}}(\lambda) = -\sum_{i=1}^{N} \left[(1-\lambda)\widetilde{M}_{2i} + \lambda \widetilde{R}^\dagger_{2i}\widetilde{R}_{2i+2}\right] + h.c. \\ &H_{01}^{\text{odd}}(\lambda) = -\sum_{i=1}^{N} \left[\lambda \widetilde{M}_{2i+1} + (1-\lambda)\widetilde{R}^\dagger_{2i-1}\widetilde{R}_{2i+1}\right] + h.c. \end{aligned} \tag{B.17}$$

It is important to note that Equation (B.17) is supplemented with the spatially twisted boundary condition

$$\widetilde{R}_{2N+1} := \widetilde{B}\widetilde{R}_1 \quad \text{and} \quad \widetilde{R}_{2N+2} := \widetilde{B}\widetilde{R}_2 \tag{B.18}$$

and the constraint Equation (B.14). In addition, after the transformation the two generators of the $Z_n \times Z_n$ group become

$$\widetilde{B} \quad \text{and} \quad \prod_{j=1}^{N} \widetilde{M}_{2j}. \tag{B.19}$$

On the surface Equation (B.17) describes two decoupled Z_n clock models living on even and odd sites, respectively. However the notion of "decoupled chains" is deceptive because the constraint in Equation (B.14) couples them together.

B.3 The notion of "orbifold"

A useful way to implement the constraint Equation (B.14) is to apply the projection operator

$$\frac{1}{n}\sum_{q=0}^{n-1} Q^q \tag{B.20}$$

to states in the Hilbert space, where the operator Q is given by

$$Q := \prod_{j=1}^{2N} \widetilde{M}_j. \tag{B.21}$$

Because the eigenvalues of Q are $1, \eta_n, ..., \eta_n^{n-1}$. Equation (B.20) projects onto those states in the Hilbert space that are symmetric under the action of Q. The partition function of the Hamiltonian (B.17), subject to constraint Equation (B.14) and summed over twisted spatial boundary condition sectors is therefore

$$Z = \frac{1}{n}\sum_{q_\tau=0}^{n-1}\sum_{q_s=0}^{n-1} \mathrm{Tr}\Big[Q^{q_\tau} e^{-\beta(H^{even}+H^{odd})}\Big]_{q_s}, \tag{B.22}$$

where $\mathrm{Tr}[...]_{q_s}$ denotes the trace under the spatially twisted boundary condition

$$\widetilde{R}_{2N+1} = \eta_n^{q_s}\widetilde{R}_1 \text{ and } \widetilde{R}_{2N+2} = \eta_n^{q_s}\widetilde{R}_2. \tag{B.23}$$

Moreover in the path integral the action of Q^{q_τ} at $\tau = \beta$ and be viewed as imposing a twisted boundary condition in the time direction.

Thus Equation (B.22) can be written as

$$Z = \frac{1}{n} \sum_{q_s,q_\tau=0}^{n-1} Z^{\text{n-clock}}_{q_s,q_\tau} \times Z^{\text{n-clock}}_{q_s,q_\tau} \tag{B.24}$$

where $Z^{\text{n-clock}}_{q_s,q_\tau}$ represents clock model partition function under the space and time twisted boundary condition characterized by q_s and q_τ. In Equation (B.24) $Z^{\text{n-clock}}_{q_s,q_\tau}$ appears twice on right-hand side because without orbifold (i.e., summing over space and time twisted boundary conditions) we have two independent n-state clock models. Averaging over the partition function under space and time boundary condition twists is the "orbifolding" [42]. Note that here the spatial boundary condition twist is generated by one of the Z_n generator, namely $\tilde{B}$, in Equation (B.19). However, the time twist is generated by $Q = \prod_{j=1}^{2N} \widetilde{M}_j$, which is a symmetry of the $Z_n \times Z_n$ clock Hamiltonian, Equation (B.17), but it is not the generator for the other Z_n in Equation (B.19).

B.4 The modular invariant partition function and the primary scaling operators of the orbifold critical $Z_2 \times Z_2$ clock model

Review of modular invariant partition function for the Ising model

The Ising model shows an order-disorder phase transition. At the critical point, the Hamiltonian is given by

$$H_{Ising} = -\sum_i [M_i + R_i R_{i+1}]$$

where M_i, R_i are Pauli matrices σ^x and σ^z respectively (we use M, R rather than σ^x, σ^z for the consistency of notation). The central charge of a single critical Ising chain is $c = \frac{1}{2}$. Its conformal field theory is the $\mathcal{M}(4,3)$ minimal model. The primary scaling operators are labeled by two pairs of indices (r,s) and (r',s') each label the "holomorphic" and the "anti-holomorphic" part of the operator. The ranges of these indices are given by $1 \le s \le r \le 2$ and $1 \le s' \le r' \le 2$. The scaling dimensions of the holomorphic and anti-holomorphic parts of these operators are given by

$$h_{r,s} = \frac{(4r-3s)^2 - 1}{48}, \quad \bar{h}_{r',s'} = \frac{(4r'-3s')^2 - 1}{48} \tag{B.25}$$

Equation (B.25) gives rise to three primary holomorphic (and anti-holomorphic) scaling operators with distinct scaling dimensions. The corresponding (r,s) indices are $(1,1)$, $(2,1)$ and $(2,2)$. Through the operator-state correspondence, each of these primary fields and

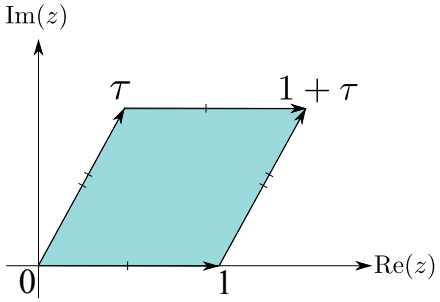

Figure B.2: (Color online) The spacetime torus with modular parameter τ is obtained from identifying opposite edges of a parallelogram with vertices $0, 1, \tau$ and $1+\tau$ in the complex plane. Here τ is a complex number in the upper complex plane.

their associated "descendants" form the basis of a Hilbert space (the "Verma module") which carries an irreducible representation of the conformal group.

Now consider the partition function of the CFT on a spacetime torus (see Fig. B.2). The prototype torus is obtained from identifying opposite edges of the parallelogram having $(0, 1, 1+\tau, \tau)$ as the complex coordinates of its four vertices ($\tau \in$ upper half complex plane). On such a torus, the partition function is given by

$$Z(\tau) = \sum_{r,s;r',s'} M_{(r,s);(r',s')} \chi_{r,s}(\tau) \bar{\chi}_{r',s'}(\bar{\tau}), \tag{B.26}$$

where $M_{(r,s);(r',s')}$ is a matrix with integer entries, and

$$\begin{aligned} \chi_{r,s}(\tau) &= q^{-\frac{c}{24}} \mathrm{Tr}_{(r,s)} q^{h_{r,s}} \\ \bar{\chi}_{r',s'}(\bar{\tau}) &= (\bar{q})^{-\frac{c}{24}} \, \mathrm{Tr}_{(r',s')} \, (\bar{q})^{\bar{h}_{r',s'}} \, , \end{aligned} \tag{B.27}$$

with $q = e^{i2\pi\tau}$ and $\bar{q} = e^{-i2\pi\bar{\tau}}$ Here the trace $\mathrm{Tr}_{(r,s)}$ and $\mathrm{Tr}_{(r',s')}$ are taken within the Verma module labeled by (r, s) and (r', s'). In the literature $\chi_{r,s}$ and $\bar{\chi}_{r',s'}$ are referred to as "characters".

For the CFT to be consistent, its partition function must be "modular invariant" [43]. The modular group consists of discrete coordinate transformations that leave the lattice whose fundamental domain is given by Fig. B.2 invariant. This group is generated by the T ($\tau \to \tau + 1$) and the S ($\tau \to -1/\tau$) transformations. When acted upon by these transformations the characters $\chi_{r,s}$ (with a similar expression for $\bar{\chi}_{r',s'}$) transform according to

$$\begin{aligned} T: \quad & \chi_{r,s}(\tau+1) = \sum_{(\rho,\sigma)} \mathrm{T}_{(r,s),(\rho,\sigma)} \; \chi_{\rho,\sigma}(\tau) \\ S: \quad & \chi_{r,s}(-1/\tau) = \sum_{(\rho,\sigma)} \mathrm{S}_{(r,s),(\rho,\sigma)} \; \chi_{\rho,\sigma}(\tau). \end{aligned}$$

Here S,T are known matrices and the transformation matrices for the anti-holomorphic $\bar{\chi}$ are the complex conjugate of those of the holomorphic ones.)

The requirement of modular invariance,namely,

$$Z(\tau+1) = Z(-1/\tau) = Z(\tau) \tag{B.28}$$

impose stringent constraints on the possible $M_{(r,s);(r',s')}$ in Equation (B.26). For $c = 1/2$ if we require $M_{(1,1),(1,1)} = 1$, i.e., a unique ground state, there is only one such possible M, namely, $M_{(r,s);(r',s')} = \delta_{(r,s),(r',s')}$. The corresponding partition function is given by:

$$Z^{\text{Ising}}(\tau) = |\chi_I(\tau)|^2 + |\chi_\epsilon(\tau)|^2 + |\chi_\sigma(\tau)|^2$$

where

$$\chi_I := \chi_{1,1},\ \chi_\epsilon := \chi_{2,1},\ \chi_\sigma := \chi_{2,2} \tag{B.29}$$

The explicit form of $\chi_{(r,s)}$ is given by equation (8.15) of Ref.[(44)]. The conformal dimensions of primary fields and their eigenvalues under the action of the Z_2 generator are summarized in table B.1 (44).

Table B.1: Conformal dimensions of the primary fields of the Ising model, and their transformation properties upon the action of the Z_2 generator.

(r,s)	(1,1)	(2,1)	(2,2)
$h_{(r,s)}$	0	1/2	1/16
Z_2	1	1	-1

Constructing the orbifold partition function for the $Z_2 \times Z_2$ critical theory

With the brief review of the modular invariant partition function of the critical Ising model we are ready to construct the partition function for the orbifolded $Z_2 \times Z_2$ model defined by of Equation (B.24):

$$Z_{Z_2\times Z_2}(\tau) = \frac{1}{2}\sum_{q_s=0}^{1}\sum_{q_\tau=0}^{1} Z^{\text{Ising}}_{q_s,q_\tau}(\tau) \times Z^{\text{Ising}}_{q_s,q_\tau}(\tau). \tag{B.30}$$

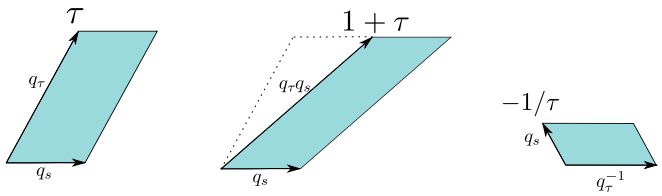

$$Z^{\text{Ising}}_{q_s,q_\tau}(\tau) = Z^{\text{Ising}}_{q_s,q_\tau q_s}(\tau+1) = Z^{\text{Ising}}_{q_\tau^{-1},q_s}(-1/\tau)$$

Figure B.3: (Color online) The transformation of the boundary twisted partition function $Z_{q_s,q_\tau}(\tau)$ under the S and T transformations.

$Z^{\text{Ising}}_{(0,1)}$ is given in Ref.[(44)]. It is also shown in the same reference that $Z^{\text{Ising}}_{q_s,q_\tau}(\tau) = Z^{\text{Ising}}_{q_s,q_\tau q_s}(\tau+1) = Z^{\text{Ising}}_{q_\tau^{-1},q_s}(-1/\tau)$ (see Fig. B.3), hence

$$\begin{aligned}
Z^{\text{Ising}}_{0,0}(\tau) &= |\chi_I(\tau)|^2 + |\chi_\epsilon(\tau)|^2 + |\chi_\sigma(\tau)|^2 \\
Z^{\text{Ising}}_{0,1}(\tau) &= |\chi_I(\tau)|^2 + |\chi_\epsilon(\tau)|^2 - |\chi_\sigma(\tau)|^2 \\
Z^{\text{Ising}}_{1,0}(\tau) &= \mathcal{S} Z^{\text{Ising}}_{0,1}(\tau) \\
Z^{\text{Ising}}_{1,1}(\tau) &= \mathcal{T} Z^{\text{Ising}}_{1,0}(\tau)
\end{aligned} \tag{B.31}$$

Using the known S,T matrices of the Ising model we can compute $Z^{\text{Ising}}_{1,0}$ and $Z^{\text{Ising}}_{1,1}$. Substitute the results into Equation (B.30) we obtain the orbifolded $Z_2 \times Z_2$ partition function:

$$Z_{Z_2\times Z_2}(\tau) = (|\chi_I|^2 + |\chi_\epsilon|^2)^2 + 2|\chi_\sigma^2|^2 + (\bar{\chi}_I\chi_\epsilon + \bar{\chi}_\epsilon\chi_I)^2 \tag{B.32}$$

where the τ dependence is suppressed. When expanded in terms of $\chi_{r,s}\bar{\chi}_{r',s'}$ the first term yields 4 terms (henceforth referred to as group I terms). The second term yields 2 terms (group II terms). The third term yields 4 terms (group III terms). Due to the prefactor 2 in the second term on the right-hand side of Equation (B.32), terms in group II appear with multiplicity 2. It turns out that this partition function is the same as the XY model. The first few energy levels with $h + \bar{h} < 2$ and their quantum numbers are listed in Table B.2.

Transformation properties under the action of $Z_2 \times Z_2$

To see how the contributing Verma modules of Equation (B.32) transform under the action of $Z_2 \times Z_2$, we construct operators that project the Hilbert space into subspaces carrying various irreducible representations of $Z_2 \times Z_2$. Let $G_A = \widetilde{B}$ and $G_B = \prod_{i\in even} \widetilde{M_i}$ be the generators of $Z_2 \times Z_2$. The operator that projects into subspace with eigenvalues (η_2^a, η_2^b) (here $\eta_2 = -1$ and $a, b = 0, 1$) under the action of G_A and G_B is given by

$$P_{ab} = \left(\frac{1+\eta_2^{-a}G_A}{2}\right)\left(\frac{1+\eta_2^{-b}G_B}{2}\right) \tag{B.33}$$

Table B.2: The quantum numbers of the first few primary operators of the orbifold $Z_2 \times Z_2$ CFT.

$h+\bar{h}$	$h-\bar{h}$	Multiplicity	Terms in $Z_{Z_2\times Z_2}$
0	0	1	$\lvert\chi_I\rvert^4$
1/4	0	2	$2\lvert\chi_\sigma\rvert^4$
1	0	4	$4\lvert\chi_I\rvert^2\lvert\chi_\epsilon\rvert^2$
1	±1	2	$\bar{\chi}_I^2\chi_\epsilon^2$ + c.c.
5/4	±1	8	$2\lvert\chi_\sigma\rvert^4$(due to the first descendant)

To filter out the Verma modules that transform according to this particular irreducible representation, we compute

$$\begin{aligned} P_{ab}Z_{Z_2\times Z_2} &:= \frac{1}{2}\sum_{q_\tau=0}^{1}\sum_{q_s=0}^{1}\mathrm{Tr}\Big[P_{ab}Q^{q_\tau}e^{-\beta(H^{\mathrm{even}}+H^{\mathrm{odd}})}\Big]_{q_s} \\ &= \frac{1}{8}\sum_{\mu,\nu=0}^{1}\sum_{q_\tau=0}^{1}\sum_{q_s=0}^{1}\eta_2^{-a\mu-b\nu}\mathrm{Tr}\Big[G_A^\mu G_B^\nu Q^{q_\tau}e^{-\beta(H^{\mathrm{even}}+H^{\mathrm{odd}})}\Big]_{q_s} \\ &= \frac{1}{8}\sum_{\mu,\nu=0}^{1}\sum_{q_\tau=0}^{1}\sum_{q_s=0}^{1}\eta_2^{-a\mu-b\nu}\Big[\eta_2^{q_s\mu}(Z^{\mathrm{Ising}}_{q_s,q_\tau})(Z^{\mathrm{Ising}}_{q_s,q_\tau+\nu})\Big] \end{aligned} \tag{B.34}$$

For example,

$$P_{00}Z_{Z_2\times Z_2} = (\lvert\chi_I\rvert^2 + \lvert\chi_\epsilon\rvert^2)^2, \tag{B.35}$$

which means only group I transform as the identity representation of $Z_2 \times Z_2$. For other P_{ab} the results are summarized in table B.3

Table B.3: Transformation properties of the contributing Verma modules in Equation (B.32) under the action of G_A and G_B. For group II, the doublet records the transformation properties of the multiplicity two Verma modules in Equation (B.32) .

Group	G_A	G_B
I	1	1
II	$(1,-1)$	$(-1,1)$
III	-1	-1

Scaling Dimension for the operator driving the $Z_2 \times Z_2$ SPT transition

The operator that drives the SPT phase transition must be (1) relevant, (2) translational invariant and (3) invariant under $Z_2 \times Z_2$. In Equation (B.32) the only term that contains operators (there are two such operators due to the multiplicity 2) satisfy these conditions is $2|\chi_I \chi_\epsilon|^2$. The scaling dimension of $(I\epsilon)(\bar{I}\epsilon)$ is $h + \bar{h} = 1 < 2$ hence it is relevant. The momentum of this operator is $h - \bar{h} = 0$ hence is translation invariant. Moreover according to Table B.3 there operators are invariant under $Z_2 \times Z_2$. It turns out that one of these two relevant operators drives a symmetry breaking transition while the other drives the SPT transition (See Fig. B.4). From the scaling dimension $h + \bar{h} = 1$ we predict the gap exponent to be $\frac{1}{2-1} = 1$.

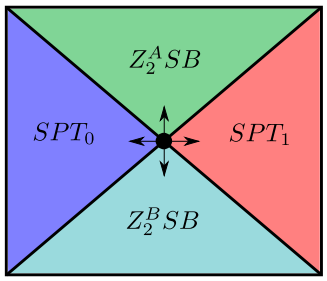

Figure B.4: (Color online) A schematic phase diagram near the $Z_2 \times Z_2$ SPT critical point (the black point). The vertical and horizontal arrows correspond to perturbations associated with the two relevant operators found in section B.4. The relevant perturbation represented by the horizontal arrows drives the transition between the trivial SPT(blue) and the non-trivial SPT (red). The perturbation represented by the vertical arrows drives a Landau forbidden transition between spontaneous symmetry breaking (SB) phases where different Z_2 symmetries are broken in the two different phases (turquoise and green).

B.5 The modular invariant partition function and the primary scaling operators of the orbifold critical $Z_3 \times Z_3$ clock model

Review of modular invariant partition function for the 3 states Potts model

The construction of the orbifold partition function for the $Z_3 \times Z_3$ case closely mirrors the $Z_2 \times Z_2$ case. But instead of two critical Ising chains, we now have two critical Potts chains. We first review the known results for the modular invariant Z_3 clock model (equivalent to the 3-state Potts model). The 3-state Potts model shows an order-disorder phase transition. At the critical point the Hamiltonian is given by

$$H_{Potts} = -\sum_i \Big[M_i + R_i^\dagger R_{i+1} + h.c. \Big]$$

where $R_j = 1, \eta_3, \eta_3^2$ ($\eta_3 = e^{i2\pi/3}$) and $R_j M_k = \eta_3^{\delta_{jk}} M_k R_j$. The conformal field theory for the critical 3-state Potts model belong to the well known "minimal" model $\mathcal{M}(6,5)$ [44;45]. The central charge is

$$c = \frac{4}{5} \tag{B.36}$$

and the primary scaling operators are labeled by two pairs of indices (r,s) and (r',s') each label the "holomorphic" and the "anti-holomorphic" part of the operator. The range of these indices are given by $1 \le s \le r \le 4$ and $1 \le s' \le r' \le 4$. The scaling dimensions of the holomorphic and anti-holomorphic parts of these operators are given by

$$h_{r,s} = \frac{(6r-5s)^2-1}{120}, \quad \bar{h}_{r',s'} = \frac{(6r'-5s')^2-1}{120}. \tag{B.37}$$

It is easy to check that $h_{r,s} = h_{5-r,6-s}$ and $\bar{h}_{r',s'} = \bar{h}_{5-r',6-s'}$ hence there are 10 distinct primary fields in the holomorphic and anti-holomorphic sector each.

Requiring modular invariance (B.28) for $c = 4/5$ yields two possible such M's: one with $M_{(r,s);(r',s')} = \delta_{(r,s),(r',s')}$ describing the "tetra-critical Ising model", and the other corresponds to the 3-state Potts model described by the following partition function [44]:

$$Z^{\text{3-Potts}}(\tau) = |\chi_I(\tau)|^2 + |\chi_\epsilon(\tau)|^2 + 2|\chi_\psi(\tau)|^2 + 2|\chi_\sigma(\tau)|^2, \tag{B.38}$$

where

$$\chi_I := \chi_{1,1} + \chi_{4,1}, \ \chi_\epsilon := \chi_{2,1} + \chi_{3,1}, \ \chi_\psi := \chi_{4,3}, \ \chi_\sigma := \chi_{3,3} \tag{B.39}$$

Note that out of the 10 possible primary operators in each holomorphic/anti-holomorphic sector only six of them contribute to the partition function. In addition, the diagonal combination of the $(3,3)$ and $(4,3)$ operators from each sector appear twice. The explicit form of $\chi_{(r,s)}$ is given by equation (8.15) of Ref.[44]. The conformal dimensions of primary fields and their eigenvalues under the action of the Z_3 generator are summarized in table B.4 [44].

Table B.4: Conformal dimensions of the primary fields of the 3-states Potts model, and their phases under the transformation of the Z_3 generator.

(r,s)	(1,1)	(2,1)	(3,1)	(4,1)	$(3,3)_{1,2}$	$(4,3)_{1,2}$
$h_{(r,s)}$	0	2/5	7/5	3	1/15	2/3
Z_3	1	1	1	1	$(\eta_3, \bar{\eta}_3)$	$(\eta_3, \bar{\eta}_3)$

Constructing the orbifold partition function for the $Z_3 \times Z_3$ critical theory

With the brief review of the modular invariant partition function of the critical 3-state Potts model we are ready to construct the partition function for the orbifolded $Z_3 \times Z_3$ model defined by of Equation (B.24):

$$Z_{Z_3\times Z_3}(\tau) = \frac{1}{3}\sum_{q_s=0}^{2}\sum_{q_\tau=0}^{2} Z^{\text{3-Potts}}_{q_s,q_\tau}(\tau) \times Z^{\text{3-Potts}}_{q_s,q_\tau}(\tau) \tag{B.40}$$

$Z^{\text{3-Potts}}_{(01)}$ and $Z^{\text{3-Potts}}_{(02)}$ are given in Ref.[(44)]. Using $Z^{\text{3-Potts}}_{q_s,q_\tau}(\tau) = Z^{\text{3-Potts}}_{q_s,q_\tau q_s}(\tau+1) = Z^{\text{3-Potts}}_{q_\tau^{-1},q_s}(-1/\tau)$, we have

$$\begin{aligned}
Z^{\text{3-Potts}}_{(00)}(\tau) &= |\chi_I(\tau)|^2 + |\chi_\epsilon(\tau|^2 + 2|\chi_\psi(\tau)|^2 + 2|\chi_\sigma(\tau)|^2 \\
Z^{\text{3-Potts}}_{(01)}(\tau) &= |\chi_I(\tau)|^2 + |\chi_\epsilon(\tau)|^2 + (\eta_3+\bar{\eta}_3)|\chi_\psi(\tau)|^2 + (\eta_3+\bar{\eta}_3)|\chi_\sigma(\tau)|^2 \\
Z^{\text{3-Potts}}_{(02)}(\tau) &= Z^{\text{3-Potts}}_{(01)}(\tau) \\
Z^{\text{3-Potts}}_{(10)}(\tau) &= Z^{\text{3-Potts}}_{(01)}(-1/\tau) = \mathcal{S} Z^{\text{3-Potts}}_{(01)}(\tau) \\
Z^{\text{3-Potts}}_{(20)}(\tau) &= \mathcal{S} Z^{\text{3-Potts}}_{(02)}(\tau) \\
Z^{\text{3-Potts}}_{(12)}(\tau) &= Z^{\text{3-Potts}}_{(10)}(\tau+1) = \mathcal{T} Z^{\text{3-Potts}}_{(10)}(\tau) \\
Z^{\text{3-Potts}}_{(11)}(\tau) &= \mathcal{T} Z^{\text{3-Potts}}_{(12)}(\tau) \\
Z^{\text{3-Potts}}_{(21)}(\tau) &= \mathcal{T} Z^{\text{3-Potts}}_{(20)}(\tau) \\
Z^{\text{3-Potts}}_{(22)}(\tau) &= \mathcal{T} Z^{\text{3-Potts}}_{(21)}(\tau)
\end{aligned} \tag{B.41}$$

Using the S,T matrices of the 3-states Potts model we can compute all these terms. Substituting the results into Equation (B.40) we obtain the orbifolded $Z_3 \times Z_3$ partition function:

$$Z_{Z_3\times Z_3} = (|\chi_I|^2 + |\chi_\epsilon|^2)^2 + 4(|\chi_\psi|^2 + |\chi_\sigma|^2)^2 + 4|\chi_I\bar{\chi}_\psi + \chi_\epsilon\bar{\chi}_\sigma|^2, \tag{B.42}$$

where the τ dependence is suppressed. When expanded in terms of $\chi_{r,s}\bar{\chi}_{r',s'}$ the first term yields 64 terms (henceforth referred as group I terms). The second term yields 16 terms (group II terms). The third term yields 64 terms (group III terms). Due to the prefactor of 4 in the last two terms of Equation (B.42) group II and III terms appear with multiplicity 4. Thus there are in total 144 terms, each corresponds to a primary scaling operator. In Table B.5 we give the first few energy $(h+\bar{h})$ and momentum $(h-\bar{h})$ eigenvalues

Table B.5: The quantum numbers of the first few primary operators of the orbifold $Z_3 \times Z_3$ CFT.

$h+\bar{h}$	$h-\bar{h}$	Multiplicity	Terms in $Z_{Z_3\times Z_3}$
0	0	1	$\lvert\chi_I\rvert^4$
4/15	0	4	$4\lvert\chi_\sigma\rvert^4$
4/5	0	2	$2\lvert\chi_I\rvert^2\lvert\chi_\epsilon\rvert^2$
14/15	0	4	$4\lvert\chi_\epsilon\rvert^2\lvert\chi_\sigma\rvert^2$
17/15	±1	8	$4(\bar{\chi}_I\bar{\chi}_\sigma\chi_\psi\chi_\epsilon + \text{c.c})$
4/15+1	±1	16	$4\lvert\chi_\sigma\rvert^4$(due to the first descendants)
4/3	0	4	$4\lvert\chi_I\rvert^2\lvert\chi_\psi\rvert^2$
22/15	0	8	$8\lvert\chi_\sigma\rvert^2\lvert\chi_\psi\rvert^2$
8/5	0	1	$\lvert\chi_\epsilon\rvert^4$

Transformation properties under the action of $Z_3 \times Z_3$

Following the same procedure in B.4 we construct operators that project the Hilbert space into subspaces carrying various irreducible representation of $Z_3 \times Z_3$ which is generated by $G_A = \widetilde{B}$ and $G_B = \prod_{i\in even} \widetilde{M_i}$. The projector into subspace with eigenvalues (η_3^a, η_3^b) (here $\eta_3 = e^{i2\pi/3}$ and $a, b = 0, 1, 2$) under the action of G_A and G_B is given by

$$P_{ab} = \left(\frac{1+\eta_3^{-a}G_A + \eta_3^a G_A^2}{3}\right)\left(\frac{1+\eta_3^{-b}G_B + \eta_3^b G_B^2}{3}\right) \tag{B.43}$$

Analogous to Equation (B.34) we filter out the Verma modules that transform according to this particular irreducible representation by computing

$$P_{ab}Z_{Z_3\times Z_3} := \frac{1}{27}\sum_{q_\tau,q_s,\mu,\nu=0}^{2} \eta_3^{-a\mu-b\nu}\left[\eta_3^{q_s\mu}(Z^{\text{3-Potts}}_{q_s,q_\tau})(Z^{\text{3-Potts}}_{q_s,q_\tau+\nu})\right] \tag{B.44}$$

For example,

$$P_{00}Z_{Z_3\times Z_3} = (\lvert\chi_I\rvert^2 + \lvert\chi_\epsilon\rvert^2)^2, \tag{B.45}$$

which means only group I transform as the identity representation of $Z_3 \times Z_3$. For other P_{ab} the results are summarized in table B.6

Scaling Dimension for the operator driving the $Z_3 \times Z_3$ SPT transition

From Table B.5 and Equation (B.45) it is seen that the translation-invariant (*i.e.* $h-\bar{h}=0$), relevant(*i.e.* $h+\bar{h}<2$), $Z_3 \times Z_3$ invariant operators either have scaling dimensions 4/5 or

Table B.6: Transformation properties of the contributing Verma modules in Equation (B.42) under the action of G_A and G_B. For group II and group III, the quadruplet records the transformation properties of the multiplicity four Verma modules in Equation (B.42) .

Group	G_A	G_B
I	1	1
II	$(\eta_3, \bar{\eta}_3, 1, 1)$	$(1, 1, \eta_3, \bar{\eta}_3)$
III	$(\eta_3, \eta_3, \bar{\eta}_3, \bar{\eta}_3)$	$(\eta_3, \bar{\eta}_3, \eta_3, \bar{\eta}_3)$

8/5. Through a comparison with the numerical result for the gap exponent in section 9 of the main text, we identify one of the operators with scaling dimension 4/5 as responsible for the opening of the energy gap in the SPT phase transition. The predicted gap exponent is $\frac{1}{2-4/5} = 5/6$ which agrees reasonably well with the numerical gap exponent. Moreover similar to the $Z_2 \times Z_2$ case there are two operators with the same scaling dimension (4/5). Again one of these operators drives a symmetry breaking transition while the other drives the SPT transition, hence the phase diagram is similar to Fig. B.4.

B.6 The modular invariant partition function and the primary scaling operators of the orbifold critical $Z_4 \times Z_4$ clock model

Review of modular invariant partition function for the Z_4 clock model

The Z_4 clock model undergoes an order-disorder transition. The Hamiltonian at criticality between the ordered is given by

$$H_{Z_4} = -\sum_{i=1}^{N} \Big[M_i + R_i^\dagger R_{i+1} + h.c. \Big] \tag{B.46}$$

where $R_j = 1, \eta_4, \eta_4^2, \eta_4^3$ where $\eta_4 = e^{i2\pi/4}$, and $R_j M_k = \eta_4^{\delta_{jk}} M_k R_j$. With periodic boundary condition, $R_{N+1} = R_1$, it can be exactly mapped onto two decoupled periodic Ising chains [46] as follows. For the Z_4 clock model the Hilbert space for each site j is 4-dimensional. In the following, we shall regard this 4-dimensional Hilbert space as the tensor product of two 2-dimensional Hilbert spaces associated with site $2j-1$ and $2j$. We then view each of the 2-dimensional space as the Hilbert space of an Ising spin. In this way the Z_4 clock model with N sites can be viewed as an Ising model with $2N$ sites.

More explicitly, under the unitary transformation $U = \prod_i U_i$, where

$$U_i = \begin{pmatrix} 0 & 1 & 0 & 0 \\ 1 & 0 & 0 & 0 \\ 0 & 0 & 1 & 0 \\ 0 & 0 & 0 & 1 \end{pmatrix},$$

Equation (B.46) becomes

$$\begin{aligned} U^\dagger H_{Z_4} U &= -\sum_{i=1}^{N} (X_{2i-1} + Z_{2i-1}Z_{2i+1}) - \sum_{i=1}^{N} (X_{2i} + Z_{2i}Z_{2i+2}) \\ &= H_{odd}^{\text{Ising}} + H_{even}^{\text{Ising}} \end{aligned} \tag{B.47}$$

where X_i and Z_i denote the 2×2 Pauli matrices σ_i^x and σ_i^z. Thus the partition function of the Z_4 clock model under periodic boundary condition is given by

$$Z_{(0,0)}^{\text{4-clock}}(\tau) = Z_{(0,0)}^{\text{Ising}}(\tau) \times Z_{(0,0)}^{\text{Ising}}(\tau)$$

The fact that Ising model has central charge $c = 1/2$ implies the central charge of the critical Z_4 clock model to be $1/2 + 1/2 = 1$.

CFT with $c = 1$ has infinitely many Verma modules[47]. The scaling dimension of the primary fields, which can take any non-negative values, is parametrized by $h = x^2/4$ where x is a non-negative real number. The characters associated with these Verma modules are given[48] by

$$\chi_h(q) = \begin{cases} \frac{1}{\eta(q)} q^{x^2/4}, & \text{for } x \notin \mathbb{Z} \\ \frac{1}{\eta(q)} \left(q^{x^2/4} - q^{(x+2)^2/4} \right), & \text{for } x \in \mathbb{Z} \end{cases} \tag{B.48}$$

where

$$\eta(q) = q^{1/24} \prod_{n=1}^{\infty} (1 - q^n). \tag{B.49}$$

Because later on we shall perform orbifolding it is necessary to consider the Z_4 clock model under twisted spatial boundary condition. With the spatial boundary condition twisted by the Z_4 generator, i.e., $R_{N+1} = \eta_4 R_1$, the last two terms, namely $Z_{2N}Z_2 + Z_{2N-1}Z_1$ in Equation (B.47), are replaced by

$$Z_{2N}Z_2 + Z_{2N-1}Z_1 \to Z_{2N}Z_1 - Z_{2N-1}Z_2$$

In the language of Ising model, the above replacement creates an overpass connecting the

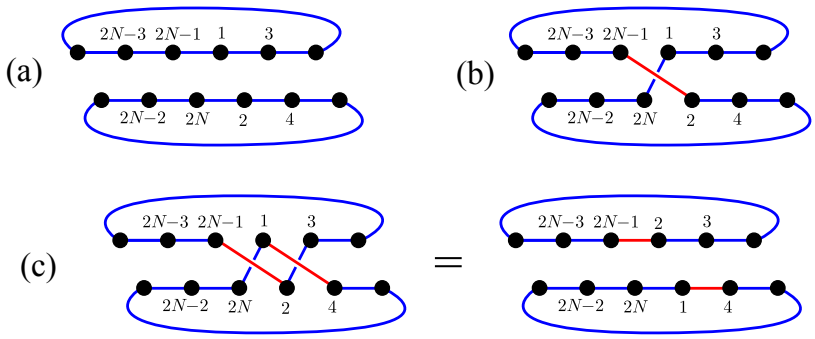

Figure B.5: (Color online) The mapping of Z_4-clock model with different spatially twisted boundary conditions to Ising models. Each black dot represents the X_i term in the Hamiltonian and each blue bond represents the term Z_iZ_j (an antiferromagnetic bond). The red bond represents $-Z_iZ_j$. (a)With periodic boundary condition, the Z_4 clock model maps to two decoupled Ising chains. (b)When the boundary condition is twisted by a Z_4 generator, the Z_4 clock model maps to a single Ising chain twice as long with one antiferromagnetic bond. (c)When the boundary condition is twisted by the square of the Z_4 generator, the Z_4 clock model maps to two decoupled Ising chains, each having an antiferromagnetic bond.

even chain to the odd chain and a sign change of one bond (the red bond in Fig. B.5(b)). Thus we arrive at an Ising chain twice as long and with the spatial boundary condition twisted by the Z_2 generator. As a result

$$Z^{\text{4-clock}}_{(1,0)}(\tau) = Z^{\text{Ising}}_{(1,0)}(\tau/2). \tag{B.50}$$

The reason the modular parameter of the Ising partition function is half that of the Z_4 clock partition function is because the Ising chain has twice the length in the spatial direction. The same argument applies if the boundary is twisted by the inverse of the Z_4 generator ($R_{N+1} = \eta_4^3 R_1$) instead, i.e.,

$$Z^{\text{4-clock}}_{(3,0)}(\tau) = Z^{\text{Ising}}_{(1,0)}(\tau/2). \tag{B.51}$$

Similarly, when the spatial direction is $R_{N+1} = \eta_4^2 R_1$, the Hamiltonian of the Ising model becomes that of two decoupled Ising chain each having a sign-flipped bond equivalent to the Z_2 twisted boundary condition (See Fig. B.5(c)). The resulting partition function is given by

$$Z^{\text{4-clock}}_{(2,0)}(\tau) = Z^{\text{Ising}}_{(1,0)}(\tau) \times Z^{\text{Ising}}_{(1,0)}(\tau)$$

Using the known S and T matrices for the Ising model, other $Z^{\text{4-clock}}_{(q_s,q_t)}(\tau)$ can be determined

$$\begin{aligned}
Z^{\text{4-clock}}_{(0,1)}(\tau) &= Z^{\text{4-clock}}_{(0,3)}(\tau) = \mathcal{S} Z^{\text{4-clock}}_{(1,0)}(\tau) = Z^{\text{Ising}}_{(0,1)}(2\tau) \\
Z^{\text{4-clock}}_{(1,3)}(\tau) &= Z^{\text{4-clock}}_{(3,1)}(\tau) = \mathcal{T} Z^{\text{4-clock}}_{(3,0)}(\tau) = Z^{\text{Ising}}_{(1,0)}(\tau/2+1/2) \\
Z^{\text{4-clock}}_{(1,1)}(\tau) &= Z^{\text{4-clock}}_{(3,3)}(\tau) = \mathcal{S} Z^{\text{4-clock}}_{(1,3)}(\tau) = Z^{\text{Ising}}_{(1,1)}(\tau/2+1/2) \\
Z^{\text{4-clock}}_{(1,2)}(\tau) &= Z^{\text{4-clock}}_{(3,2)}(\tau) = \mathcal{T} Z^{\text{4-clock}}_{(1,3)}(\tau) = Z^{\text{Ising}}_{(1,1)}(\tau/2) \\
Z^{\text{4-clock}}_{(2,1)}(\tau) &= Z^{\text{4-clock}}_{(2,3)}(\tau) = \mathcal{S} Z^{\text{4-clock}}_{(1,2)}(\tau) = Z^{\text{Ising}}_{(1,1)}(2\tau) \\
Z^{\text{4-clock}}_{(0,2)}(\tau) &= \mathcal{S} Z^{\text{4-clock}}_{(2,0)}(\tau) = Z^{\text{Ising}}_{(0,1)}(\tau) \times Z^{\text{Ising}}_{(0,1)}(\tau) \\
Z^{\text{4-clock}}_{(2,2)}(\tau) &= \mathcal{T} Z^{\text{4-clock}}_{(2,0)}(\tau) = Z^{\text{Ising}}_{(1,1)}(\tau) \times Z^{\text{Ising}}_{(1,1)}(\tau)
\end{aligned} \tag{B.52}$$

Orbifold partition function for the critical $Z_4 \times Z_4$ CFT

Using these result and Equation (B.24) we can calculate the orbifolded $Z_4 \times Z_4$ partition function

$$\begin{aligned}
Z_{Z_4\times Z_4}(\tau) &= \frac{1}{4}\sum_{q_s=0}^{3}\sum_{q_\tau=0}^{3} Z^{\text{4-clock}}_{q_s,q_\tau}(\tau) \times Z^{\text{4-clock}}_{q_s,q_\tau}(\tau) \\
&= \left(|\chi_I|^2 + |\chi_J|^2 + 2|\chi_Y|^2 + |\chi_\epsilon|^2 + \bar\chi_\alpha\chi_\beta + \bar\chi_\beta\chi_\alpha\right)^2 \\
&+ \left(\bar\chi_I\chi_J + \bar\chi_J\chi_I + 2|\chi_Y|^2 + |\chi_\epsilon|^2 + \bar\chi_\alpha\chi_\beta + \bar\chi_\beta\chi_\alpha\right)^2 \\
&+ 2\left(|\chi_\alpha|^2 + |\chi_\beta|^2 + |\chi_\epsilon|^2 + \bar\chi_Y\left(\chi_I+\chi_J\right) + \left(\bar\chi_I+\bar\chi_J\right)\chi_Y\right)^2 \\
&+ 4\left(|\chi_\sigma|^2 + |\chi_\tau|^2\right)^2 + 4\left(\bar\chi_\sigma\chi_\tau + \bar\chi_\tau\chi_\sigma\right)^2 \\
&+ 4|\bar\chi_{O_1}\chi_{O_3} + \bar\chi_{O_3}\chi_{O_2} + \bar\chi_{O_2}\chi_{O_4} + \bar\chi_{O_4}\chi_{O_1}|^2,
\end{aligned} \tag{B.53}$$

where

$$\begin{aligned}
\chi_I &= \chi_0 + \sum_{n>0} \left(\chi_{8n^2} + \chi_{4n^2}\right) \\
\chi_J &= \sum_{n>0} \left(\chi_{8n^2} + \chi_{(2n-1)^2}\right) \\
\chi_Y &= \sum_{n>0} \chi_{2(2n-1)^2};\ \chi_\epsilon = \sum_n \chi_{(4n+1)^2/2} \\
\chi_\alpha &= \sum_n \chi_{(8n+1)^2/8};\ \chi_\beta = \sum_n \chi_{(8n+3)^2/8} \\
\chi_\sigma &= \sum_n \chi_{(8n+1)^2/16};\ \chi_\tau = \sum_n \chi_{(8n+3)^2/16} \\
\chi_{O_1} &= \sum_n \chi_{(16n+1)^2/32};\ \chi_{O_2} = \sum_n \chi_{(16n+7)^2/32} \\
\chi_{O_3} &= \sum_n \chi_{(16n+3)^2/32};\ \chi_{O_4} = \sum_n \chi_{(16n+5)^2/32}.
\end{aligned} \tag{B.54}$$

The χ_h in the above equations are given by Equation (B.48). The scaling dimensions of the highest weight states associated with the Verma modules that generate these χ_h are summarized in Table B.7.

Table B.7: Scaling dimensions of the extended primary fields of the Z_4 clock model.

field	I	J	Y	ϵ	α	β	σ	τ	O_1	O_2	O_3	O_4
h	0	1	2	1/2	1/8	9/8	1/16	9/16	1/32	49/32	9/32	25/32

Let's refer to the six terms in Equation (B.53) as Group I, II, III, IV, V, and VI respectively. Due to the prefactor of 2, Group III elements appear in doublets. Due to the prefactor of 4, Group IV, V and VI elements appear with multiplicity 2. In Table B.8 we list the first few primary fields with scaling dimension $h+\bar{h} < 2$ and their quantum numbers.

Transformation properties under the action of $Z_4 \times Z_4$

Similar to section B.4 and B.5 we resolve the Verma modules that generate the partition function in Equation (B.53) into different irreducible representation spaces of $Z_4 \times Z_4$. As done in previous sections we construct the symmetry projection operators

$$P_{ab} Z_{Z_4 \times Z_4} := \qquad \frac{1}{64} \sum_{q_\tau, q_s = 0}^{3} \sum_{\mu,\nu=0}^{3} \eta_4^{-a\mu - b\nu + q_s \mu} \left[Z^{\text{4-clock}}_{q_s, q_\tau} Z^{\text{4-clock}}_{q_s, q_\tau + \nu} \right] \tag{B.55}$$

The results are summarized in Table B.9.

Table B.8: The quantum numbers of the first few low scaling dimension primary operators of the orbifold $Z_4 \times Z_4$ CFT.

$h+\bar{h}$	$h-\bar{h}$	Multiplicity	Terms in $Z_{Z_4\times Z_4}$
0	0	1	$\lvert\chi_I\rvert^4$
1/4	0	4	$4\lvert\chi_\sigma\rvert^4$
1/2	0	2	$2\lvert\chi_\alpha\rvert^4$
5/8	0	4	$4\lvert\chi_{O_1}\chi_{O_3}\rvert^2$
1	0	2	$2\lvert\chi_I\chi_\epsilon\rvert^2$
9/8	±1	8	$4\left(\bar{\chi}_{O_1}^2\chi_{O_3}\chi_{O_4}+\text{c.c.}\right)$
5/4	0	16+4	$16\lvert\chi_\sigma\chi_\tau\rvert^2+4\lvert\chi_\alpha\chi_\epsilon\rvert^2$
5/4	±1	8+4	$4\left(\bar{\chi}_\sigma\chi_\tau\right)^2+2\lvert\chi_I\rvert^2\bar{\chi}_\alpha\chi_\beta+\text{c.c.}$
5/4	±1	16	$4\lvert\chi_\sigma\rvert^4$(first descendants)
3/2	±1	8	$2\lvert\chi_\alpha\rvert^4$(first descendants)
13/8	0	4	$4\lvert\chi_{O_1}\chi_{O_4}\rvert^2$
13/8	±1	16	$4\lvert\chi_{O_1}\chi_{O_3}\rvert^2$(first descendants)

Table B.9: Transformation properties of the contributing Verma modules in Equation (B.53) under the action of G_A and G_B. For Group III to VI, the multiplet records the transformation properties of the corresponding degenerate Verma modules in Equation (B.53).

Group	G_A	G_B
I	1	1
II	-1	-1
III	$(1,-1)$	$(-1,1)$
IV	$(1,1,\eta_4,\bar{\eta}_4)$	$(\eta_4,\bar{\eta}_4,1,1)$
V	$(-1,-1,\eta_4,\bar{\eta}_4)$	$(\eta_4,\bar{\eta}_4,-1,-1)$
VI	$(\eta_4,\eta_4,\bar{\eta}_4,\bar{\eta}_4)$	$(\eta_4,\bar{\eta}_4,\eta_4,\bar{\eta}_4)$

The term $2|\chi_I\chi_\epsilon|^2$ in Equation (B.53) yields two primary fields with scaling dimension $h+\bar{h}=1$ (hence are relevant) and are invariant under $Z_4\times Z_4$ and translation. Hence they are qualified as the gap generating operator. The gap exponent is $\frac{1}{2-1}=1$. Similar to the $Z_2\times Z_2$ and $Z_3\times Z_3$ cases there are two operators with the same scaling dimension (1). As the above two cases one of these operators drives a symmetry breaking transition while the other drives the SPT transition, hence the phase diagram is similar to Fig. B.4.

B.7 Some details of the density matrix renormalization group calculations

The truncation error estimate

We determine the ground state phase diagram and properties of the model Hamiltonian in Equation (3.9) by extensive and highly accurate density-matrix renormalization group [22] (DMRG) calculations. We consider both periodic (PBC) and open (OBC) boundary conditions. Careful study of the dependence on the finite system sizes enables the extrapolation to the thermodynamic limit. For OBC, we keep up to $m = 1000$ states in the DMRG block with around 24 sweeps to get converged results. The truncation error is estimated to be no bigger than $\epsilon = 5 \times 10^{-9}$. For PBC, we keep up to $m = 1100$ states with around 60 sweeps for converged results. In this case, the truncation error is of the order $\epsilon = 10^{-5}$.

The entanglement entropy

For conformal invariant system in one dimension, the central charge can be extracted by fitting the von Neumann entanglement entropy to the following analytical form [34]

$$S(x) = \frac{c}{3\eta} \ln(x) + \text{constant}. \tag{B.56}$$

Here $\eta = 1(2)$ for the periodic (open) boundary condition, respectively. The parameter x is given by $x = \frac{\eta N}{l} \sin(\frac{\pi l}{N})$ for a cut dividing the chain into segments of length l and $N - l$. For each system size under both OBC and PBC, we first calculate the entanglement entropy by keeping a fixed number of states m, hence yielding finite truncation error ϵ. We then perform systematic m dependence study which allows us to extrapolate to the $\epsilon = 0$ limit. For each system size the resulting entanglement entropy is fit to Equation (B.56) to generate the data shown in Fig. 3.4. This result enables us to estimate the central charge to be $c = \frac{8}{5}$. The exponent for the energy gap is obtained in a similar way.

B.8 The on-site global symmetry of conformal field theories

In order to determine which CFT can describe the critical points between bosonic SPT phases, it is important to understand the on-site symmetries of CFTs. This is because the critical theory should at least contain the protection symmetry (which is on-site for bosonic SPTS) of the SPT phases on either side. In Ref. [49] it is shown that a particular type of lattice models (the "RSOS models") reproduce the minimal model CFTs in the continuum

limit. Moreover, the symmetry of such lattice model is related to that of the Dynkin diagrams which are used to classify the modular invariant partition functions[50;49]. However this elegant result does not answer the question whether the continuum theory has emergent symmetry beyond that of the lattice model. In this appendix we briefly review the results of Ref.[51;35] which answers this question.

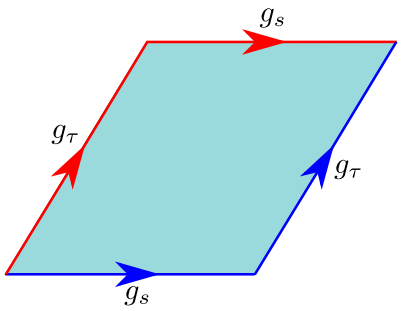

Figure B.6: (Color online) The space-time torus with spatial and temporal boundary condition twisted by group elements g_s and g_τ. The path in red picks up the group element $g_\tau g_s$, while the path in blue picks up the group element $g_s g_\tau$. Since the path in red can be deformed into the path in blue, g_s and g_τ need to commute so that the boundary condition is self-consistent.

The key idea of Ref.[35] is the following. Let's assume the CFT in question has an on-site symmetry group G. This means G commutes with the Virasoro algebra hence each Verma module must carry an irreducible representation of G. Let Z_m be any abelian subgroup of G. We can use Z_m to perform orbifolding. (Note that in order for the space and time symmetry twists to be consistent with each other on a torus the respective elements we use to twist the space and time boundary conditions must commute (see figure B.6). Moreover, if the Z_m irreducible representations are correctly assigned to the Verma modules the resulting orbifolded partition is modular invariant. Therefore to detect whether an on-site symmetry group contains Z_m as an abelian subgroup we just need to see whether it possible to assign Z_m irreducible representations to the Verma modules so that after orbifolding the partition function is modular invariant. For discrete groups after knowing all abelian subgroups we can reconstruct the total group G. This is essentially the strategy followed by Ref.[35].

More explicitly, let the Hilbert space consistent with a spatial boundary condition involving a twist generated by ρ^{g_s} (ρ is the generator of certain abelian subgroup Z_m and $g_s = 0, ..., m-1$)

$$\mathcal{H}^{(g_s)} = \oplus_{i,j} \oplus_{k=1}^{\mathcal{M}_{ij}^{(g_s)}} (\mathcal{V}_i \otimes \bar{\mathcal{V}}_j)_k \tag{B.57}$$

where $\mathcal{V}_i$ ($\bar{\mathcal{V}}_i$) is the ith Verma module in the holomorphic (anti-holomorphic) sector and $\mathcal{M}_{ij}^{(g_s)}$ is a non-negative integer labeling the multiplicity of the $\mathcal{V}_i \otimes \bar{\mathcal{V}}_j$ modules. Moreover, for the CFT to have a unique ground state, we require the vacuum module ($i = 1$) only shows up once in the periodic sector, i.e., $\mathcal{M}_{11}^{(g_s)} = \delta_{0,g_s}$.

Next we assign irreducible representation to the Verma modules:

$$\rho^{g_\tau}(\mathcal{V}_i \otimes \bar{\mathcal{V}}_j)_k = \eta_m^{Q(g_\tau;g_s,i,j,k)}(\mathcal{V}_i \otimes \bar{\mathcal{V}}_j)_k \tag{B.58}$$

where $g_\tau = 0, ..., m-1$, $\eta_m = e^{\frac{i2\pi}{m}}$ and $Q(g_\tau; g_s, i, j, k) \in 0, ..., m-1$ is called "symmetry charge" in Ref.[35]. Combine Equation (B.57) and Equation (B.58) we obtain the following space-time boundary twisted partition function on a torus with modular parameter τ

$$Z_{g_s,g_\tau}(\tau) = \ Tr_{\mathcal{H}^{(g_s)}}(q^{L_0-c/24}\bar{q}^{\bar{L}_0-c/24}q_\tau) = \ \sum_{i,j}\left[\sum_{k=1}^{\mathcal{M}_{ij}^{(g_s)}} \zeta_N^{Q(g_\tau;g_s,i,j,k)}\chi_i(\tau)\bar{\chi}_j(\tau)\right] \tag{B.59}$$

The consistency conditions

So far the abelian subgroup Z_m as well as $\mathcal{M}_{ij}^{(g_s)}$ and $Q(g_\tau; g_s, i, j, k)$ are unknown. They need to be determined subjected to the following consistency conditions. (1) When there is no spatial boundary condition twist the Hilbert space in Equation (B.57) must return to that of the periodic boundary condition. Moreover in the case where there is also no time boundary condition twist the partition function must agree with the modular invariant partition function $Z_{0,0}(\tau)$. (2) The $Z_{g_s,g_\tau}(\tau)$ in Equation (B.59) must transform under the generators (S and T) of the modular transformation as (see Fig. B.3):

$$Z_{g_s,g_\tau}(\tau) = Z_{g_s,g_\tau g_s}(\tau+1) = Z_{g_\tau^{-1},g_s}(-1/\tau)$$

(3) $\mathcal{M}_{11}^{(g_s)} = \delta_{0,g_s}$, $\mathcal{M}_{ij}^{(g_s)}$ = non-negative integer, and $Q(g_\tau; g_s, i, j, k) = 0, ..., m-1$. (1)-(3) pose strong constraints on the possible abelian subgroup Z_m and the allowed assignment of the irreducible representations (i.e. $Q(g_\tau; g_s, i, j, k)$) to each Verma module.

The on-site symmetry of minimal models

Under constants (1)-(3) in the previous subsection Ref.[35] solved the possible abelian subgroups and their symmetry representations for the all minimal models. By patching these abelian subgroups together the author reached the following conclusion: the on-site symmetries of the unitary minimal models are exactly the same as those predicted by the lattice RSOS models[49]. Hence there is no emergent symmetry! Thus, for most of the unitary

minimal models the symmetry is Z_2. The only exceptions are 3-states Potts and tri-critical 3-state Potts models where the symmetry is S_3. Finally for the minimal model labeled by E_7, E_8, where there is no symmetry.

Bibliography

[1] L. Landau, "On the theory of phase transitions," *Zh. Eksp. Teor. Fiz.*, vol. 7, pp. 19–32, 1937.

[2] D. C. Tsui, H. L. Stormer, and A. C. Gossard, "Two-dimensional magnetotransport in the extreme quantum limit," *Physical Review Letters*, vol. 48, no. 22, p. 1559, 1982.

[3] A. P. Schnyder, S. Ryu, A. Furusaki, and A. W. Ludwig, "Classification of topological insulators and superconductors in three spatial dimensions," *Physical Review B*, vol. 78, no. 19, p. 195125, 2008.

[4] A. Kitaev, "Periodic table for topological insulators and superconductors," *AIP conference proceedings*, vol. 1134, 2009.

[5] X. Chen, Z.-C. Gu, Z.-X. Liu, and X.-G. Wen, "Symmetry protected topological orders and the group cohomology of their symmetry group," *Phys. Rev. B*, vol. 87, p. 155114, June 2011.

[6] X. Chen, F. Wang, Y.-M. Lu, and D.-H. Lee, "Critical theories of phase transition between symmetry protected topological states and their relation to the gapless boundary theories," *Nucl. Phys. B*, vol. 873, p. 248, Feb. 2013.

[7] A. Kapustin, "Symmetry protected topological phases, anomalies, and cobordisms: Beyond group cohomology," *arXiv preprint arXiv:1403.1467*, 2014.

[8] Y.-M. Lu and D.-H. Lee, "Quantum phase transitions between bosonic symmetry-protected topological phases in two dimensions: Emergent qed 3 and anyon superfluid," *Physical Review B*, vol. 89, no. 19, p. 195143, 2014.

[9] T. Grover and A. Vishwanath, "Quantum phase transition between integer quantum hall states of bosons," *Physical Review B*, vol. 87, no. 4, p. 045129, 2013.

[10] X. Chen, Y.-M. Lu, and A. Vishwanath, "Symmetry-protected topological phases from decorated domain walls," *Nature communications*, vol. 5, 2014.

[11] M. Levin and Z.-C. Gu, "Braiding statistics approach to symmetry-protected topological phases," *Phys. Rev. B*, vol. 86, p. 115109, Feb. 2012.

[12] S. C. Morampudi, C. Von Keyserlingk, and F. Pollmann, "Numerical study of a transition between z 2 topologically ordered phases," *Physical Review B*, vol. 90, no. 3, p. 035117, 2014.

[13] X.-G. Wen, "Topological orders and edge excitations in fractional quantum hall states," *Advances in Physics*, vol. 44, no. 5, pp. 405–473, 1995.

[14] C. Wang, A. C. Potter, and T. Senthil, "Gapped symmetry preserving surface state for the electron topological insulator," *Physical Review B*, vol. 88, no. 11, p. 115137, 2013.

[15] C. Wang and T. Senthil, "Interacting fermionic topological insulators/superconductors in three dimensions," *Physical Review B*, vol. 89, no. 19, p. 195124, 2014.

[16] F. Burnell, X. Chen, L. Fidkowski, and A. Vishwanath, "Exactly soluble model of a 3d symmetry protected topological phase of bosons with surface topological order," *arXiv preprint arXiv:1302.7072*, 2013.

[17] M. A. Metlitski, C. Kane, and M. Fisher, "A symmetry-respecting topologically-ordered surface phase of 3d electron topological insulators," *arXiv preprint arXiv:1306.3286*, 2013.

[18] X. Chen, L. Fidkowski, and A. Vishwanath, "Symmetry enforced non-abelian topological order at the surface of a topological insulator," *Physical Review B*, vol. 89, no. 16, p. 165132, 2014.

[19] P. Bonderson, C. Nayak, and X.-L. Qi, "A time-reversal invariant topological phase at the surface of a 3d topological insulator," *Journal of Statistical Mechanics: Theory and Experiment*, vol. 2013, no. 09, p. P09016, 2013.

[20] A. Vishwanath and T. Senthil, "Physics of three-dimensional bosonic topological insulators: surface-deconfined criticality and quantized magnetoelectric effect," *Physical Review X*, vol. 3, no. 1, p. 011016, 2013.

[21] L. Fidkowski, X. Chen, and A. Vishwanath, "Non-abelian topological order on the surface of a 3d topological superconductor from an exactly solved model," *Physical Review X*, vol. 3, no. 4, p. 041016, 2013.

[22] S. R. White, "Density matrix formulation for quantum renormalization groups," *Phys. Rev. Lett.*, vol. 69, pp. 2863–2866, Nov 1992.

[23] F. D. M. Haldane, "Fractional quantization of the hall effect: a hierarchy of incompressible quantum fluid states," *Physical Review Letters*, vol. 51, no. 7, p. 605, 1983.

[24] I. Affleck and F. Haldane, "Critical theory of quantum spin chains," *Physical Review B*, vol. 36, no. 10, p. 5291, 1987.

[25] I. Affleck and F. Haldane, "Critical theory of quantum spin chains," *Physical Review B*, vol. 36, no. 10, p. 5291, 1987.

[26] Z. Bi, A. Rasmussen, and C. Xu, "Classification and description of bosonic symmetry protected topological phases with semiclassical nonlinear sigma models," *arXiv preprint arXiv:1309.0515*, 2013.

[27] J. Oon, G. Y. Cho, and C. Xu, "Two-dimensional symmetry-protected topological phases with psu (n) and time-reversal symmetry," *Physical Review B*, vol. 88, no. 1, p. 014425, 2013.

[28] A. A. Belavin, A. M. Polyakov, and A. B. Zamolodchikov, "Infinite conformal symmetry in two-dimensional quantum field theory," *Nuclear Physics B*, vol. 241, no. 2, pp. 333–380, 1984.

[29] A. Mesaros and Y. Ran, "A classification of symmetry enriched topological phases with exactly solvable models," *Phys. Rev. B*, vol. 87, p. 155115, Dec. 2012.

[30] L. Tsui, H.-C. Jiang, Y.-M. Lu, and D.-H. Lee, "Quantum phase transitions between a class of symmetry protected topological states," *Nuclear Physics B*, vol. 896, pp. 330–359, 2015.

[31] L. H. Santos, "Rokhsar-Kivelson models of bosonic symmetry-protected topological states," *Physical Review B*, vol. 91, no. 15, p. 155150, 2015.

[32] G. Y. Cho, K. Shiozaki, S. Ryu, and A. W. Ludwig, "Relationship between symmetry protected topological phases and boundary conformal field theories via the entanglement spectrum," *arXiv preprint arXiv:1606.06402*, 2016.

[33] J. V. José, L. P. Kadanoff, S. Kirkpatrick, and D. R. Nelson, "Renormalization, vortices, and symmetry-breaking perturbations in the two-dimensional planar model," *Physical Review B*, vol. 16, no. 3, p. 1217, 1977.

[34] P. Calabrese and J. Cardy, "Entanglement entropy and quantum field theory," *Journal of Statistical Mechanics: Theory and Experiment*, no. 06, p. 002, 2004.

[35] P. Ruelle and O. Verhoeven, "Discrete symmetries of unitary minimal conformal theories," *Nuclear Physics B*, vol. 535, no. 3, pp. 650–680, 1998.

[36] L. Tsui, F. Wang, and D.-H. Lee, "Topological versus landau-like phase transitions," *arXiv preprint arXiv:1511.07460*, 2015.

[37] X. Chen, Z.-X. Liu, and X.-G. Wen, "Two-dimensional symmetry-protected topological orders and their protected gapless edge excitations," *Physical Review B*, vol. 84, no. 23, p. 235141, 2011.

[38] E. Lieb, T. Schultz, and D. Mattis, "Two soluble models of an antiferromagnetic chain," *Annals of Physics*, vol. 16, no. 3, pp. 407–466, 1961.

[39] I. Affleck and E. Lieb, "A proof of part of haldane's conjecture on spin chains," *Letters in Mathematical Physics*, vol. 12, no. 1, pp. 57–69, 1986.

[40] C. Xu and A. W. Ludwig, "Nonperturbative effects of a topological theta term on principal chiral nonlinear sigma models in 2+ 1 dimensions," *Physical Review Letters*, vol. 110, no. 20, p. 200405, 2013.

[41] P. Calabrese and J. Cardy, "Entanglement entropy and quantum field theory," *Journal of Statistical Mechanics: Theory and Experiment*, no. 06, p. 002, 2004.

[42] R. Dijkgraaf, C. Vafa, E. Verlinde, and H. Verlinde, "The operator algebra of orbifold models," *Communications in Mathematical Physics*, vol. 123, no. 3, pp. 485–526, 1989.

[43] J. L. Cardy, "Operator content of two-dimensional conformally invariant theories," *Nuclear Physics B*, vol. 270, pp. 186–204, 1986.

[44] P. Francesco, P. Mathieu, and D. Sénéchal, *Conformal field theory*. Springer, 2012.

[45] V. S. Dotsenko, "Critical behavior and associated conformal algebra of the $\mathbb{Z}_3$ potts model," *Journal of Statistical Physics*, vol. 34, no. 5-6, pp. 781–791, 1984.

[46] W. Li, S. Yang, H.-H. Tu, and M. Cheng, "Criticality in translation-invariant parafermion chains," *Physical Review B*, vol. 91, no. 11, p. 115133, 2015.

[47] B. L. Feigin and D. Fuks, "Verma modules over the virasoro algebra," *Functional Analysis and its Applications*, vol. 17, no. 3, pp. 241–242, 1983.

[48] I. Runkel and G. M. Watts, "A non-rational CFT with c=1 as a limit of minimal models," *Journal of High Energy Physics*, no. 09, p. 006, 2001.

[49] V. Pasquier, "Lattice derivation of modular invariant partition functions on the torus," *Journal of Physics A: Mathematical and General*, vol. 20, no. 18, p. L1229, 1987.

[50] V. Pasquier, "Two-dimensional critical systems labelled by dynkin diagrams," *Nuclear Physics B*, vol. 285, pp. 162–172, 1987.

[51] J. Zuber, "Discrete symmetries of conformal theories," *Conformal Invariance and Applications to Statistical Mechanics*, vol. 3, p. 406, 1998.